CRANFIELD UNIVERSITY
SILSOE COLLEGE

A FIELD METHOD FOR PREDICTING THE DRAUGHT FORCES OF TILLAGE IMPLEMENTS

A DISSERTATION SUBMITTED TO
THE FACULTY OF AGRICULTURAL ENGINEERING
FOOD PRODUCTION AND RURAL LAND USE
IN CANDIDACY FOR THE DEGREE OF PhD

AGRICULTURAL AND ENVIRONMENTAL
ENGINEERING DEPARTMENT

BY

VAHIT KIRISCI

SUPERVISOR: Prof.R.J.GODWIN

Co-SUPERVISOR: B.S.BLACKMORE

SILSOE, BEDFORDSHIRE

MARCH, 1994

This Thesis is
Dedicated
to My Dear Wife and Lovely Son

"Knowledge should mean a full of grasp of knowledge
Knowledge means to know yourself, heart and soul
If you have failed to understand yourself
Then all of your reading has missed its call

What is the purpose of reading these books
*So that **Man** can know the **All-Powerful***
If you have read, but failed to understand
Then your efforts are a borren toil"
Yunus Emre

ABSTRACT

A literature review was conducted on several models which have been developed, based on Terzaghi's passive earth pressure theory, to describe the forces acting upon tillage implements during tillage operations. These models require a knowledge of cohesion (c) and angle of internal shearing resistance (ϕ) data which are not easy to obtain especially in remote areas.

The main objective of the study was to establish a prediction model for the draught force required for a range of primary tillage implements under different field and soil conditions. The data obtained from the model were used to investigate whether the model was adequate for the mechanisation planning of the GAP region (South Eastern Anatolia Integrated Development Project) in Türkiye where by the year 2012, approximately 1.7 million ha of land will be opened to irrigation.

An effective three-point linkage dynamometer system was developed to measure the draught of implements under different soil conditions. The system consists of bi-axial Linkage Extended Octagonal Ring Transducers (LEORTs) for the lower links, a modified top link and a rotary position transducer sensing the angle of the cross-shaft, together with a 21x datalogger and a portable computer. All transducers outputs were repeatable and linear with a coefficient of determination of ≥ 0.999. The output hysteresis effect was small for all transducers; the largest deviation from the mean was 1.006 % [f.s.] which occurred in the top link. Cross-sensitivity errors for the LEORTs were not significant at a maximum of 0.001 $\mu V\ V^{-1}N^{-1}$.

A spreadsheet model was developed in order to download the data from the instrumentation system to the computer. The model is user friendly and can be used to calculate and plot the forces on the linkage system.

Field experiments were conducted to determine draught force requirements of tillage implements such as a disc plough, mouldboard plough, chisel and subsoiler both under sandy loam soil conditions in UK and clay soil conditions in Türkiye. The standard tine which has a 45^{o} rake angle was used as a reference tine. The field tests were conducted to examine the validation of a model for different soil conditions in UK such as dry, wet, light and heavy soil conditions.

A prediction model has been developed based upon Godwin and Spoor's (1977) which describes the three-dimensional soil failure for a narrow tine above the critical depth, i.e. where only soil loosening takes place. The model has two major components, a geometrical factor (GF) and a soil strength factor (SSF). A simple tine with a 45° rake angle remains at the centre of the model as a reference for the tillage implements. For prediction two stages of work were proposed 1) to measure the draught force acting upon the standard tine; 2) to determine the soil strength factor for the field by using measured tine draught and a geometrical factor from Desbiolles (1994). Having calculated these two components the predictions were made for a disc plough, mouldboard plough, chisel and subsoiler used in the fields. The predicted values were then compared with measured draughts. The difference between the predicted and measured draughts were expressed as a ratio representing the combination of variations in two major factors.

The model predicts the draught requirements of the tillage implements within an error of ±20 %, if two extreme cases are ignored. This error range is acceptable when considering the variation in both the geometrical and soil strength factors. Furthermore, the variations in soil strength characteristics even in the same field can produce a variation of ±10 %. Hence, the ratio of the measured to the predicted draught is between 0.80 and 1.20. It would be difficult to obtain meaningful cohesion (c) and angle of shearing resistance (ϕ) data and implement prediction model which would be any more accurate (Payne, 1956; O'Callaghan and Farrelly, 1964; Hettiaratchi and Reece, 1967; Godwin and Spoor, 1977).

The model was compared with other current prediction approaches such as ASAE D497 Agricultural Machinery Management Data and Witney (1988). This model showed very good predictions when compared with the others. These results are confident and decisive since the model is based on experimental data including both specific field soils and the characteristics of a particular implement. The other techniques particularly ASAE can give values showing a range which vary by a factor of up to 5 times i.e. 2.9-13.1 kN per unit width for a chisel at 0.18-0.23 m depths. These predictions from Witney (1988) contain anomalies which cannot be explained. The ASAE data are not specific for a mechanisation planning in a particular area.

The model provides a novel and simple approach for predicting the mechanisation requirements of a specific area in the future, thus eliminating the need to take particular implements to the field.

ACKNOWLEDGMENTS

First, I would like to thank sincerely Allah (c.c.) for giving me this extremely valuable opportunity to be able to study on a specific subject as a scientist. I am very grateful to the Turkish government for awarding me the scholarship that enabled to make this study possible and I would also like to thank to my employers, the Agricultural Machinery Department of the Faculty of Agricultural of Çukurova University, for giving me permission to study at Silsoe College.

I would like to express my gratitude to my supervisor Prof.R.J.Godwin, to the co-supervisor Mr.B.S.Blackmore, and to the Chairman of the thesis committee, Mr.J.Kilgour for their endless helpful comments, constructive criticisms and suggestions during this study.

Many thanks are expressed to Prof.M.J.O'Dogherty for valuable assistance in checking the text.

I wish to acknowledge the assistance given by colleagues in the Agricultural and Environmental Engineering Department at Silsoe College.

Grateful thanks are given to staff at the Faculty of Agricultural Engineering, Food Production and Rural Land Use for their invaluable assistance and comments.

The author acknowledges to Ms. R.Louise Varley who is the first secretary of the Science and Technology, The British Council in Ankara, Türkiye for assistance in donating the tractor dynamometer system to Çukurova University within the H.M. Ambassador's Gift Scheme.

Many thanks are also due to colleagues and staff working in the Agricultural Machinery Department of Agricultural Faculty of Çukurova University in Türkiye.

Last, but by no means least, I am very indebted and grateful to my dear wife Hanife, my lovely son Mustafa Burak and all my parents for their endless support, encouragement and boundless understanding and invaluable prayers throughout this study. I hope, for your sake, that this study will be beneficial for mankind.

TABLE OF CONTENTS

	Page No
ABSTRACT	
ACKNOWLEDGEMENTS	
TABLE OF CONTENTS	IV
LIST OF TABLES	VI
LIST OF FIGURES	VIII
LIST OF PLATES	XI
LIST OF APPENDICES	XII
LIST OF FILES ON THE FLOPPY DISC	XIII
1. INTRODUCTION	1
1.1. Background of the Study	3
1.1.1. The Country	3
1.1.2. The Southeast Anatolia Project (GAP) Region	4
1.1.3. GAP's Position in National Economy	6
1.1.4. The GAP	7
1.1.5. The Present Problem Structure in the GAP Region	8
1.1.6. Mechanisation Level in the GAP Region	10
1.2. The Structure of the Study	
1.2.1. Justification of the Study	13
1.2.2. Broad Aim of the Study	13
1.2.3. Objective of the Study	13
1.3. Chapter Summary	13
2. REVIEW OF LITERATURE	
2.1. Introduction	14
2.2. Soil-Tine Interaction Models	14
2.3. Instrumentation Systems	26
2.4. Implement Draught Predictions	33
2.5. Chapter Summary	35
3. CONCEPT AND OUTLINES	36

Page No

4. MATERIAL AND METHODS

4.1. Introduction 43

4.2. Tractor Force System for Mounted Implements 43

4.3. Linkage Dynamometer

4.3.1. Design and Construction 48
4.3.2. Lower Link Transducers 48
4.3.3. Top Link Transducer 53
4.3.4. Linkage Position Indicator 53
4.3.5. Instrumentation 54

4.4. The Spreadsheet Model 71

4.5. The Outline of the Study 72

4.6. Soil Characteristics 74

4.7. Standard Tine 76

4.8. Implement Specifications 78

5. RESULTS AND DISCUSSIONS

5.1. Introduction 79

5.2. Draught Force Measurement 79

5.3. Draught Force Predictions 82

5.4. Comparison of Measured and Predicted Draught 85

5.5. Validation of the Concept 95

5.6. Comparison Between the Models 99

6. CONCLUSIONS AND RECOMMENDATIONS

6.1. Conclusions 103

6.2. Recommendations 105

REFERENCES 106

APPENDICES 113

LIST OF TABLES

Table No	Definition of the Table	Page No
1	The Area of the Provinces in the GAP Region	5
2	Population Statistics of the GAP Region and Türkiye	5
3	Gross Regional Product of the GAP Region (1985)	6
4	Basic Features of the GAP	7
5	Number of the Agricultural Machinery and Tractors in the GAP Provinces in 1990 and a Comparison with Türkiye	10
6	Production Capacities in the Tractor Manufacturing Industry in Türkiye	12
7	Variables Used and Assumption made in Force Prediction Procedure	47
8	Some Technical Specifications for the Tractors Used	48
9	Sensing Elements Used on the Three-Point Linkage Dynamometer	49
10	Some Specifications of the Material Used for EOR	51
11	Transducer Calibration Result by Using Datalogger	61
12	Multipliers and Offset Values for Transducers	66
13	Calibration Results of the Transducers Used in 1993	69
14	Mechanical Analysis of the Soil: Downings Field	74
15	Mechanical Analysis of the Soil: GAP in Türkiye	74
16	Mechanical Analysis of the Soil: Showground Field	75
17	Mechanical Analysis of the Soil: Millbrook Field	75
18	Mechanical Analysis of the Soil: Copse Field	75
19	Some Specifications of the Implements	78

Table No	Definition of the Table	Page No
20	Draught Force Requirements of the Implements and Standard Tine Used under Sandy Loam Soil Condition: Downings Field-UK in 1991	79
21	Draught Force Requirements of the Implements and Standard Tine Used under Clay Soil Condition: GAP-Türkiye in 1991	81
22	Geometrical Factors for Tools and Standard Tine Used in 1991	82
23	Soil Strength Factors (SSF) for the Fields in UK and Türkiye in 1991	83
24	Index (I_{GF}) Regression Equations of the Tools Used in 1991	93
25	Regression Equations for the Standard Tine in UK in 1993	95
26	Comparison of Measured Draught and Predicted for Field Tests in UK in 1993	96

LIST OF FIGURES

Figure No	Definition of the Figure	Page No
1	The location map of Türkiye	4
2	The location map of the GAP region	4
3	The problem structure in the GAP region	9
4	Some mechanisation criteria for the GAP region	11
5	Three-dimensional failure wedge in front of a single narrow tine for depths less than critical depth	37
6	Block diagram of the study conducted in Silsoe College	41
7	The forces acting upon a tillage implements	43
8	Forces acting between a tractor and mounted implements	44
9	A force system for a three-point linkage system in XY and XZ Planes	45
10	The position of the resultant	46
11	Sensing elements used in the dynamometer system	49
12	Forces exerted on a lower link	50
13	Basic dimensions of extended octagonal ring	52
14	Bridge arrangements for LEOR	54
15	Poisson arrangement on top link turnbuckle	55
16	Calibration procedure for transducers	57
17	Instrumentation system	59
18	Characteristics of Rotary Position Transducer (RPT)	63
19	Characteristics of FTL bridge on Modified Top Link	63
20	Characteristics of FPL bridge on Left-LEORT	64
21	Characteristics of FCL bridge on Left-LEORT	64

Figure No	Definition of the Figure	Page No
22	Characteristics of FPR bridge on Right-LEORT	65
23	Characteristics of FCR bridge on Right-LEORT	65
24	Three-point linkage dynamometer on the tractor	67
25	Block diagram of the second stage of the study conducted	73
26	A simple 45^{o} raked angle tine	76
27	Measured draughts for the implements and standard tine used under sandy loam soil condition: Downings field-UK in 1991	80
28	Measured draughts for the implements and standard tine used under clay soil condition: GAP-Türkiye in 1991	81
29	Geometrical factors for the tools and standard tine used in 1991	82
30	Predicted-Measured force relationships for the implements used in sandy loam soil condition: Downings field-UK in 1991	86
31	Predicted-Measured force relationships for the implements used in clay soil condition: GAP-Türkiye in 1991	86
32	The ratio of predicted to measured draught for the implements used in sandy loam soil: Downings field-UK in 1991	87
33	The ratio of predicted to measured draught for the implements used in clay soil: GAP-Türkiye in 1991	87
34	Prediction errors for disc plough in sandy loam soil: Downings field-UK in 1991	89
35	Prediction errors for mouldboard plough in sandy loam soil: Downings field-UK in 1991	89
36	Prediction errors for chisel in sandy loam soil: Downings field-UK in 1991	90
37	Prediction errors for subsoiler in sandy loam soil: Downings field-UK in 1991	90
38	Prediction errors for disc plough in clay soil: GAP-Türkiye in 1991	91

Figure No	Definition of the Figure	Page No
39	Prediction errors for mouldboard plough in clay soil: GAP-Türkiye in 1991	91
40	Prediction errors for chisel in clay soil: GAP-Türkiye in 1991	92
41	Prediction errors for subsoiler in clay soil: GAP-Türkiye in 1991	92
42	Index curves based on geometrical factor for the tools used in 1991	93
43	Index values based on the measured draught for the tools used in sandy loam soil: Downings-UK in 1991	94
44	Index values based on the measured draught for the tools used in clay soil: GAP-Türkiye in 1991	94
45	Draught-Depth relationship for standard tine in 1993	95
46	Prediction errors for the field tests in UK in 1993	97
47	Comparison between draught forces predicted by different methods for disc plough	100
48	Comparison between draught forces predicted by different methods for mouldboard plough	100
49	Comparison between draught forces predicted by different methods for chisel	101
50	Comparison between draught forces predicted by different methods for subsoiler	101

LIST OF PLATES

Plate No	Definition of the Plate	Page No
1	Linkage Extended Octagonal Ring and Top Link	52
2	Modification on the Lower Links	53
3	Avery Test Machine	56
4	Support Frame and Apparatus Used with Avery Test Machine	58
5	The Dynamometer Fitted on to the Tractor	66
6	Shear Load Cell	68
7	Extended Octagonal Ring Transducer between Tine and Frame	69
8	The Measurement of the Rolling Resistance for the Tractor and Implement	70
9	The Measurement of the Draught and Rolling Resistance	70
10	Standard Tine Hitched on to the Tractor	77

LIST OF APPENDICES

Appendix No	Definition of the Appendix	Page No
1	Tractor Force System for Mounted Implements	113
2	Ring Theory	120
3	Lower Link Transducer Design	126
4	Datalogger Program	138
5	Three-Point Linkage Model	146
6	Field Test Results (Sandy Loam Soil: Downings Field in UK-1991	150
7	Field Test Results (Clay Soil: GAP in Türkiye-1991	155
8	Geometrical Factors and Error Bands for Tools Used in Field Experiments in 1991	157
9	Tine Interactions for the Chisel Used in UK	158
10	Tine Interactions for the Chisel Used in Türkiye	161
11	Comparison of Measured and Predicted Draughts	164
12	Comparison of Index Values	166
13	Soil Strength Factors for the Fields in 1993	168
14	Geometrical and Soil Strength Factors for the Validation Tests in 1993	170
15	Predicting the Draught Forces	172

LIST OF FILES ON FLOPPY DISC

File Name	File Type	Content of the File
LLEORT01.XLS	Worksheet	Calibration results of Left-LEORT in tables, with DVM
LLEORT02.XLS	Worksheet	Regression statistics of LLEORT01.XLS
LLEORT03.XLS	Worksheet	Calibration results of Left-LEORT in tables, with Datalogger
LLEORT04.XLS	Worksheet	Regression statistics of LLEORT03.XLS
RLEORT01.XLS	Worksheet	Calibration results of Right-LEORT in tables, with DVM
RLEORT02.XLS	Worksheet	Regression statistics of RLEORT01.XLS
RLEORT03.XLS	Worksheet	Calibration results of Right-LEORT in tables, with Datalogger
RLEORT04.XLS	Worksheet	Regression statistics of RLEORT03.XLS
RPT01.XLS	Worksheet	Calibration results of Rotary Position Transducer in tables, with DVM
RPT02.XLS	Worksheet	Regression statistics of RPT01.XLS
RPT03.XLS	Worksheet	Calibration results of Rotary Position Transducer in tables, with Datalogger
RPT04.XLS	Worksheet	Regression statistics of RPT03.XLS
TOP01.XLS	Worksheet	Calibration results of Modified Top Link in tables, with DVM
TOP02.XLS	Worksheet	Regression statistics of TOP01.XLS
TOP03.XLS	Worksheet	Calibration results of Modified Top Link in tables, with Datalogger
TPL.WKI	Worksheet	Model for Three-Point Linkage Linkage

1. INTRODUCTION

Tillage is one of the most fundamental and essential operations in agricultural production. The aim of tillage is to give the optimum environment for germination and crop development and to enable mechanisation and soil and water management practices to take place. However , soil tillage is the most energy consuming work among the field operations. Soil dynamics, which is a phase of soil science and mechanics concerned with soils in motion, provides knowledge relating to the development of tillage implements. The practical importance of soil dynamics in tillage and traction has been known for many years; however, soil dynamics research has been conducted only since 1920 (Gill and Vanden Berg, 1968; Kepner et al., 1982; Kawamura, 1985).

Originally, the mathematical solution for calculating forces was based on the Terzaghi's passive earth pressure theory (Terzaghi, 1962). Based on this theory, several models have been developed to describe the relationship soil tillage-tine. Many of the models are theoretically suitable only for two-dimensional soil failure with wide tines (blades) (Osman, 1964; Reece, 1965; Siemens et al., 1965; Hettiaratchi et al., 1966; Hettiaratchi and Reece, 1974). Models are also available for the three-dimensional soil failure situation with narrow tines (Payne, 1956; O'Callaghan and Farrelly, 1964; Hettiaratchi and Reece, 1967; Godwin and Spoor, 1977; McKyes and Ali, 1977; Perumpral et al., 1983).

In addition to the above models, with the accessibility of computers, numerical based models have been also developed to characterise the soil-tine interaction. Yong and Hanna (1977) first proposed finite element analysis model for the two-dimensional soil failure with wide tine (blade). Chi and Kushwaha (1989) presented a finite element analysis model for the two-dimensional soil failure with narrow tine.

Some of the above models accounts for the effect of the tine shapes and the cutting speed (Söhne, 1956; Stafford, 1979a; Swick and Perumpral, 1988; Chi and Kushwaha, 1989).

Consequently, many of the existing models are inappropriate or are too complex to describe the soil forces upon the tine under field conditions as they require cohesion (c) and angle of internal shearing resistance (ϕ) data which are not easy to obtain especially in remote areas.

Agriculture plays an important role in the economy of the Southeastern Anatolia Region in Türkiye. Agriculture is the dominant activity in the region contributing about 40 % to the region's GRP (Gross Regional Product) while manufacturing contributes 12 %. The majority of the region's population (around 70 %) are earning their living from the agricultural sector (SPO, 1989). However, arid farming has been practised due to the lack of an irrigation scheme.

The Southeastern Anatolia Integrated Development Project, referred to as GAP (shortly in Turkish), comprising 13 energy and irrigation sub-projects, has been introduced by the Turkish Government in order to increase the region's agricultural productivity, and to accelerate the industrialisation and development of the region.

With the completion of the GAP project in Türkiye, which will be by the year 2012, around 1.7 million ha of land (approximately 19 % of the total irrigable area in Türkiye) will be opened up to irrigation and the national agricultural production will double itself. North Mesopotamia which served mankind for thousand of years will achieve advancement again. It is obvious that the farmers will need to use extensive mechanisation due to the shift from arid to irrigated farming in the region's agriculture and new second and industrial crops. Therefore, the farmers should be encouraged to choose proper agricultural machinery, particularly tractors, which are the biggest proportion in both farm inputs and agricultural mechanisation.

In this respect, matching a tractor and implement especially for tillage activities, which represent the most costly single item in the budget of an arable farm (Culpin, 1986), is always important. To improve productivity and efficiency in farm operations, through research, it is necessary to have detailed information about the forces between the tractors and implements.

Implements are attached to the tractor by two methods either the drawbar or the three-point linkage. To measure these forces for a trailed implement, a single load cell is inserted between the drawbar and implement. The majority of current cultivation implements are attached to the tractor through a three-point linkage, either Category I, II or III, instead of one single point. Thus the tractor-implement system becomes much more complex and the force measuring system that is used for trailed implement cannot be used. Therefore, an effective three-point linkage dynamometer is an essential research tool for evaluating the performance of implements and determining tractors pulling required. There are several types of dynamometers available. However, none of them are good enough and each dynamometer has some advantages and disadvantages to others.

Information provided from the proper soil mechanics model tests using the force measurement of the tillage implements can be used to match the tractor and implement required for a particular area such as GAP Region in Türkiye.

1.1. Background of the Study

This chapter gives brief information about Türkiye and the Southeast Anatolia region which is the subject of the study. The importance of agriculture within both the national and the region's economy is also described and the scope of the Southeast Anatolia Project (GAP, shortly in Turkish) is introduced. The reason for selecting the subject from this area and the structure of the study are presented.

1.1.1. The Country

Türkiye is a country at a meeting-point of Europe, Asia and the Middle East. To define it as "a natural bridge" between the continents would be appropriate not only in terms of geographical position but also due to its widespread mosaic of different cultures.

Türkiye lies between the latitudes of 36° and 42° north and the longitudes of 26° and 45° east. Three sides of the country are surrounded by sea and it has a border with Georgia, Ermenia and Nahcivan in the north-east, Iran in the east, Iraq in the south-east, Syria in the south-east, Greece and Bulgaria in the north west, with the land borders of 2 753 km (Fig. 1).

The total area in Türkiye is 779 452 km^2 of which Anatolia (the Asian part) is 755 688 km^2 and Thrace (the European part) is 23 764 km^2 (SIS, 1993).

According to the 1990 census, the population of the country was about 56.473 million with an annual growth rate of about 2.2 %. The average population density is 73 capita per km^2 (SIS, 1993).

Türkiye is situated in the temperate zone. Thus, it has a variety of climatic features. The country is subject to both a continental type of climate, which is characterised by rainy weather throughout the year, and to a sub-tropical climate distinguished by dry summers. The average annual rainfall in Türkiye varies between 325 mm and 1 200 mm depending on location and region.

Figure 1. The location map of Türkiye

1.1.2. The Southeast Anatolia Project (GAP) Region

The Southeast Anatolia Project (GAP) Region used to cover six provinces, Adıyaman, Diyarbakır, Gaziantep, Mardin, Siirt and Şanlıurfa. Recently, two new provinces, Batman and Şırnak, have been included into the project region in Türkiye (Fig. 2).

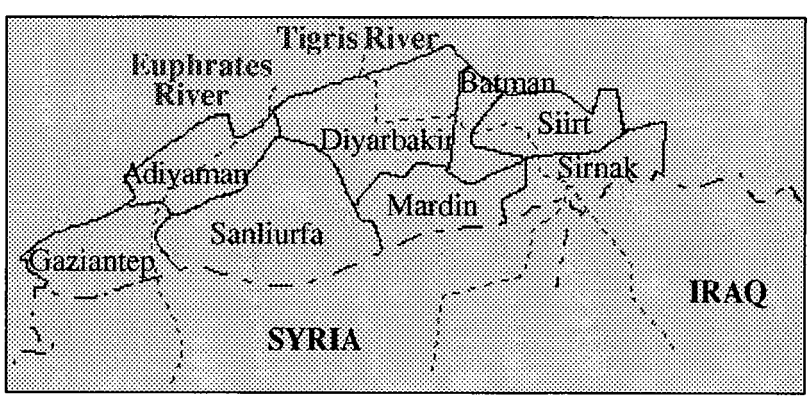

Figure 2. The location map of the GAP region

The region area is approximately 76 263 km^2 which is almost 9.8 % of Türkiye's total land area. The area of each province and the proportion in both Türkiye and the GAP region is shown in Table 1.

Table 1. The Area of the Provinces in the GAP Region

Provinces	Area [km2]	% of GAP TOTAL	% of Türkiye TOTAL
Adıyaman	7 423	9.73	0.95
Batman	4 694	6.16	0.60
Diyarbakır	14 908	19.55	1.91
Gaziantep	8 015	10.51	1.0
Mardin	8 594	11.27	1.10
Siirt	6 186	8.11	0.80
Şanlıurfa	19 271	25.27	2.47
Şırnak	7 172	9.40	0.92
GAP TOTAL	76 263	100.00	9.78
TÜRKİYE TOTAL	779 452	-	100.00

Source: SIS (1993)

According to the 1990 census, the population of the region was about 5 milyon which is 9 % of the nation's total population (Table 2). The density in the region varies between 37 (in Şırnak) and 149 (in Gaziantep) having an average of 68 capita per km^2. The average density differs 5 capita per km^2 from the national average which is 73 capita per km^2. However, the growth rates of population in the region have been higher than that of Türkiye since 1945.

Table 2. Population Statistics of the GAP Region and Türkiye (according to the 1990 census)

Provinces	Population				
	Total	Rural Numbers	[%]	Density [cap/km2]	Growth [%]
Adıyaman	513 131	293 827	57.3	67	3.501
Batman	344 669	151 048	43.8	73	3.772
Diyarbakır	1 094 996	494 356	45.1	71	3.170
Gaziantep	1 140 594	319 467	28.0	149	3.304
Mardin	557 727	308 695	55.3	63	2.587
Siirt	243 435	133 296	54.8	45	1.250
Şanlıurfa	1 001 455	450 331	45.0	54	4.616
Şırnak	262 006	136 742	52.2	37	3.898
GAP	5 158 013	2 387 762	46.3	68	3.732
TÜRKİYE	56 473 035	23 146 684	41.0	73	2.171

Source: SIS (1993)

The share of the region in the national population has been slightly increasing from 7.0 % in 1945 to 9.1 % in 1990, despite the intensive migration of people from the region to the big cities outside, and very high birth rates.

The economically active population has a share of 47 % (people aged from 15 to 64) of the region's population. 70 % of these are working in agriculture while services and industry sectors have 21 % and 8 %, respectively. Table 2 shows that 46 % of the region's population live in rural areas.

The continental climate, characterised by two distinct seasons of a dry and hot summer and a cold and rainy winter, is dominant in the region. The average annual rainfall in the region varies between 467 mm and 757 mm (Sındır, 1992).

1.1.3. GAP's Position in the National Economy

The Gross Regional Product (GRP) of the GAP region in 1985 is compared with the Gross Domestic Product (GDP) of Türkiye and given in Table 3.

Table 3. Gross Regional Product of the GAP Region (1985)

Sectors	GAP billion US$	% to GAP	Türkiye billion US$	GAP as % of Türkiye
Agriculture	846	39.59	9 442	8.96
Industry	335	15.68	16 898	1.99
Manufacturing	250	11.70	13 422	1.86
Services	956	44.74	26 864	3.56
GDP or GRP Total	2 137	100.00	53 205	4.02

Source: SPO (1989)

So far agriculture has been the dominant production sector, claiming its share in the region's GRP of close to 40 %. In this sector the region contributes to around 9 % of the agricultural value-added of Türkiye. Manufacturing accounts for 12 % of the GRP, contributing only 1.9 % of this sector's value-added of the country.

As a whole, the region's economy claims a modest share of 4 % in Türkiye's GDP, much lower than its population share of 8.5 % in 1985. The per capita GRP of the region was only 47 % of the per capita GDP of the country in 1985.

1.1.4. The GAP

The GAP stands for the Southeastern Anatolia Project in Turkish. The GAP is an integrated development project which was originally planned by the State Water Affairs (SWA) primarily for irrigation and hydropower generation. With its 13 energy and irrigation sub-project packages, it comprises the construction of 21 dams and 17 hydroelectric power plants on the Fırat (Euphrates) and Dicle (Tigris) rivers and their tributaries.

The GAP has been introduced in order to mainly increase the region's agricultural productivity and to speed up the industrialisation and development of the region by all means. The basic features of the project, including the total land to be under rainfed and irrigation in the region, without and with the presence of the GAP, are illustrated in Table 4. Although the project has been planned to be completed by 2002, the experts interviewed indicated that this would not be possible before the year 2012.

Table 4. Basic Features of the GAP

	Without Project	With Project
Irrigation means (ha)		
Total Cultivable Land	3 081 182	3 081 182
Land Under Irrigation	120 740	1 641 282
Land Under Rainfed	2 960 442	1 439 900
Power Generation Means		
Installed Capacity (MW)	16	7 561
Energy Generation (GWh/year)	48	25 003
Crop Production Means ('000 tonnes)		
Wheat	1 994	3 279
Cotton	177	859
Tomato	215	1 584
Groundnut	-	156
Soybean	-	316
Maize	16	281

Source: SPO (1989)

1.1.5. The Present Problem Structure in the GAP Region

The GAP region at present faces many problems which vary between the most fundamental and the most immediate ones. These problems are interacting with each other. Major problems and interactions are shown in Figure 3. In the light of Figure 3, the most immediate development problems indicating the objectives for the region's development are summarised by the State Planning Organisation (SPO) as follows;

- Low income level due to immature economic structure, characterised by a small share of the manufacturing industry sector and dominance of low productivity rain-fed agriculture and livestock,
- Migration from villages to larger cities in and out of the region.

The most fundamental ones can be given as;

- Unfavourable topographic and climatic conditions, specially maldistribution of water resources and low productivity land without land/water management,
- Distortion of land distribution/ownership,
- Low levels of education and health services,
- Lack of proper planning and management for resource utilisation.

To overcome these problems, the main objectives for the development of the GAP region are set by the State Planning Organisation (SPO) as follows;

- To raise the income levels in the GAP region by improving the economic structure in order to narrow the income disparity between the region and other regions,
- To increase the productivity and employment opportunities in rural areas,
- To enhance the assimilative capacity of larger cities in the region,
- To contribute to the national objectives of sustained economic growth, export promotion, and social stability by efficient utilisation of the region's sources.

There are some major constraints to the agricultural development in the region. These are also summarised by the State Planning Organisation (SPO) as follows;

- Agro-ecological conditions: i.e. low and non uniform rainfall distribution, very hot summer season, and extended dry periods,
- The prevalence of low yield agricultural technologies with limited input use and commercialisation,
- Low level of farm mechanisation and modernisation.

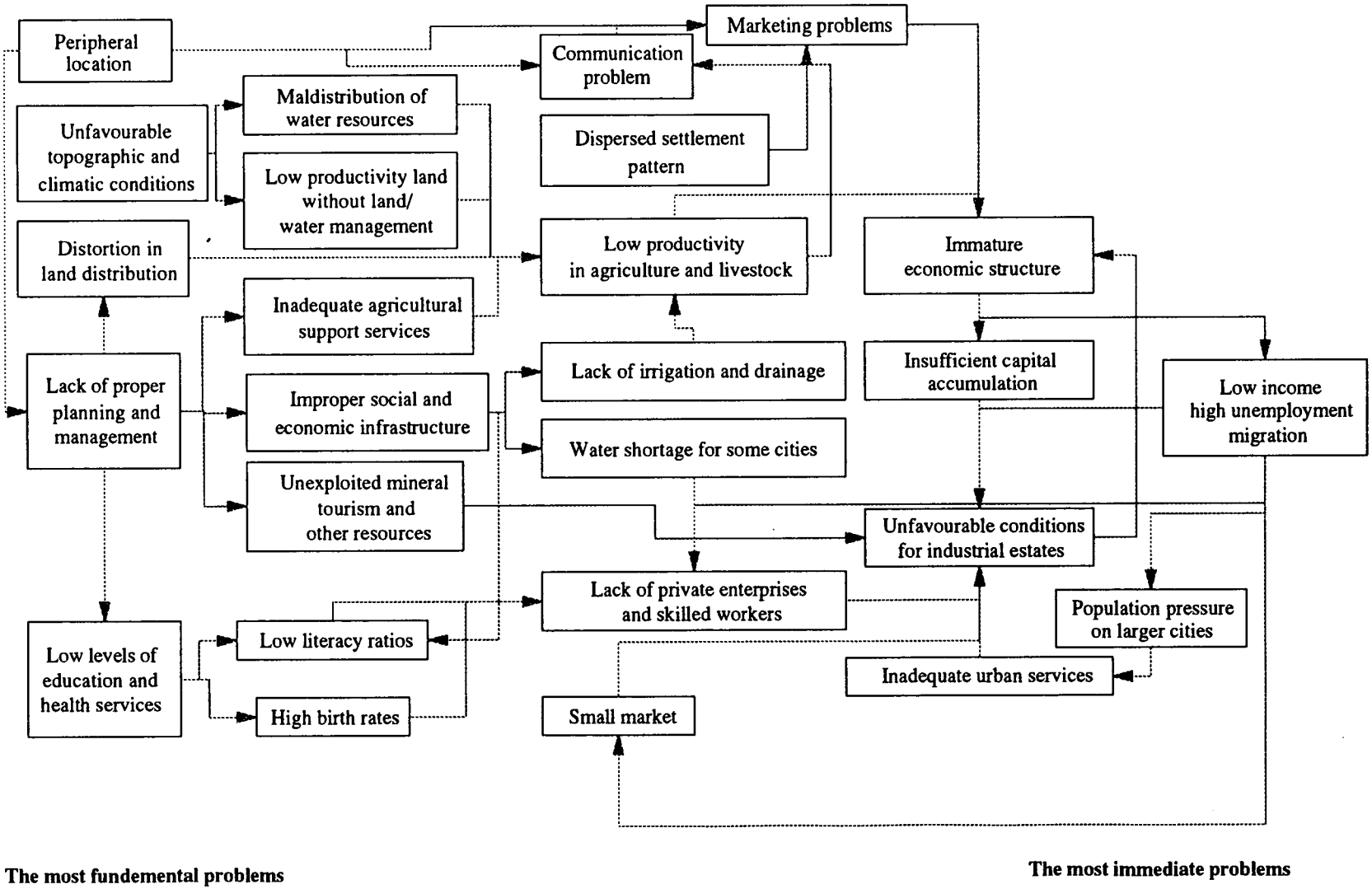

Source: SOP (1989)

Figure 3. The problem structure in the GAP region

1.1.6. Mechanisation Level in the GAP Region

The number of tractors and machinery in the region are shown in Table 5. The region is relatively much less well equipped with these machinery and implements than the country as a whole. This is due to dry land farming system, fragmented land ownership and land tenure systems and the difficulty of farmers with very low income is obtaining farm credit.

Table 5. Number of the Agricultural Machinery and Tractors in the GAP Provinces in 1990 and a Comparison with Türkiye.

Machine	GAP	Türkiye	GAP as % of Türkiye
Tractor Plough	35 979	770 833	4.67
Furrow Opener	563	31 243	1.80
Rotary Cultivator	215	12 318	1.75
Cultivator	21 571	284 677	7.58
Roll	3 846	39 198	9.81
Disc & Other Harrows	4 194	152 390	2.75
Spike Tooth Harrow	1 340	356 171	0.38
In Row Cultivator	1 814	90 103	2.01
Cereal Drill	12 069	162 061	7.45
Universal Planter	493	58 838	0.84
Fertiliser Spreader	15 233	176 015	8.65
Baler	18	7 170	0.25
Thresher	7 785	197 869	3.93
Combine Harvester	478	11 742	4.07
Mower	1 897	20 104	9.44
Knap-Sack Sprayer	8 010	418 736	1.91
PTO Driven Sprayer	2 775	117 583	2.36
Engine Driven Sprayer	371	57 381	0.64
Water Pump	14 061	418 546	3.36
Sprinkler System	559	104 224	0.54
Milking Machine	173	9 636	1.80
Trailer	29 790	648 844	4.60
Tractor	33 111	692 454	4.78

Source: SIS (1993)

There are no organised tractor and machinery hiring services in the region but such services are very common in Türkiye especially for harvesting operations. For example, combine harvesters move from one region to another depending on crop maturity. Tractors and machinery are usually hired from local farmers in the same village.

The measure "*number of tractors per 1 000 ha*" in the GAP in 1988 was 10, almost one third of the national average of 27 (Fig. 4) while the average figure was approximately 28 for developed countries, 4.4 for developing countries and 15.7 for the whole world. Other measures, "tractor horsepower per hectare" and "area in hectares per tractor" are also shown as a comparison with Türkiye, the world, the developed and developing countries.

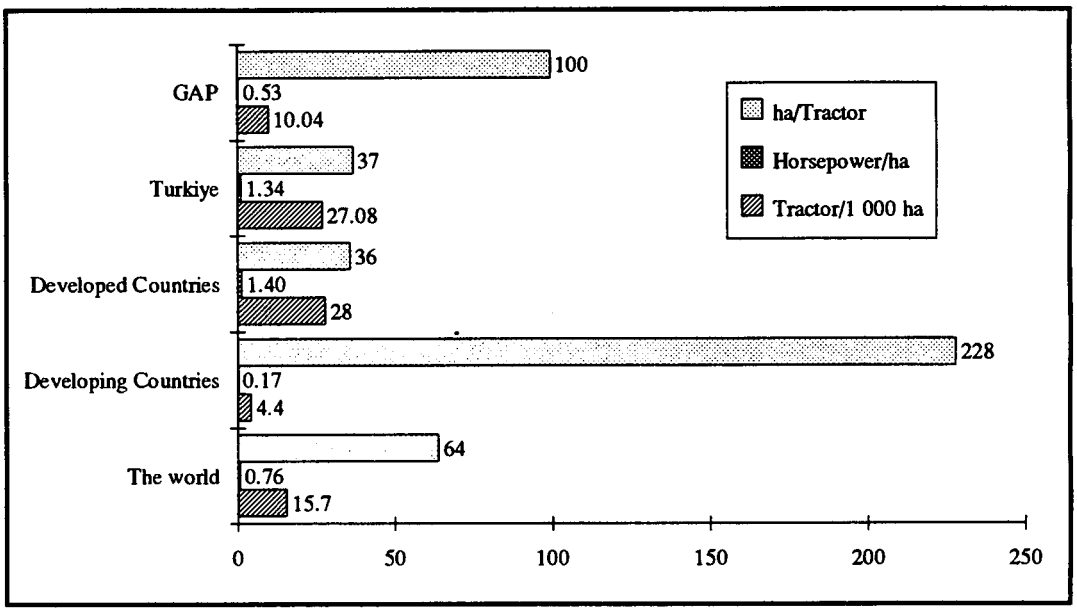

Source: SIS (1988); Sağlam (1987)

Figure 4. Some mechanisation criteria for the GAP region

In the region most of the machinery used in agriculture is produced locally in order to meet the local market demands. However, there is no tractor manufacturing establishment in the region. All of the tractors used are provided from the tractor manufacturers in other regions which are shown in Table 6.

Table 6. Production Capacities in the Tractor Manufacturing Industry in Türkiye

Company	Brand	Production [number of units per year]		
		Real Capacity	in 1989	in 1990
Çumitaş	John Deere	10 000	0	0
Hema	Ford	10 000	344	57
Iltor	Goldoni	3 400	463	648
TOE	TOE	4 000	0	0
Türk Traktör	Fiat	22 500	7 594	12 303
TZDK	Steyr	15 000	2 064	4 474
Uzel	MF	30 000	8 419	14 955
TOTAL		94 000	18 884	14 955

Source: AMA (1990)

1.2. The Structure of the Study

1.2.1. Justification for the Study

It is indicated above that, with the completion of the GAP project in Türkiye, which will be by the year 2012, around 1.7 million ha of land (approximately 19 % of the total irrigable area in Türkiye) will be opened up to irrigation and the national agricultural production will double itself. North Mesopotamia which served mankind for thousand of years will achieve advancement again. It is obvious that the farmers will need to use extensive mechanisation due to the shift from arid to irrigated farming in the region's agriculture and new second and industrial crops. Therefore, the farmers should be encouraged to choose proper agricultural machinery, particularly tractors, which are the biggest proportion in both farm inputs and agricultural mechanisation. In this respect, matching a tractor and implement especially for tillage activities, which is one of the most fundamental and essential operations in agricultural production, represents the most costly single item in the farm budget.

1.2.2. Broad Aim of the Study

It has been highlighted above that the Integrated Regional Development Project (GAP) will produce enormous changes in the agricultural sector which has an important role in the region's economy. Therefore, the broad aim of this study was to determine tractor power which farmers will require in the GAP region concerned with agricultural mechanisation, specifically for tillage operations.

1.2.3. Objective of the Study

The main objective of this study was to determine the relationship between the draught force required for a range of tillage implements and soil properties in various soil conditions in GAP in particular.

1.3. Chapter Summary

This chapter has given an introduction and background information about Tü rkiye and the study area (GAP region). The role of agriculture in the regional and national economy and the current situation and the present problem structure of the region's agriculture are described and the scope of the Southeastern Anatolia Project (GAP) is explained. The events leading up to the identification and selection of the topic for the present study are defined and its aim and objectives are presented.

2. REVIEW OF LITERATURE

2.1. Introduction

The literature related to the study objectives is presented in this chapter. To make the chapter understandable, all of the previous work will be reviewed under three sub-headings concerned with the contents of the study: 1) soil-tine interaction model; 2) instrumentation systems; 3) force predictions for tillage implements.

2.2. Soil-Tine Interaction Models

Soil mechanics, a phase of soil science and mechanics concerned with soils in motion, can be defined as the relation between forces applied to the soil and the resultant soil reaction (Gill and Vanden Berg, 1968). The practical importance of soil dynamics has been known for many years; however, soil-dynamics research has been conducted only since 1920.

In operation, a tillage tine is subjected to three independent force systems: tine weight, soil forces and the forces acting between the tillage tine and prime mover (Vanden Berg, 1966; Kepner et al., 1982). When moving at a constant velocity, these three forces must be in equilibrium. The weight of tine is constant and can be easily determined. The forces between the tine and prime mover vary to achieve equilibrium conditions, so that they are equal but opposite to the resultant of tine weight and soil forces. Soil forces thus can be measured by determining soil-tine interactions.

There have been numerous investigations explaining the soil-tine interaction both in Europe and the USA. A mathematical solution for calculating forces was originally based on the Terzaghi Passive Earth Pressure theory (Terzaghi, 1962). The semi-graphical method of Terzaghi was satisfactory for vertical tines. Based on this theory, several models have been developed to describe the relationship soil-tine.

Zelenin (1950) studied on vertical, horizontal and inclined "soil cutters", and attempted to use fundamental soil mechanics for an empirical approach. He observed a change in the soil failure mechanism at depth with very narrow tines.

Rogers and Hawkins (1956) listed the following methods of reporting data on tillage tines:

(a) a force with a couple in a plane perpendicular to the force, i.e. a wrench.

(b) a force and a couple inclined to the force.

(c) two forces, one on a chosen line.

(d) three forces on mutually perpendicular axes and three couples in the planes of intersection of the axes.

(e) three forces in three major planes.

Soil engaging implements may be divided into three main groups based on depth/width ratio as follows (Godwin and Spoor, 1977; Smith et al., 1989):

Blades:	where the soil failure is two-dimensional, forward and upward only, and small end effects which are generally ignored.
Narrow tines:	where the soil failure is three-dimensional with the soil moving forward, upward and sideways in a crescent shape; the end effects are very significant.
Very narrow tines:	where close to the surface a small three-dimensional crescent occurs, but the soil below a certain depth (critical depth) appears to move forwards only, with no distinct shear plane being formed (lateral failure).

The first comprehensive study was made by Payne (1956). He attempted to apply the civil engineering principle to agricultural soils in order to treat it as an engineering material. He postulated a hypothesis based upon relating measured soil properties to the soil failure patterns and the horizontal force caused by narrow flat rectangular tines which have a rake angle of 90^{o}. The hypothesis was based upon the classical soil mechanics theories of Terzaghi (1962), assuming that the force on the tine faces and front of the soil wedge formed on the front of the tine could be determined from retaining wall theory. He defined blades as those tines with a depth/width ratio of < 0.5 and narrow tines with a depth/width ratio of > 1.0. He carried out the tests both in a soil bin and in the field. Agreement between the predicted and measured values was good for narrow tines. However, the difference was significant for wide tines (blades). He showed that it seemed likely that the theory can be extended to include much more complicated shapes.

Kostritsyn (1956) studied the physics of cutting a cohesive medium by knives and cones. He developed a semi-empirical model based upon experimentally determined constants for calculating the draught of implements. However, the work is only concerned with the behaviour of soil at depths below 0.20 m when it is cut by a knife 30 mm wide. For vertical tines, he found that the critical depth occurred at an aspect ratio of approximately 7, whereas studies with dry sand in glass-sided box by Miller (1971) detected the transition to be at aspect ratios of 12-14. O'Callaghan and McCullen (1965) considered the critical depth to be at an aspect ratio of 0.6 for vertical tines increasing to 2.7 in the Godwin and Spoor (1977) model. He also confirmed the observations of Zelenin (1950) concerning soil failure mechanisms depending on the critical depth.

Söhne (1956) has proposed a formulae for calculating the draught of simple cutting tines by assuming that rupture occurred on planes at 45° to the surface and extending upwards from the base of the tine. He has also estimated the proportion of the total work used in the failure process in lifting, shearing and accelerating the soil. This work applies only to tines with a very small depth/width ratio for two-dimensional soil-tine interactions.

Similar studies to Payne (1956) and Söhne (1956) were also reported by Siemens et al. (1965) studied the mechanics of agricultural soil and compared the experimental results with the theory used for passive earth pressure against retaining walls. They observed that tines caused progressive failure rather than instantaneous failure assumed in the prediction equations and concluded that the predicted tine forces using passive earth pressure theories were higher than the measured values, because the soil shear strength properties were not determined under exactly the same stress conditions that occurred in front of the tine in practice.

Further work on inclined tines was carried out at Silsoe Research Institute (SRI) by Payne and Tanner (1959). They studied rectangular plate tines which had a range of inclination to the horizontal (direction of travel) of 20° to 160° as rake angles and range of depth/width ratio of 1.5 to 6.0. They also measured vertical force as well as horizontal force, and detected the extent to which the soil was disturbed. However, they did not compare predicted values with measured ones. They showed that changes in draught due to depth/width ratios or tine rake angles were dependent on changes in the length of the shear path in the direction of travel, and the soil specific resistance was much more sensitive to the rake angle than depth/width ratios. Draught was relatively intensive to inclination between 20° and 50°, thereafter increasing very

rapidly, the 160° tines having at least five times greater draught than the 20° tines. With tines inclined at less than 45°, the soil provided a component force to assist penetration, but at greater angles it opposed penetration. The same effect was measured by Dransfield et al. (1964).

Osman (1964) developed a model of the mechanics of simple two-dimensional soil cutting blades based upon theories concerning the passive pressure on large retaining walls. He modified Coulomb's work considering the effects of cohesion, adhesion and surcharge in order to yield an analytical solution. He also demonstrated that the logarithmic spiral technique developed by Terzaghi (1962) for rough passive retaining walls would predict the disturbances and force relationships for cutting blades within acceptable limits. The force on a cutting blade depends only on the soil properties c, ϕ, γ, soil-blade properties c_a, δ and geometrical blade constants z, α and curvature l/r, and the surcharge h. The logarithmic spiral technique requires a number of trial solutions to determine the minimum passive force, and does not take account of very small rake angles ($\leq 30°$) and those much greater than 90°. By means of dimensional analysis he presented the following equation in terms of a set of dimensionless groups as below:

$$\frac{P}{\gamma z^2} = f\left(\frac{c}{\gamma z}, \frac{c_a}{\gamma z}, \frac{q}{\gamma z}, \phi, \delta, \alpha\right) . \qquad [1]$$

where

P = soil load (kN),

γ = soil bulk density (kN / m^3),

ϕ = angle of shearing resistance (deg),

c = apparent cohesion (kN / m^2),

δ = angle of soil – interface friction (deg),

c_a = soil – interface adhesion (kN / m^2),

α = rake angle from the forward horizontal (deg),

z = depth of cut (m)

q = surcharge pressure on soil free - surface (kN / m^2).

O'Callaghan and Farrelly (1964) confirmed the two modes of failure at a critical depth described by Zelenin (1950) and Kostritsyn (1956) and developed a three-dimensional model for vertical tines using Mohr-Coulomb soil mechanics theory. O'Callaghan and McCullen (1965) proposed a model which is an extension of the O'Callaghan and Farrelly (1964) model for the cleavage of soil by tined implements. In the tests they used a plate tine raked forward in the direction of travel. They detected two different modes of rupture for shallow and deep tines, and showed that the transition from one mode to the other depends on the rake angle and depth/width ratio of the tine. Giving a forward rake to the tine provided reductions in draught. Wedge-shaped tines required the same draught as plane tines of the same dimensions, but they modified the rupture pattern.

Reece (1965) proposed the following simple additive equation with four terms representing the gravitational, cohesive, adhesive and surcharge contributions to the force. He postulated that equation [1] can be written more specifically in the form of the additive equation as shown below:

$$P = \gamma z^2 N_\gamma + czN_c + c_a zN_a + qzN_q \qquad [2]$$

where

$\gamma z^2 N_\gamma$ = gravitational component of the soil reaction

czN_c = cohesive component of the soil reaction

$c_a zN_a$ = adhesive component of the soil reaction

qzN_q = surcharge component of the soil reaction

N_γ, N_c, N_a, N_q = dimensionless factors

This equation was applied to a wide range of cutting blades by Hettiaratchi et al. (1966). They presented computed values of Reece *N-factors* for the solution of simple two-dimensional problem.

Hettiaratchi and Reece (1967) developed a three-dimensional model based upon the *Passive Earth Pressure Theory* for narrow tines. The analysis of three-dimensional failure assumes that the failure configuration consists of a forward and sideways failure pattern. The total force on the tine due to the three-dimensional failure is the vector sum of the forces due to forward failure (P_f), the sideways force (P_s), and the adhesion force on the interface.

The relationship developed for (P_f) employs the earlier analysis of plane soil wedges in two-dimensional soil failure by Hettiaratchi et al. (1966). They assumed that the forward failure pattern in front of a loaded interface extends the full width and depth of the interface, the expression for the force due to forward failure is:

$$P_f = \gamma d^2 w N_\gamma + cdwN_c + c_a dwN_a + qdwN_q \qquad [3]$$

where

γ = soil bulk density
d = depth of tine
w = width of tine
c = cohesion
c_a = soil - interface adhesion
q = surcharge pressure on the soil - free surface
$N_\gamma, N_c, N_{c_a}, N_q$ = dimensionless earth pressure coefficients

The *N-factors* in this equation can be obtained from graphs available from Hettiaratchi et al. (1966). The forward failure force component (P_f) makes an angle δ (the soil-metal friction angle) with the normal to the interface.

The side ways force (P_s) comprises cohesive and gravitational forces. This force can be expressed as:

$$P_s = \gamma\left(d + q/\gamma\right)^2 bN_{s\gamma} + cdbN_{sc} \qquad [4]$$

where

d = effective depth of failure wedge
b = effective width of failure wedge
$N_{c\gamma}$ and N_{sc} = dimensionless factors due to gravitation and cohesion respectively

The *N-factors* in equation [2] depend upon the roughness of the interface. Separate relationships are given for perfectly smooth (δ = 0) and perfectly rough (δ = ϕ) interfaces and are computed using the charts from Hettiaratchi et al. (1966). The *N-factors* computed are, therefore, suitable for predicting sideways failure force on a vertical tine. For inclined interfaces, multiplication of equation [2] by the inclination factor (K_α) is recommended. The inclination factor is given by the expression:

$$K_\alpha = \frac{\tan^{-1}\left(\sin\alpha \cot\psi\right)}{\frac{\pi}{2} - \psi} \qquad [5]$$

where

$$\psi = \left(\frac{\pi}{4} + \frac{\phi}{2}\right) \qquad [6]$$

The generalised relationship for the sideways force due to a sideways failure is:

$$P_s = \left[\gamma\left(d + q/\gamma\right)^2 bN_{s\gamma} + cdbN_{sc}\right]K_\alpha \qquad [7]$$

By combining equations [3] and [7] and including the adhesion force on the interface, the draught and lift (vertical) forces on a tillage tine can be expressed as:

$$H = P_f \sin(\alpha + \delta) + P_s \sin\alpha + c_a dw \cot\alpha \qquad [8]$$

$$V = P_f \cos(\alpha + \delta) + P_s \cos\alpha + c_a dw \qquad [9]$$

Hettiaratchi and Reece (1967) also conducted two separate experimental investigations to examine the validity of the model. Comparison of experimental and simulated results for a vertical tine at low depth/width ratios showed that the model over-predicted the tine forces. However, the general shape of the predicted curve was similar to that developed from the experimental results. In the case of inclined tines, the model had a tendency to under-predict the tine forces.

Godwin (1974) developed a prediction model based upon Mohr-Coulomb soil mechanics theory for a wide range of flat fronted narrow tines. In that model, two major failure mechanisms were described, an upper three-dimensional crescent failure and a lower two-dimensional failure. Good agreement was found between the predicted values and experimental results. Later, Godwin and Spoor (1977) developed a force prediction model for rigid narrow tillage tines with a wide range of working depth/width ratios. Two separate models were developed for tines operating at depths less, or greater than critical depth. They attempted to use both physical and numerical techniques, and carried out extensive soil bin tests to determine soil failure pattern changes with changes of tine depth (d), width (w), and rake angle (α). The depth to width ratios varied from 1 to 30 and rake angles from 90° to 45°.

They observed that, with deep working narrow tines, the soil failure below a critical depth was different from that nearer the surface, and assumed for simplicity that the failed soil was bounded by a shear surface of logarithmic spiral shape and the crescent had a constant radius (r), and attempted to predict the critical depth of a tine, at the depth that a transition from a crescent failure to a lateral one takes place.

The total wedge for depths less than critical depth was divided into a centre wedge with a width the same as the tine width and two side crescents. They considered the forces contributed by each section to obtain the total force on the tine. The relationship developed by Hettiaratchi et al. (1966) for wide tines (Eqn. 3) was used to obtain the magnitude of the resultant passive force from the centre position of the wedge. The equation for the maximum crescent angle, ρ′, is given by:

$$\rho' = \cos^{-1}\left(\frac{\cot\alpha}{m}\right) \qquad [10]$$

where

ρ' = maximum limit of angle of crescent element from the direction of travel

m = rupture distance ratio $(= r / d_c)$

r = crescent radius

d_c = crtical depth

To obtain a relationship for the force due to the crescents, a wedge-shaped elemental volume ($d\rho$) and forces (dP) acting upon it were considered.

The relationships for the total horizontal (draught) and vertical force components in the direction of travel acting upon tine for the linear (centre wedge) and two curved sections (crescents) were developed. Total horizontal force can be expressed as:

$$H_T = \left[\gamma d_c^2 N_\gamma + c d_c N_c + q d_c N_q\right]\left[w + r\sin\rho'\right]\sin(\alpha+\delta) + c_a w d_c\left[N_a \sin(\alpha+\delta) + \cos\alpha\right] \qquad [11]$$

while the vertical force is expressed as follows:

$$V_T = -\left[\gamma d_c^2 N_\gamma + c d_c N_c + q d_c N_q\right]\left[w + \frac{\pi}{180} r\sin\rho'\right]\cos(\alpha+\delta) - c_a w d_c\left[N_a \cos(\alpha+\delta) - \sin\alpha\right] \qquad [12]$$

The rupture distance (r) should be given to be able to use equations [11] and [12]. The authors also developed a graph to determine the rupture distance for the particular rake angle from experimental results based upon the information from Payne (1956), Payne and Tanner (1959), and Hettiaratchi and Reece (1967).

They conducted low speed verification tests in a sandy loam soil in a soil bin. The experimental results were compared with the predicted total force. The predicted draught force compared reasonably well with the experimental results in two soil conditions with high angles of shearing resistance while poorer comparisons were

obtained for the predicted vertical force. However, as the depth/width ratio increased, the agreement between the predictions and experimental data improved.

The lateral failure which takes place when tine depths are greater than the critical depth was calculated from the bearing capacity solution developed by Meyerhof (1951). A graph of actual depth/width ratio was provided to enable critical depth estimates. However, the critical depth can be predicted by minimising total draught force between the crescent and lateral failure sections.

Later, the crescent failure pattern in the model was simplified by Godwin et al. (1984) so that it enables forces on interacting tines to be predicted. They reviewed crescent radius (r) and expressed the force equations. They considered the influence of tine arrangement on the pattern of soil disturbance, draught force and specific resistance from soil bin experiments, and presented a mathematical model based upon Mohr-Coulomb soil mechanics to predict the soil forces acting upon combination of tines positioned at similar working depths and spacing. Their models can be used to predict the forces within acceptable limits. However, these models are not sufficiently sensitive to predict the additional soil disturbance that can be achieved between neighbouring interacting tines.

Both models predict changes in force pattern with the tine width (w).

McKyes and Ali (1977) developed the three-dimensional model which is similar to that of Godwin and Spoor (1977) for shallow tines. The one major difference is that the McKyes-Ali model does not require empirical data on crescent size, such as the rupture distance, for determining the forces acting upon the tine.

The curved failure surface from the tip of the tine was assumed to be straight and makes an unknown failure angle with the horizontal. The horizontal component of crescent force on the tine is predicted by integrating the elemental force segments from passive retaining-wall theory using trial failure wedges instead of the *General Soil Mechanics Equation.*

Most of the models so far reviewed either assumed that the forward speed of the tool was sufficiently small so that speed effects could be neglected, or that the draught force does not vary with speed. It is generally accepted that the draught force on mouldboard ploughs increases approximately with the square of speed (Gill and Vanden Berg, 1968; Söhne, 1956). The influence of speed on the interaction between narrow tines still has been investigated. Stafford (1979a) evaluated the performance of a tine in terms of the effect of soil type, moisture content and tine speed on soil forces

and soil failure. He emphasised the influence of forward speed on predicting the draught force, and added that the square law explaining the relationship between draught and speed is not universal and cannot be used for all tools. He also observed that the soil forces were determined primarily by the related factors of moisture content and shear strength.

However, while Payne (1956) observed a rise of only 20-30 % over a speed range of 0.2-2.7 m/s, Dransfield et al. (1964) observed no change in draught with speed in the range 0.4-2.2 m/s. In contrast, Siemens et al. (1965) found a 100 % increase of draught in the speed range of 0.2-0.9 m/s. Luth and Wismer (1971) measured a similar increase of draught in the range 0.2-2.5 m/s in an air-dry sand. Wang and Liang (1970) developed a method based on Schuring and Emori (1965) in order to predict the draft requirements of tillage tools considering forward speed. The prediction error was more than 20 %. The authors described the error as acceptable and explained that differences of more than 10 % are expected between test results of the same tine in some soils. Willatt and Willis (1965) found that the effect of speed of the tine was small up to 2.1 m/s.

Spoor and Godwin (1978) showed that the soil at depth can fail in one of two ways: (i) forward and upward in a brittle manner, with well defined failure planes, termed crescent failure, (ii) locally with a compressive type of failure. The brittle failure causes soil loosening, whereas the compressive failure causes soil compaction in a compressible soil. The type of failure depends upon the resistance to deformation in each case. Depth of work, therefore, has an important effect upon the type of soil disturbance. Implement geometry is also critical. The critical depth is dependent upon the width, inclination and lift height of the tine foot and on the moisture and density status of the soil. They mention that the attachment of wings to the tine foot and the use of shallow tines to loosen the surface layers ahead of the deep tine increases soil disturbance, particularly at depth, reduces the specific resistance, increases the critical depth and allows more effective soil rearrangement. They also showed that complete soil loosening at depth and smooth soil surfaces can be achieved by selecting an appropriate tine spacing. This spacing can be increased through the use of wings and shallow leading tines. So transition or critical depth at which a change from brittle to compressive failure occurs is deeper for the very narrow tines (Godwin and Spoor, 1977).

Perumpral et al. (1983) developed a model which is similar to models developed by Godwin and Spoor (1977) and McKyes and Ali (1977). However, the side wedges bounding the centre wedge were replaced by two sets of forces acting upon the side of centre wedge. They assumed that the slip surface was straight as in the work of McKyes and Ali (1977). Dynamic forces are included in the model. The model considers soil failure to occur when a shear plane forms and separates from the undisturbed soil wedge of soil immediately in front of the tine.

Stafford (1981) considered the soil failure caused by a rigid tine and the associated draught force characteristics in the light of the concepts of the critical state model of soil mechanics. The research was basically an extension to the model of Stafford (1979b) and Hettiaratchi et al. (1966) which took tine speed into account. He identified the two modes of soil failure; brittle and flow, and showed that the type of failure can be obtained by variation of tine speed, tine geometry, soil moisture content or soil density. He also identified shear failure with conditions of low confining stress around the tine and flow failure with high confining stresses. He showed that both the draught force magnitude and the relationship between speed and force depended on the mode of failure.

Most of the models discussed above were criticised by Stafford (1984) in that they do not take account of interface speed and only consider brittle failure condition. The critical soil property in all these models is shear strength and force prediction is much less sensitive to self-weight, interface adhesion or the assumed shape of the failure surface. The author listed assumptions made in these models as:

1) Yielding of soil in shear obeys the Mohr-Coulomb criterion.

2) A distinct rupture surface forms in front of the tine, bounding a volume of soil in a state of plastic equilibrium.

3) Rate effects on the relevant soil parameters are negligible.

Reece and Hettiaratchi (1989) presented a procedure the called slip-line method for calculating the forces on plane soil loading surfaces having any rake angle. Basically, they proposed to reduce the calculation procedure of Sokolovski's (1960) method to the solution of a set of relatively simple closed expressions. The method developed applies to two-dimensional passive soil failure situations.

Hanna et al. (1993) tested the Goryachkin crushing and lifting theory prediction of soil flow across a sweep by comparing it with measurements from observed soil flow. They observed soil flow changed with rake angle, but not with speed or depth.

The Goryachkin model does not include forces in undisturbed soil reacting on the wedge of soil being moved. However, the models include a soil-metal frictional force as a linear function of the normal force, but neglects the effect of soil-metal adhesive force.

Grisso and Perumpral (1985) reviewed four narrow tillage tine models for three-dimensional soil-cutting problems. They also compared the simulated results with the experimental results for two soils using different tine widths and rake angles. They concluded that, with the exception of the over prediction of the draught force by the model Hettiaratchi and Reece (1967) and the vertical force by the model of McKyes and Ali (1977), the models were adequate for predicting soil failure resistance and rupture distance. All of the models except the model by Hettiaratchi and Reece (1967) gave reasonable predictions.

Plasse et al. (1985) wrote a simulation program to study the influence of soil properties, the tine surface condition and its geometry on narrow tine performance. The computer simulation and experimental test results were compared with four narrow tillage tine models developed for three-dimensional soil-cutting problems. They showed that all models, except that of Hettiaratchi and Reece (1967), gave a reasonable estimation of draught force. The major factor influencing the draught force is the soil cohesion; adhesion and tine surface roughness are two other major factors.

In addition to the mathematical models, numerical methods were also developed to solve the soil cutting problem. Yong and Hanna (1977) first proposed a finite element model for two-dimensional soil failure with a wide blade. Chi and Kushwaha (1989) developed a three-dimensional finite element model for a narrow cutting blade.

2.3. Instrumentation Systems

To measure the tractive ability of the tractor and the power requirement of the implement it is essential to know the direction and magnitude of the forces between the tractor and implement.

The instrumentation and data logging system can be used in a wide range of field experiments;

- on tractor and implement performance,
- soil and tillage, and/or,
- machinery management.

Implements are attached to the tractor in two ways, either by drawbar or by three-point linkage. Mounted implements are attached to the tractor using the three-point linkage instead of one single point. The draught of trailed implements has been determined by a spring-type, hydraulic type or strain-gauge type dynamometer (Jensen, 1954; Kepner et al., 1982; Zoerb, 1963).

Rogers and Johnston (1953) indicated the need for data on implement forces. They used single acting hydraulic cylinders for the links of a three-point linkage to measure the draught of mounted implements. This technique required photographing pressure gauges attached to hydraulic cylinders at regular intervals.

Many three-point linkage dynamometers have been designed and built since the 1960s. All the recent designs have used electrical resistance strain gauges to measure the forces in specially constructed load cells (Kirişci et al., 1992).

Lal (1959) stated that, for a complete definition of the tractor-implement force relationships for mounted implements, it would be necessary to measure:

- the axial forces in the three links,
- the axial forces in the lift rods, and
- the angular position of one link.

He placed strain gauges to sense both horizontal and vertical force components on the cross-shaft of a mouldboard plough. He connected a framework to the top link of the tractor that would transfer the vertical component of top link force down to the plough cross-shaft. The top link was also gauged to measure axial stresses. The top link bridge and the bridge which sensed horizontal force in the bottom links were wired so that one channel could measure the sum of the two horizontal forces and another

channel could sense the top link axial force alone. Using this system, forces could be obtained to an accuracy of ± 5 %.

Some of the designs measure all the forces acting between the tractor and implement by using a six-dynamometer suspension system (Barker et al., 1981; Chaplin et al., 1987). Others only measure the horizontal and vertical forces, neglecting the side forces as being small (Scholtz, 1964; Garner and Dodd, 1985; Kilgour et al., 1988; Reid et al., 1985). The most basic system just measured the horizontal (draught) force but this is only suitable in certain circumstances (Kirişci et al., 1992).

However, dynamometers can be divided into two groups: 1-Frame type 2-Link type (Chaplin et al. 1987). The frame types consist of transducers mounted on a specially built frame inserted between the tractor and implement. The link type has the force transducers built in the three links themselves (Bandy et al., 1985).

All the frame types have disadvantages (Barker et al., 1981; Chaplin et al., 1987; Garner and Dodd, 1985; Kilgour et al., 1988; Reid et al., 1985; Kirişci et al., 1992). These can be summarised as follows:

- a special frame needs to be constructed.
- the frame moves the implement back from its original position by 200 to 300 mm.
- the mass of the frame itself can be up to 2 kN.
- the frame often creates difficulty in interchanging the implements.
- the frame causes fouling problems in front of the bottom link pins with some implements.

Their main advantage is that they are not specific to a particular tractor or implement. The frames have been designed in many shapes with adjustments so that they will fit a wide range of implements to allow free use of the P.T.O. shaft.

The main advantage of the link type dynamometer is that it does not change the position of the implement in relation to the tractor. This enables the linkage to function as originally intended. This type does not restrict the use of the P.T.O. The strain gauges may be fixed directly to the link but calibration and cross sensitivity can be a problem. The system needs small changes before fixing the transducers (Kilgour et al., 1988). These systems are not interchangeable between tractors.

Reece (1961) developed strain-gauged cantilever pins which were one of the earliest attempts at using strain gauges to measure the forces between tractor and implement. The pins were mounted on the tractor to support the ball joints at the inner end of three links. These pins could only measure the horizontal forces. They had a cross-sensitivity of up to 10 %. The accuracy was 3 % due to friction at the ball joints resulting in hysteresis. This method of draught measurement was limited to tractors using a free linkage (unrestrained) and assumed that the horizontal forces in the left and right lift rods were equal and opposite. The system allowed the use of neither position nor draught control.

Scholtz (1964) improved the system proposed by Lal (1959). The system was based on three transverse beams which were mounted to the tractor frame and served as the front attachment points of the links. However, the system had problems of high hysteresis (15 %) which Scholtz (1964) discovered was due to friction at the ball joints. He reduced this effect by using self-aligning ball bearings instead of plain ball joints and/or by increasing the cantilever length. This increased the bending moment being measured. This measuring system was limited to a specific tractor. The P.T.O. was obstructed and could not be used.

Scholtz (1966) listed the requirements of three-point linkage dynamometers and stated that a dynamometer must:

- be able to measure the forces acting in a vertical plane.
- fit as many implements as possible without requiring modification to either implement or dynamometer.
- permit the use of a P.T.O. shaft.
- use the minimum number of measuring channels.

He designed a frame-type three-point linkage dynamometer to measure the horizontal and vertical forces between the tractor and implement. The dynamometer was made in one L-shaped transducer for the top hitch point and two U-shaped transducers for the lower hitch points. The frame had a special shape so that it permitted the use of P.T.O. power. The friction at the ball joints was minimised. Cross-sensitivity was 0.5 % for the draught force. He listed some limitations of the dynamometer as follows:

- not suitable for use with any mounted implement without modification.
- had a mass of 1.2 kN due to the sub-frame.

- moves the hitch point of the tractor 229 mm to the rear.
- produces some extra resilience in the hitch.

One of the most common methods used to measure specific forces on tines is the Extended Octagonal Ring Transducer (EORT). EORT was introduced by Loewen and Cook (1956) and has been used in agricultural and other engineering fields (Cook et al., 1954; O'Dogherty, 1975; Godwin, 1975; Bandy et al., 1985).

Godwin (1975) built an extended octagonal ring transducer to measure the two force components and moment in the plane of the two soil reaction forces acting upon simple rigid tines. He found the sensitivities of the strain gauge outputs significantly higher than predicted sensitivities. He also detected the smallest cross-sensitivity when the gauges for vertical force were placed at 34°. He also stated that the extended octagonal ring transducer advantages over the other multi-dynamometer system as:

- alleviation of the frictional problems arising from the dynamometer suspension bushes.
- single component construction, compactness and simple mounting; which reduces the difficulties with precision alignment necessary for accuracy when a multi-dynamometer suspension system is used.
- simultaneous monitoring of the two force components and the moment in the plane of these two forces.

He was satisfied with the system calibration results in terms of linearity, hysteresis, and cross-sensitivity. He mentioned that the cuurent design formulae for the normal ring should be modified for the Extended Octagonal Ring (EOR).

O'Dogherty (1975) designed a dynamometer to measure the forces acting upon on a sugar beet topping knife. The dynamometer was an application of an extended octagonal ring transducer. He mentioned that the design formulae for the ring should be modified for the EOR. He found some interactions between channels which was equal to 4.1 % for horizontal force and 6.5 % for vertical force. Hysteresis was less than 1.0 % for both force bridges.

Johnson and Voorhees (1979) developed a dynamometer capable of simultaneously measuring draught, vertical force and torque in a vertical longitudinal plane. This dynamometer required three channels of signal conditioning and data recording. This dynamometer used a sub frame assembly. The design of the sub frame was based on a quick-attaching coupler which was a feature of this dynamometer

made to hook-up to most category II and III implements in a simple manner. This dynamometer cannot be used with implements which require power transmitted through a P.T.O. shaft due to obstructions. The dynamometer resulted in an implement hitch point which was 310 mm to the rear of the normal hitch position. The mass of the dynamometer was approximately 2.3 kN.

Godwin (1982) proposed a wide range of instrumentation systems using the extended octagonal ring transducer to measure forces on various tillage tools and even on a specific parts of tools.

Smith and Barker (1982) constructed a dynamometer which used six commercial load cells mounted in a triangular pattern to measure the three orthogonal components of force between the tractor and implement. Three of the load cells were mounted at the vertices of the triangle to measure draught force. Two cells were mounted in the legs of the triangle to measure horizontal and vertical forces and one cell was mounted in the base of triangular pattern to measure only horizontal force. Thus it was possible to identify both the vertical and horizontal components of implement reaction. An inclinometer was mounted in the frame to sense the angular position of the tractor lower links. The implement was moved back by 190 mm.

Reid et al. (1983) designed a dynamometer using strain gauges mounted on vertically cantilevered aluminium beams to sense the implement forces, including side forces. Designed for use with Category I or II implements, it did not allow quick hitching. Gauges for the three sensing beams were placed in one bridge circuit so that the outputs were electrically summed. The single channel output was then proportional to total draught. With this dynamometer the hitch point was moved 130 mm to the rear.

Chung et al. (1983) listed the following criteria for their design of a dynamometer:

- ease of mounting,
- ability to measure three-dimensional forces,
- permits the use of a P.T.O. shaft,
- suitable for category II implements,
- minimum rearward implement displacement,
- economy,
- simplicity.

They equipped a propriety quick-attaching hitch with strain-gauged pins set in a "strain beam" to measure the three force components on each lower link pin of a three-point hitch. The top link pin was equipped with gauges to measure force in only one direction. The hitch point was extended 210 mm.

Upadhyaya et al. (1985) mounted strain gauges directly on the hitch links to measure draught and vertical forces for three-point hitch mounted implements. They attempted to assess a force system of the three-point linkage system for either symmetric or asymmetric implements in both a free and restrained link modes.

O'Dogherty (1986) designed a dynamometer to measure three orthogonal forces independently acting on soil working components in a soil bin. The design consisted of four beams to which were attached strain gauges arranged in three bridges. The dynamometer showed a linear response of output voltage to applied force, and the hysteresis was within acceptable limits. The sensitivities of the draught and vertical force bridges were 0.0396 and 0.0416 mV $kN^{-1}V^{-1}$, respectively, whereas the calculated sensitivities were 12 % less than the measured values. The sensitivity for the lateral force (measured as a moment) was 0.573 mV $kN^{-1}m^{-1}V^{-1}$. He found that the interactions between the bridges were generally less than 2 %.

Chaplin et al. (1987) designed a frame type three-point linkage dynamometer to measure the implement forces on tractors with Category II and III. They used, initially, an instrumentation similar to that of Johnson and Voorhees (1979), and later rejected it due to it not allowing measurement of side force component, and the effect of a large moment about the top link by large implements. A rectangular frame arrangement used six load cells to measure all components of draught. The frame was susceptible to shock loads during transport due to the large moments imposed on the top link by large mounted implements. A clamp to lock the two sub frame assemblies was required to protect the dynamometer during equipment transport. The instrument was accurate to within 5 % for draught forces between 5 kN to 45 kN; below this greater errors occurred. The dynamometer hung extra bulky load on the tractor and shifted the implements approximately 300 mm backwards.

Garner et al. (1988) constructed a three-point linkage dynamometer originally designed by Johnson and Voorhees (1979). They used a strain gauged steel tube as a sensing element instead of an aluminium one.

Thomson and Shinners (1989) developed a frame type dynamometer system to measure draught force for trailed or mounted implements. The dynamometer employed two A-shaped sub-frames and three Strainsert strain gauge (clevis pin) load cells which interconnected the frames. The frames were bulky and caused a rearward displacement of 240 mm of the implement from the original hitch location.

Godwin et al. (1993) designed a dynamometer to measure the forces and moments acting on a full-size tillage implement components for use both in a soil bin and in the field. The dynamometer consists of two extended octagonal ring transducers mounted with their axes at right angles and a torque tube. The instrument is capable of measuring the three orthogonal forces acting on the implement and three moments acting about the orthogonal axes.

McLaughlin et al. (1993) developed an instrumentation and data logging system to monitor tractor and implement performance in the field. They modified the three-point links in order to accommodate strain-gauge load cells for measurement of axial forces in the links. A mathematical model was develop to calculate the three-point hitch geometry from the angular position of the rock shaft.

2.4. Implement Draught Predictions

Zoz (1972) developed a graphical method of predicting tractor field performance for agricultural machinery decisions based upon tyre performance criteria. This procedure considers the effects of engine power, ground speed, rolling resistance, ballast or added weight, and type of implement hitch on the dynamic weight shift from the front to the rear axle. It predicts drawbar pull, drawbar power, travel speed, and travel reduction of a 2WD tractor. in either firm, tilled, or soft field conditions and concrete. The method is limited to 2WD tractors with single tyres.

Gee-Clough (1980) used the empirical equations found at Silsoe Research Institute (SRI) to make a choice of tyre sizes for off-road vehicles. However, the results provided by these equations were far from practical values, and made estimations within a wide range. Therefore, based on this procedure many tests of several makes of tyres of each size were carried out in a wide range of field conditions (Dwyer and Febo, 1987).

Witney and Oskoui (1982) considered the feasibility of a comprehensive computer model for the selection of economically-viable tractor-plough combinations by predicting traction, plough draught and available work days for a given climate and soil type within a machinery, labour and timeliness penalty cost framework. They emphasised that tractor power was determined by the heavy draught work on soil tillage for arable crops, and the weight of the tractor and implement and tillage method chosen interacted with the soil type in order to determine not only the traction available but also the draught required.

Hunt (1983) presented the draught, power, and energy requirements for some field machines. The values given were cursory for any individual operation ignoring soil and tine specifications. In addition, the values had a wide range for a single operation. For example, the draught for chiselling at 0.18 to 0.23 m depths varies between 2.9 to 13.1 kN per unit width. The ratio of the upper to the lower limit is almost five. Zoz (1972) which is concerned with the tractor selection and Hunt (1983) were combined and presented as ASAE Standard.

Zoz (1987) developed Lotus templates to predict tractor performance and ballast requirements on soil and concrete. Prediction included tractor performance for 2WD or 4WD. The templates have two calculation modes; "Performance" and "Weight". In the "Performance" mode, the static front and rear weights along with defined soil and tyre parameters are used to calculate slip and drawbar pull values. In the "Weight" mode, a

specified slip and percentage of the dynamic weight remaining on the front axle are used to calculate the static front and rear weights and the drawbar performance values.

Witney (1988) developed a graphical method to estimate the power requirement of the various characteristics of a particular plough. It can be also used to obtain an estimate of the tractor drawbar and engine power considering the working speed, plough type, number of plough bodies, soil condition, working depth and width and tractive efficiency. However, it is limited to mouldboard plough. Furthermore, the prediction chart appears to be incorrect particularly for the ploughing resistance and gives unexpected predictions.

Grisso at al. (1992) proposed Lotus templates similar to that of Zoz (1987).

2.5. Chapter Summary

This chapter has given an extensive review of literature related to the aims and objectives and the concept employed in the present study.

The major emphasis in previous tine studies has been directed towards force assessment and prediction, and to defining the general soil disturbance pattern and major soil failure planes. It can be concluded from previous work that changes in the nature of soil failure occur with changing tine working depth and soil conditions. The models evaluated so far require cohesion (c) and angle of internal shearing resistance (ϕ) data which are not easy to obtain especially in remote areas under the field conditions. Therefore, the models can work well if this data are provided. Any new approach should be aware of the need for measuring c and ϕ,. Such a method assuming that draught is a final production of the combination of the implement geometry and soil strength factor is described in detail in the next chapter.

The second major conclusion from previous work is that an effective three-point linkage dynamometer having some advantages over frame type ones is an essential research tool for evaluating the relationship between soil and an implement which is integrally mounted on to the tractor. This is a need for a wide range of people which extends from engineers designing tractors and implements to the ultimate user, the farmer. Current three-point linkage dynamometers require extensive modifications and can cause some problems so that the implement moves back from original position, or the system is bulky and not practical. However, the extended octagonal ring transducer similar to that proposed by Godwin (1975) is one of the most common sensing units. In addition, to date, no application of the extended octagonal ring transducer as a three-point linkage dynamometer has been available at Silsoe College for tillage studies. The dynamometers are also not capable of sensing the linkage position. Furthermore, no attempt has been made to use the top link as a transducer.

The current draught prediction models provide a global approach giving prediction over a wide range and are not descriptive for any individual operations. Hence, these models cannot be used for acute mechanisation planning works. However, if the concept mentioned earlier predicts the draught requirements of the implements within an acceptable limits the model can be used for predicting the draught forces of the tillage implements in a particular area.

3. CONCEPT AND OUTLINES

There are four main constituents of soil: mineral matter, organic matter, air and water which make the soil very complex. Therefore, agricultural soil is heterogeneous. The characteristics of soil, even in the same field, vary from place to place depending on these basic components. Thus, it is difficult to describe the soil characteristics for particular field. Many of the existing models predicting the soil forces upon the tine are either too complex or far from practicality due to the values of the cohesion (c) and angle of internal shearing resistance (ϕ) data which are not easy to obtain under field conditions. However, some models, such as the model of Godwin and Spoor (1977), could provide a reasonable approach for soil-tine interactions if the main parameters in the model are examined cautiously. Basically, these parameters are reflected from two main sources viz. soil and tine geometry.

Godwin and Spoor (1977) proposed a force prediction model to describe the three-dimensional soil failure for the narrow tine above the critical depth i.e. where only soil loosening takes place (Fig. 5). The draught force can be given as follows:

$$D = \left[\gamma d^2 N_\gamma + cdN_c + qdN_q\right]\left[w + md\sin\left(\cos^{-1}\left(\frac{\cot\alpha}{m}\right)\right)\right]\sin(\alpha+\delta) + c_a wd\left[N_a\sin(\alpha+\delta)+\cos\alpha\right] \quad [13]$$

where

D = horizontal or draught force [kN],

γ = soil bulk density [kN/m^3],

δ = angle of soil – interface friction [deg],

c = cohesion [kN/m^2],

c_a = soil – interface adhesion [kN/m^2],

q = surcharge pressure [kN/m^2],

N = dimensionless number [N_γ, N_c, N_q, N_a],

m = rupture distance ratio,

w = width of tine [m],

α = rake angle from the forward horizontal [deg],

d = depth of tine [m].

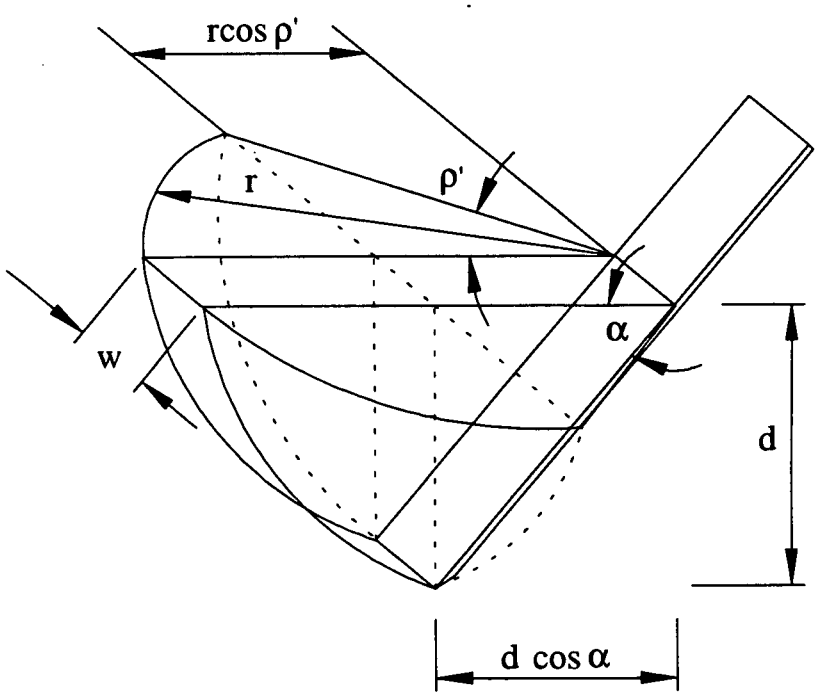

Figure 5. Three-dimensional failure wedge in front of a single narrow tine for depths less than critical depth (Godwin and Spoor, 1977)

However, under the non-adhesive and non-surcharged soil conditions, i.e. reference soil conditions, c_a and q are not relevant. In this case, equation [13] can be written as follows:

$$D = \left[\gamma d^2 N_\gamma + cdN_c\right]\left[w + md\sin\left(\cos^{-1}\left(\frac{\cot\alpha}{m}\right)\right)\right]\sin(\alpha+\delta) \qquad [14]$$

This was later modified by Godwin et al. (1984) to

$$D = \left[\gamma dN_\gamma + cdN_{ca} + qdN_q\right]\left[\left[w + d\left(m - \frac{1}{3}(m-1)\right)\right]\sin(\alpha+\delta)\right] \qquad [15]$$

where the cohesive and adhesive N factors have been combined into N_{ca} after Hettiaratchi and Reece (1974).

When loosening a compacted sandy-loam soil of no adhesion, formula [14] has been expressed by Desbiolles (1994) for a simple, tine assuming that there is no major difference between equations [14] and [15], as follows:

$$D = \left[\left(\gamma\, dN_\gamma + cN_c\right)(\sin\delta + \cos\delta)d\right]\left[\left[w + md\sin\left(\cos^{-1}\left(\frac{\cot\alpha}{m}\right)\right)\right]\cos\alpha\right] \qquad [16]$$

In equation [16], γ, c, δ, N_γ and N_C are all soil characteristics related to the dynamic performance of the implement, while w, m and α are the characteristics of the tine geometry.

Thus, equations [14] and [15] can be split into two main components. These can be given as follows:

$$D = Soil\ Strength\ Factor\ (SSF) \times Tine\ Geometrical\ Factor\ (TGF) \qquad [17]$$

where

$$SSF = \left[\left(\gamma\, dN_\gamma + cN_c\right)(\sin\delta + \cos\delta)d\right] \qquad [18]$$

$$TGF = \left[\left(w + md\sin\left(\cos^{-1}\left(\frac{\cot\alpha}{m}\right)\right)\right)\cos\alpha\right] \qquad [19]$$

The Soil Strength Factor (SSF, kN/m) represents a bulk specific resistance as a function of the tine depth (d). However, the Tine Geometrical Factor (TGF, m) describes an overall effective length which is also dependent the tine depth (d). The tine geometrical factor can be rewritten as given below:

$$\sin\alpha = \cos\alpha \ (\text{for } 45^\circ) \text{ i.e. } \sin(\alpha + \delta) = \frac{1}{\sqrt{2}}(\sin\delta + \cos\delta)$$

$$TGF = [0.7071w + 1.2247d] \qquad [20]$$

The soil strength factor (SSF) is calculated from the following equation after measuring the draught force ($D_{S.Tine}$) of a simple 45° raked angle tine (called Standard Tine (ST)) in soil-bin conditions.

$$SSF = \frac{D_{S.Tine}}{GF_{S.Tine}} = \frac{D_{S.Tine}}{(0.7071w + 1.2247d)} \qquad [21]$$

where

SSF = soil strength factor
$D_{S.Tine}$ = draught for standard tine
$GF_{S.Tine}$ = geometrical factor for standard tine
w = width of standard tine
d = working depth of standard tine

With these two parameters determined, the concept can be used to estimate the force for a range of tillage tools and implements. The geometrical factor for tools GF_{Tool} can be calculated from either equation [20] or the tests conducted in soil-bin. In this study GF_{Tool} were determined from soil-bin tests. The same geometrical factor can also be used for an implement having a single-tine on its own frame. The geometrical factor is corrected for a multiple-tined implement using the approach developed by Godwin et al. (1984).

Therefore, the force required for an implement can be predicted through comparing its equivalent width, with that of the standard tine.

Having predicted the forces acting upon tillage implements the error called prediction error between the predicted draught and measured will come naturally. The prediction error is calculated by using the equation [22].

$$Prediction\ Error\ [\%] = \frac{\left(D_{Predicted} - D_{Measured}\right)}{D_{Measured}} \times 100 \qquad [22]$$

There are two main points which should be looked into as an extension of the concept: 1-applicability of the geometrical factor to the similar implements; 2-implementation of the soil strength factor to similar field conditions.

The next stage should be to make the prediction results meaningful for future works such as mechanisation planning. Thus, this idea is based on the ratio of either draught force or geometrical factor of the single unit (tool) of the implement to the standard tine. This can be presented for the ideal condition as below:

$$I = \frac{D_{Tool}}{D_{S.Tine}} = \frac{SSF \times GF_{Tool}}{SSF \times GF_{S.Tine}} = \frac{GF_{Tool}}{GF_{S.Tine}} \qquad [23]$$

where

I = index
D_{Tool} = draught for tool
$D_{S.Tine}$ = draught for standard tine
SSF = soil strength factor
GF_{Tool} = geometrical factor for tool
$GF_{S.Tine}$ = geometrical factor for standard tine

Inevitably, there will be a difference between the ratio of the tool geometrical factor to the tine and the ratio of the tool draught to the tine. Therefore, two different index values should be investigated. The error between these index values will reflect how much the standard tine represents the implements as a reference tine. Thus, the indexes expressed as presented below:

$$I_{GF} = \frac{GF_{Tool}}{GF_{S.Tine}} \neq I_D = \frac{D_{Tool}}{D_{S.Tine}} \qquad [24]$$

where

I_{GF} = Index based on geometrical factor
I_D = Index based on measured draught force

The general outline of the study conducted at Silsoe College by Desbiolles (1994) and the author is described in Figure 6. The first stage which is shown in the dashed frame is within the area worked by Desbiolles (1994). The dotted rectangular boxes define the experiments carried out by Desbiolles (1994) in the soil-bin. The second stage, which is an extension of the first, is conducted by the author in this study.

The prediction procedure in the second stage of the study can be described as given below:

1. Measure the draught force acting upon the standard tine,
2. Determine the soil strength factor (*SSF*) for the field from equation [21],
3. Predict the force requirements of the implements at an operating depth range from the equation $D_{Tool} = SSF \times GF_{Tool}$ using tool geometrical factors from Desbiolles (1994).

To achieve the main objective in this study the following stages were proposed:

1. To design and build a three point-linkage dynamometer,
2. To develop software to calculate the resultant, horizontal and vertical forces,
3. To conduct field tests in order to measure the forces acting upon the implement,
4. To compare the prediction results with the current methods for a particular area like GAP region.

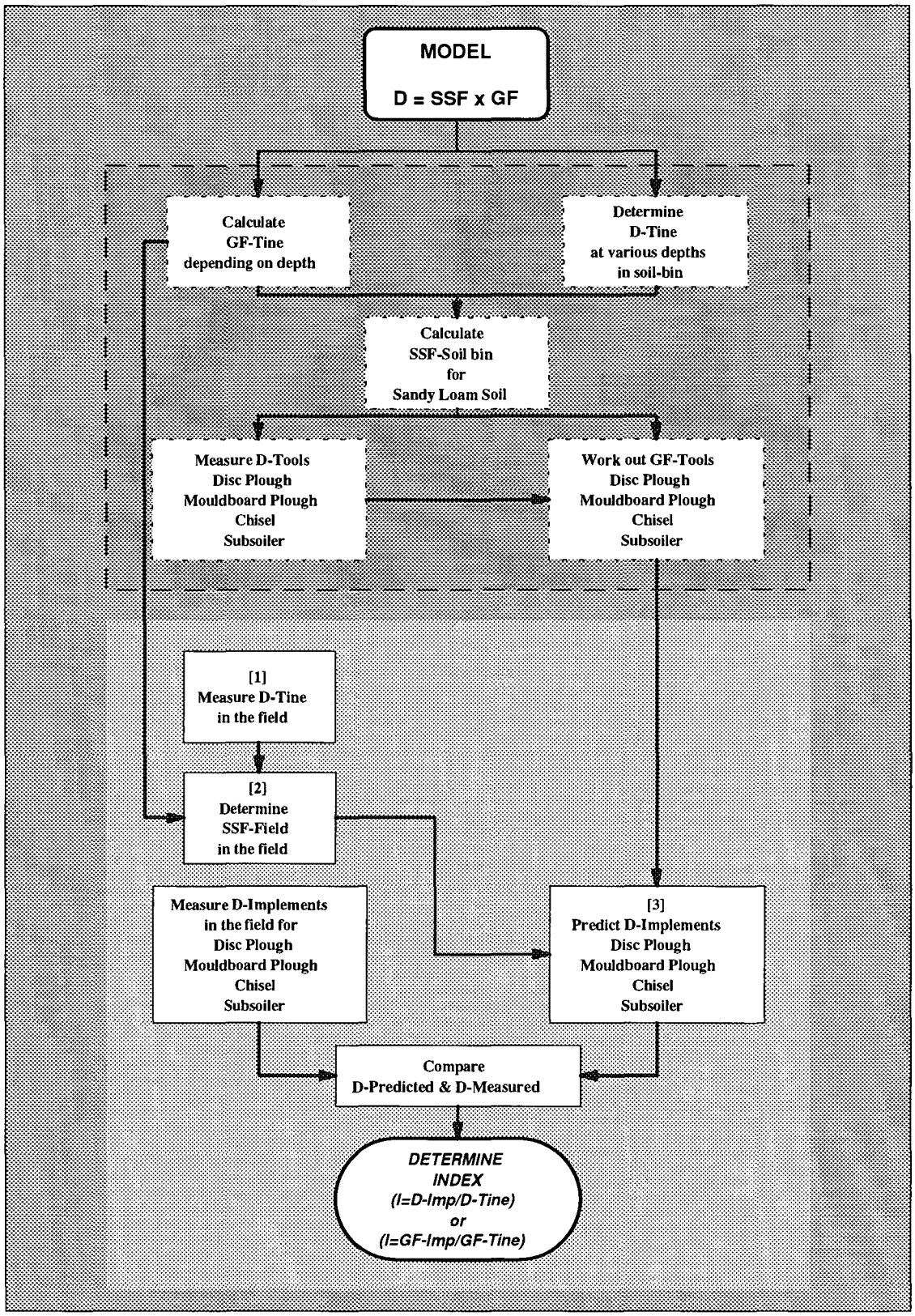

Figure 6. Block diagram of the study conducted in Silsoe College

A WORKED EXAMPLE OF THE KIRISCI MODEL

Primary Features	Example	From
Implement	: Chisel with 5 tines	Implement
Working depth	: 0.30 m	Desired depth
Soil type	: Sandy loam	Field
$GF_{S.Tine}$ at 0.30 m depth	: 0.42 m	Table 22
Draught for Standard tine ($D_{S.Tine}$)	: 5 kN	Table 20
GF_{Tool} at 0.30 m depth	: 0.46 m	Table 22
Interactions between the chisel tines	: 25 %	Godwin et.al. model 1984

Calculate

Geometrical Factor for the implement at 0.30 m depth:

GF_{Imp} = (GF_{Tool} x Number of tines) / Interaction effect

GF_{Imp} = (0.46 x 5) / 1.25

GF_{Imp} = 1.84 m

Soil Strength Factor for Sandy Loam Soil at 0.30 m depth

SSF = $D_{S.Tine}$ / $GF_{S.Tine}$

SSF = 5 / 0.42

SSF = 11.9 kN/m

Calculate the predicetd draught force required by the implement

D_{imp} = SSF x GF

D_{imp} = 11.9 x 1.84

D_{imp} = 22 kN

4. MATERIALS AND METHODS

4.1. Introduction

This chapter presents the detailed information about the tractor force system for the mounted implements which is essential for the design of three-point linkage dynamometers. The design considerations for the dynamometer are also given. The gauging, calibration procedure of transducers, and results are reported. The data processing system is described. In this chapter the second stage of the study outlined in Figure 6 is described in detail. The chapter is also aimed at defining the fields on which experiments were conducted both in UK and Türkiye presenting general soil characteristics. In addition, the specification of the implements employed in the field tests in both UK and Türkiye are presented.

4.2. Tractor Force System for Mounted Implements

The success of a three-point linkage dynamometer depends on an accurate knowledge of the geometry of the linkage. In operation at a depth and constant speed a simple tillage tool or implement, as shown in Figure 7, is subjected to soil forces. The resultant of soil forces has two major components *H* and *V* in XY-plane. The power unit should produce enough force, equal and opposite to the resultant of soil force, to be able to pull the implement.

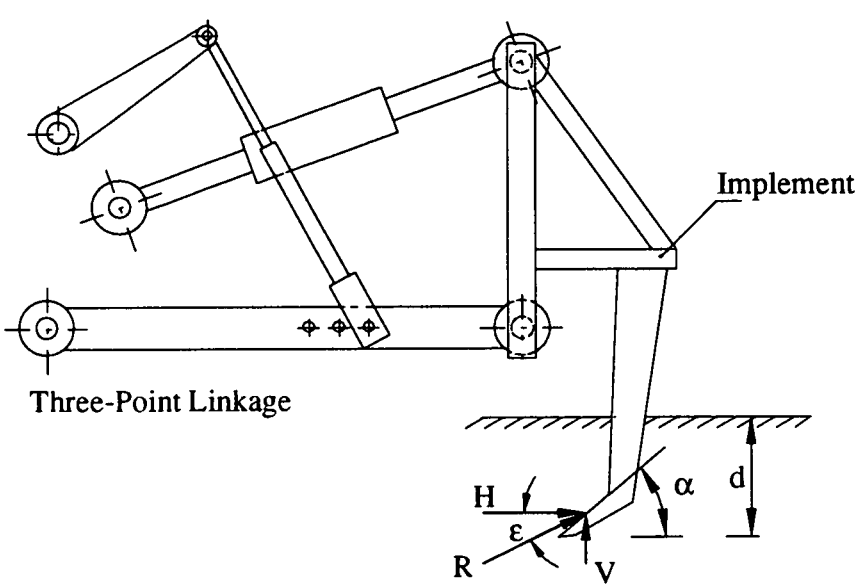

Figure 7. The forces acting upon a tillage implement

The force system between a tractor and mounted implement is much more complex than between a tractor and trailed implements due to the nature of the attachment system. Figure 8 shows the resultant exerted by a mounted implement on a conventional three-point linkage system. This force has components in all the major planes of the tractor assuming that the tractor is working along a horizontal plane surface. Therefore, the force can be resolved into three components *H*, *V*, and *L*, which are parallel to the major axes of the tractor.

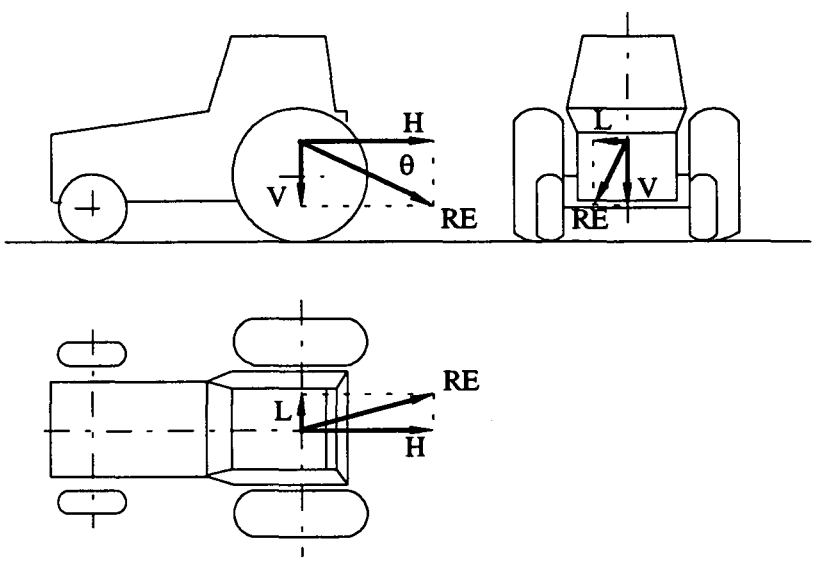

Figure 8. Forces acting between a tractor and mounted implement

The component *H* is that the main part of the resultant which is parallel to the direction of travel, and, generally, this is assumed as the draught of implement. This force should be measured to determine the traction required from the tractor. The vertical component, *V*, is the second important part of the resultant. It has the effect of adding load to the tractor rear wheels, and removing load from the front wheels. It also determines the implement penetration ability, and maintains depth as well as having the effect on the draught of the implement because of the friction forces associated with it. Finally, the side force, *L*, exists only in the case of using asymmetrical implements. It causes some stability problems for either or both tractor and implement, and increases the draught of the implement because of the friction produced. However, this force is non-existent for a symmetrical implement which are much more common, and can be neglected since it is quite small (Lal, 1959; Kilgour et al., 1988).

The force system between a tractor and implement can be also given as a resultant of the sub-component forces acting upon two tractor lower links and top link (Fig. 9).

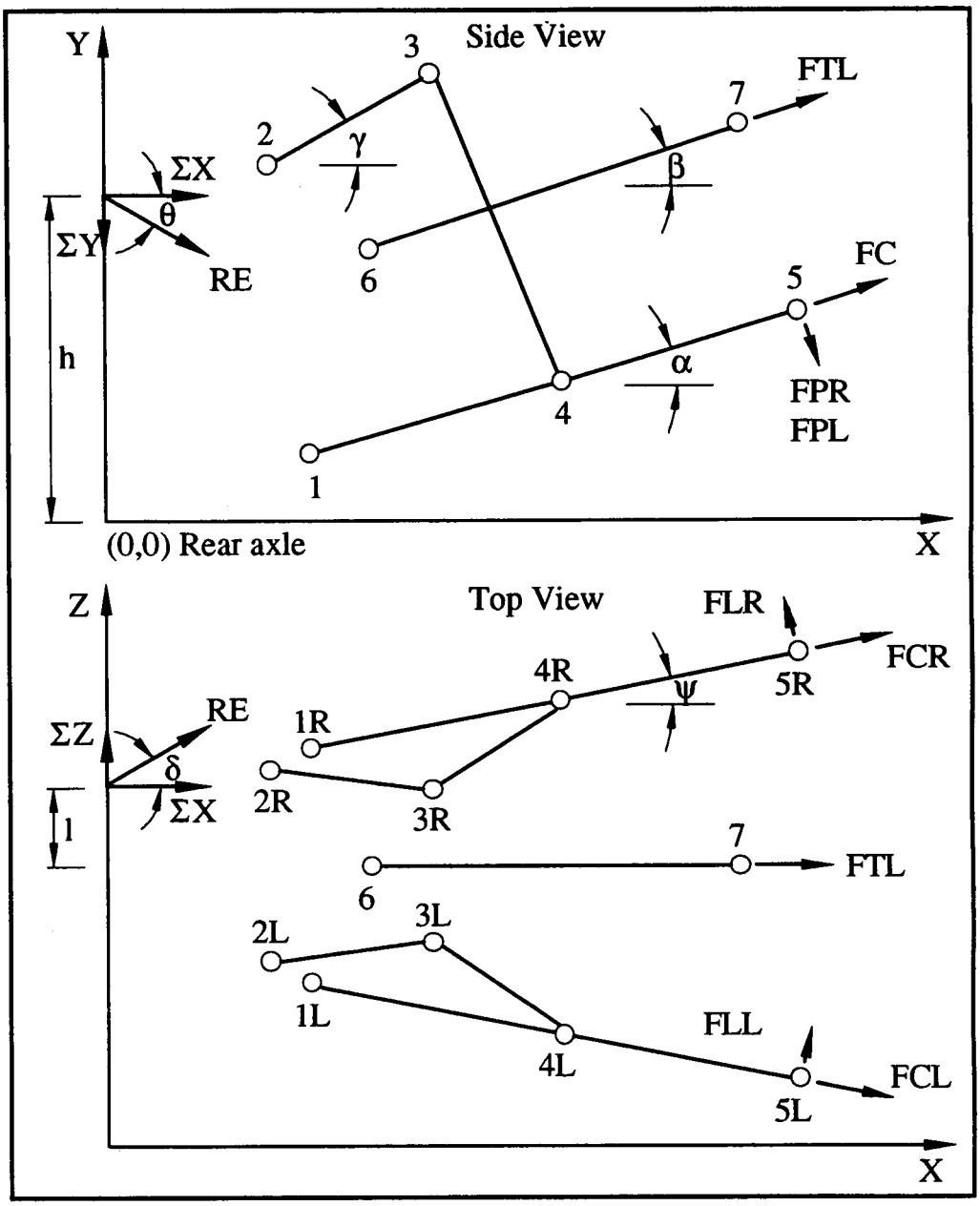

Figure 9. Force system for a three-point linkage system in XY and XZ-Planes

The resolution followed is based on three angles which are the angle of the lower links in the XY-plane (α), the angle of the top link (β), and the angle of the lower links in the XZ-plane (ψ). Numbers 1, 2 and 6 refer to pin joints to attach to the tractor while 5 and 6 to the implement.

The relative position of all the pin joints and angles can be calculated by using the cross-shaft angle (Kilgour et al., 1988). The tractor rear axle and centre line are the main references to define each joint position. The forces on the links are either compressive or tensile depending on the position of the three-point linkage.

Both the angle of lower links in the XY-plane (α) and top link angle (β) play the greatest role while the angle of lower links in the XZ-plane is less important. This angle remains constant when a quick-attach coupler is used. Normally, it varies from 10 to15° (Bandy et al., 1985).

The definitions used and assumptions made are presented in Table 7. The resultant (*RE*) is a vectored summation of its major components which are Σ*X*, Σ*Y* and Σ*Z* which must be known. However, Σ*X* and Σ*Y* include the total forces of *FX* or *FY* in the lower links and *FTL*'s component in the top link with a mounted implement on a three-point linkage system.

As the magnitude of the lateral force exerted by asymmetrical implements on the three-point linkage has been neglected as being small, the resultant (*RE*) in XY-Planes can be expressed ignoring the lateral force components in a two-dimensional system instead of a three-dimensional system.

In this case, the resultant (*RE*) can be calculated as:

$$RE = \sqrt{[(\Sigma X^2)+(\Sigma Y^2)]} \qquad [25]$$

Also, the angle (θ) of the resultant in the XY-Plane can be expressed as:

$$\theta = \arctan\left(\frac{\Sigma Y}{\Sigma X}\right) \qquad [26]$$

The resultant found in Equation [25] represents the resolution of all components exerted on the three-point linkage into one single force, oriented at an angle (θ), and acting at a distance (*a*) from the rear axle (Fig. 10).

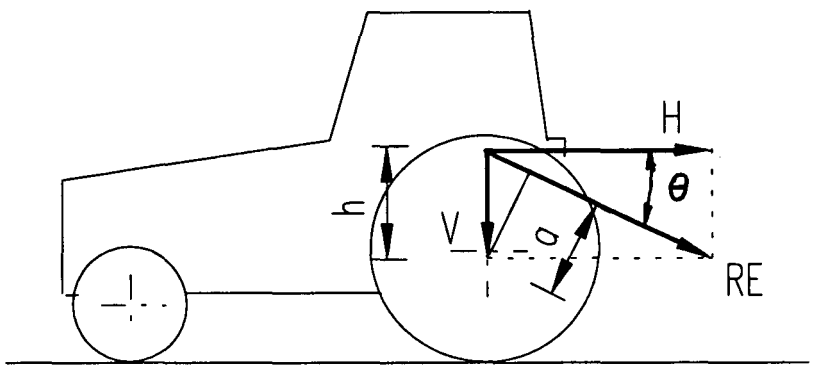

Figure 10. The position of resultant about rear axle

More information about the procedure to determine the force system is presented in Appendix 1.

Table 7. Variables Used and Assumptions Made in Force Resolution Procedure

α	Angle of lower links with respect to horizontal plane in XY-plane
β	Angle of top link with respect to horizontal plane in XY-plane
ψ	Angle of lower links with respect to the tractor centre line in XY-plane
θ	Angle of resultant in XY-plane
δ	Angle of resultant in XZ-plane
γ	Angle of cross-shaft with respect to horizontal plane in XY-plane
RE	Magnitude of resultant in XYZ-planes
ΣX	Total forces in X-direction (Draught force)
ΣY	Total forces in Y-direction (Vertical force)
ΣZ	Total forces in Z-direction (Lateral force)
FX	Total forces on lower links in X-direction
FY	Total forces on lower links in Y-direction
FZ	Total forces on lower links in Z- direction
FXR	Total forces on right lower link in X-direction
FXL	Total forces on left lower link in X-direction
FYR	Total forces on right lower link in Y-direction
FYL	Total forces on left lower link in Y-direction
FZR	Total forces on right lower link in Z-direction
FZL	Total forces on left lower link in Z-direction
FCR	Coincident force to right lower link in XY-plane (tension = +)
FCL	Coincident force to left lower link in XY-plane (tension = +)
FPR	Perpendicular force to right lower link in XY-plane (down = +)
FPL	Perpendicular force to left lower link in XY-plane (down = +)
FLR	Lateral force to right lower link in XZ-plane (right = +)
FLL	Lateral force to right lower link in XZ-plane (right = +)
FTL	Top link force (tension = +)
h	Height of resultant in XY-plane (right = +)
l	Lateral distance of resultant from tractor centre line
a	Moment arm which is a distance from tractor rear axle

4.3. Linkage Dynamometer

4.3.1. Design and Construction

The dynamometer is first proposed for the MB-trac 1 300 tractor which is available for tillage studies at Silsoe College. Later, the system was slightly changed for Ford 6410 2WD tractor due to the technical difficulties in finding the spare lower and top links for the MB-trac 1 300 tractor that has a category II and III linkage. However, the dynamometer can be fitted to any type of Ford which has a category II linkage. The Ford 6610 4WD, therefore, that has been widely used in Türkiye, is taken as an experimental tractor for the field tests in Türkiye. Technical data for the tractors is given Table 8.

Table 8. Some Technical Specifications for the Tractors Used

Technical data	MB-1 300 trac	Ford 6410 2WD	Ford 6610 4WD
Engine			
Size (cc)	5 958	4 393	4 393
Max. Power (kW)	92	63.3	63.3
Weights			
Max front axle (kN)	6	-	1.4
Max rear axle (kN)	6.5	-	2.4
Total (kN)	6.3	4	3.8
Tyres			
Front	18.4-30	13.6-24	13.6-24
Rear	18.4-30	16.9-34	16.9-34
Linkage category	II and III	II	II

The sensing elements used in the three-point linkage dynamometer are shown in Table 9 and Figure 11.

4.3.2. Lower Link Transducers

There are different ways of sensing the force exerted in the lower link. The strain gauges may be fixed directly to the link but calibration and cross-sensitivity can be a problem (Kilgour et al., 1988; Kirişci et al., 1993).

Table 9. Sensing Elements Used on the Three-Point Linkage Dynamometer

Sensor	To sense
Bi-axial LEORT for	
Left Lower Link	
Bridge I	Perpendicular Force (*FPL*)
Bridge II	Coincident Forces (*FCL*)
Right Lower Link	
Bridge I	Perpendicular Force (*FPR*)
Bridge II	Coincident Forces (*FCR*)
Modified Top Link	Top Link Force (*FTL*)
Rotary Position Transducer	Cross-Shaft Angle (*CSA*,γ)

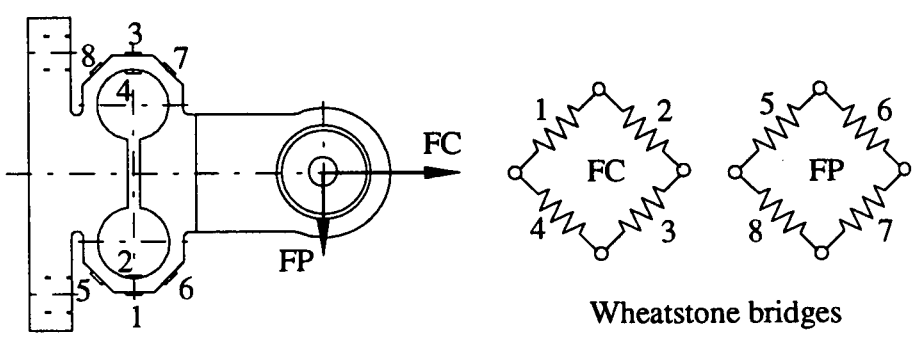

a) Bi-axial Extended Octagonal Ring Transducer (EORT)

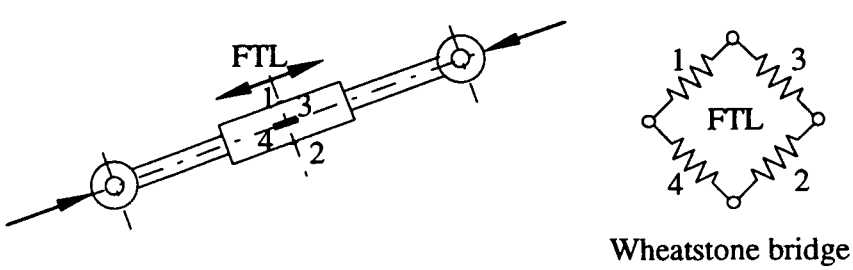

b) Modified Top Link

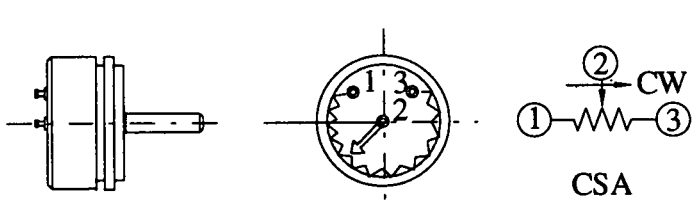

c) Rotary Position Transducer

Figure 11. Sensing elements used in the dynamometer system

To monitor the forces in the lower links an Extended Octagonal Ring Transducer (EORT) is one of the most common ways. Rings were originally developed by Cook in 1951 (Cook and Rabinowicz, 1963). Circular or octagonal rings have been used in a different way for force measurement for many years.

An extended octagonal ring is a common application of rings particularly an octagonal ring extended by $2L$ to gain stability and approximately to meet the requirement of zero rotation of the top surface. O'Dogherty (1975) and Godwin (1975) both described and designed EORTs to monitor the forces for different purposes. The design of Godwin (1975) has been successfully used in the study of farm machinery at Silsoe College for many years. In this study, the sensing elements in the lower links (Fig. 11a) are a different application of Godwin's EORT, and are similar to that proposed by Kilgour et al. (1988).

The maximum force through the lower link arms is assumed as the maximum pull exerted by the tractor which is 75 % of the tractor weight multiplied by a safety factor of three.

So, the design specification is as follows:

$$\begin{aligned} \text{Weight} &= 70 \text{ kN} \\ \text{Max. pull} &= 70 \times 0.75 \\ \text{Safety factor} &= 3 \\ \text{Design force} &= (70 \times 0.75) \times 3 \\ &= 157.5 \text{ kN} \end{aligned}$$

This force acts through two lower links and hence two Extended Octagonal Rings (EORs). Thus, each ring should be designed to carry approximately a half of the design force (Fig. 12).

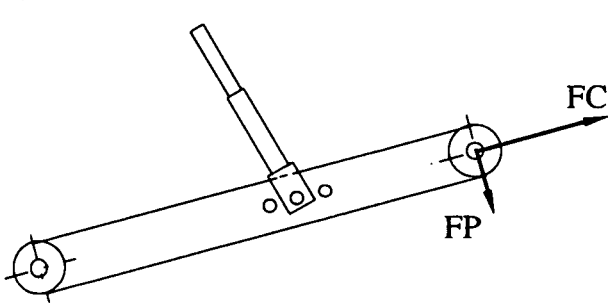

Figure 12. Forces exerted on a lower link

However, another assumption is made that the forces on each link are:

Max. coincident force (FC) $\cong$ 80 kN

Max. perpendicular force (FP) $\cong$ 40 kN

So, the resultant (RE) is going to be:

$$RE = \sqrt{(FC)^2 + (FP)^2} \Rightarrow RE = 89.4 \text{ kN} \quad [27]$$

The transducers were constructed from a solid block of pre hardened alloy mould steel that can be machined by normal workshop techniques. General specifications of the material used are shown in Table 10.

Table 10. Some Specifications of the Material Used for EOR

General							
Approximate analysis [%]	C 0.33	Si 0.3	Mn 0.8	Cr 1.8	Ni 0.9	Mo 0.2	S 0.008
Standard specification	AISI P20 Modified						
Delivery condition	Hardened and tempered to 290-330 HB						
Testing temperature	20°C						
Tensile strength [N/mm^2]	1 010						
Yield strength [N/mm^2]	800						
Reduction of area Z [%]	60						
Elongation as [%]	20						
Impact strength [kJ]	50						
Density [kg/m^3]	7 800						
Modulus of elasticity [N/mm^2]	205 000						
Material manufacturer	Uddeholm Impax Supreme						

(Source: Uddeholm catalogue)

To meet the design specifications the following theory developed for extended circular rings by Cook and Rabinowicz (1963) and Godwin (1975) were used (see Appendix 2).

$$\frac{\varepsilon E b t^2}{M} = 0.4 \text{ when } k = 1.6\left(=\frac{L}{r}\right) \text{ and } t = \sqrt{\frac{0.4M}{\varepsilon E b}} \quad [28]$$

where (Fig. 13)

ε = strain

E = modulus of elasticity

b = width of ring

t = ring thickness

M = applied moment

$2L$ = distance between ring centres

r = mean radius of ring

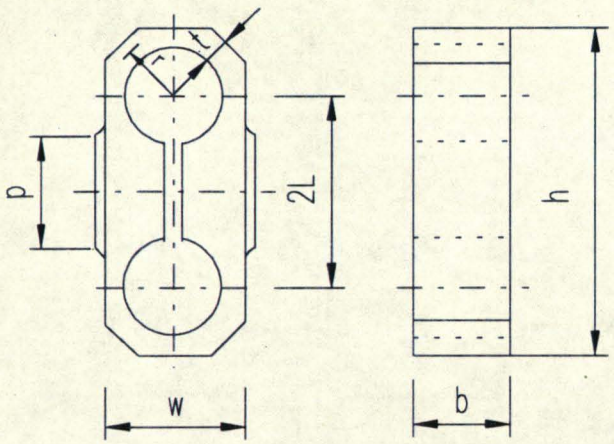

Figure 13. Basic dimensions of extended octagonal ring

It was assumed that the force was applied at a distance of 160 mm from the ring centre line. In this case, the bending moment (M) was:

$$M = FP \times x \times SF = 40\ 000 \times 160 \times 3 \Rightarrow M = 19.2 \text{ MNm} \qquad [29]$$

EORs were given a special shape so that the implement ball joints became an integral part of the linkage EOR. To make fewer modifications to the three-point linkage system, original swivel sets were used at the ball end of the rings. At the other end was a flange for two bolts fixing to the rest of the lower link (Plate 1). All calculations relating to the design of rings are given in Appendix 3.

Plate 1. Linkage Extended Octagonal Ring (EOR) and Top Link

The implement ends of the bottom links were cut off, and a pad welded on the links in such a way that the overall lengths and angles were not changed from the original dimensions (Plate 2). This modification can be easily made to other tractor linkages if required.

Plate 2. Modification on the Lower Links

4.3.3. Top Link Transducer

The turnbuckle of the original top link of Ford 6410 2WD was modified for the attachment of strain gauges to detect the force along the line of the top link keeping the dimensions the same as for the original (Fig. 11b and Plate 1). Thus, the top link is likely to fit a wide range of other tractors so this part of the dynamometer has universal application characteristics.

4.3.4. Linkage Position Indicator

The dynamometers sense the forces in directions relative to the linkage. To resolve the forces about the tractor rear axle completely, the angle of the link arms is required. The method used for ascertaining the angular position of the three-point linkage was by using a RS rotary position transducer (Fig. 11c). The transducer was fitted onto the tractor cross-shaft to sense the angle (γ).

The conductive plastic element on the transducer is rated at 1 *W* at 40°*C*. This rating is restricted to current passing between terminals 1 and 3 only of the potentiometer. The maximum permissible wiper current is 10 *mA*.

4.3.5. Instrumentation

Gauging

The sensing elements used in the two lower links are the linkage type extended octagonal ring. To be able to use them as a bi-axial transducer each one was equipped with two strain gauge bridge arrangements (Fig. 14): 1- Coincident force (*FC*) to the lower link; 2- Perpendicular force (*FP*) to the lower link. Consequently, *FC* and *FP* are two mutually perpendicular forces. From Godwin (1974) the two positions $\theta = 34^{o}$ and $\theta = 90^{o}$ were considered as the positions required of the strain nodes on the ring for each force, *FP* and *FC* respectively.

Each bridge consists of 4 active gauges for a Wheatstone full bridge. Each gauge has a resistance of 120 Ω. Gauges were selected, bonded and wired on to the ring following "*Student Manual for Strain Gage Technology*" published by Measurement Group. Due to the particular placement of the gauges on the LEOR the two mutually perpendicular forces can be measured with minimum of cross-sensitivity (Godwin, 1974). The bridge sensing *FC* was also configured as a differential cantilever i.e. it senses the force independent of its point of application.

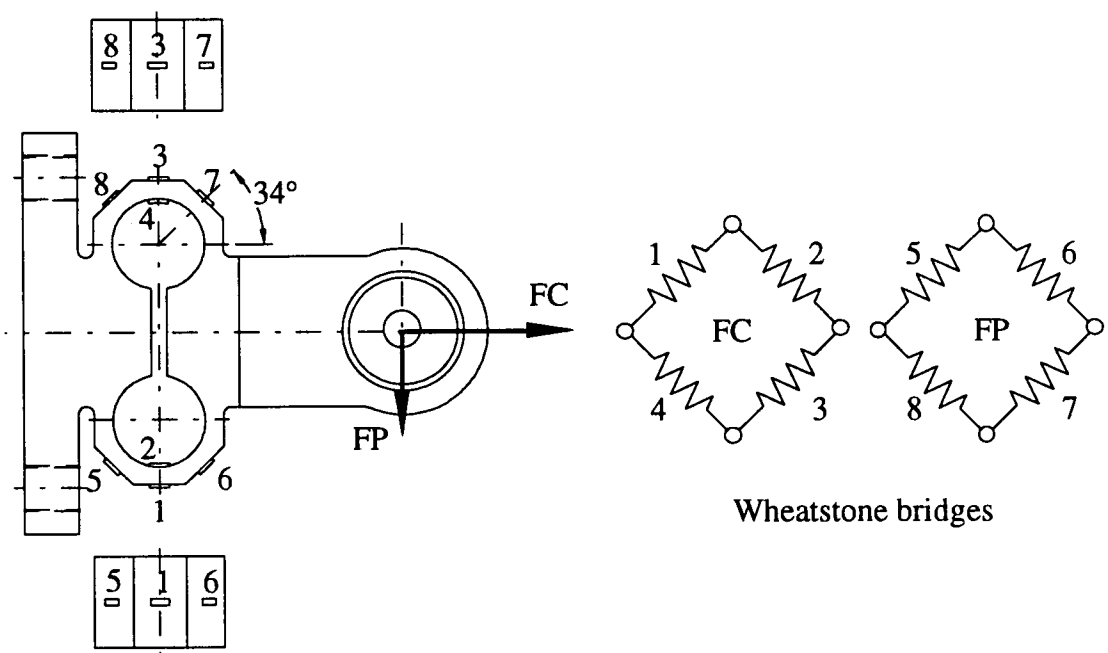

Figure 14. Bridge arrangements for LEOR

There was only one Wheatstone-bridge circuit to sense the force (*FTL*) on the top link. The stain gauges were connected in a "*Poission Arrangement*" (Perry and Lissner, 1962) as shown in Figure 15.

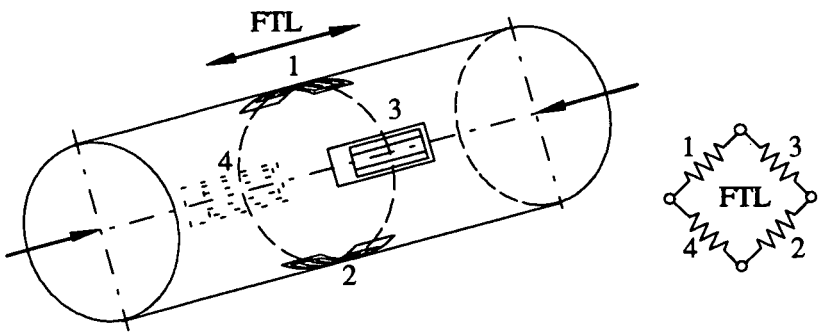

Turnbuckle of the top link Wheatstone bridge

Figure 15. Poisson arrangement on top link turnbuckle

In this arrangement, gauges 3 and 4 will be much more active in tension similarly gauge 1 and 2 in compression will actively sense the force. Each gauge has a resistance of 120 Ω in a full bridge.

The rotary position transducer was ready for direct application as a linkage position indicator.

Calibration Tests

All the transducers were calibrated to determine the following characteristics:

- sensitivity, which is the change in output from an instrument, or instrument component, per unit change at its input
- cross-sensitivity, which is the error in a non-active bridge while recording the active bridge
- hysteresis, which is the amount by which the output from an instrument, or instrument component, can differ at any point in its working range depending on the direction of change at its input
- linearity, which is the maximum deviation of any calibration point, obtained from the best straight line having overall minimum deviation obtained by using the coefficients of determination, R^2 (Steel and Torrie, 1980)
- repeatability, which is the variation in the results obtained when a measurement is repeated, under the same conditions as far as possible (Cox, 1988).

In the beginning, the LEORTs were calibrated statically for both horizontal and vertical loads by using a support frame and an Avery Test Machine (Rated to BS 1610) (Plate 3) with Digital Volt Meter (DVM) to provide some global information about the output of bridges on transducers.

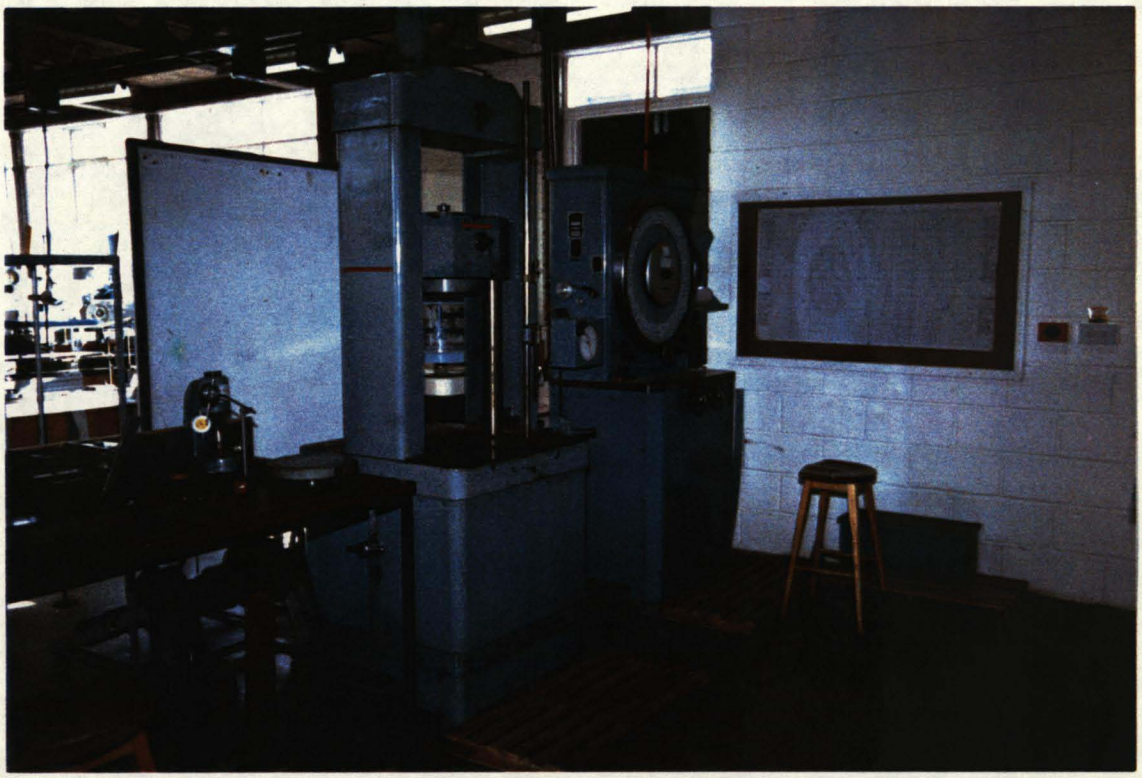

Plate 3. Avery Test Machine

The LEORTs were loaded to the working design limits which were 40 kN in the perpendicular direction and 80 kN in the coincident direction as shown in Figure 16a. During the calibration, the chosen direction was loaded while the other channel was monitored to determine signal output in this direction to determine the level of cross-sensitivity. The top link was also calibrated in tension and in compression by using the same system and loading up to 70 kN (Fig. 16b). Plate 4 shows the support frame and apparatus used for the calibration of LEORTs and the top link. Finally, the rotary position transducer was tested using a 360^{o} protractor and a pointer fitted on to the transducer's shaft for both clockwise and anti-clockwise as shown in Figure 16c. All tests were repeated three times to see how repeatable were the transducer calibrations.

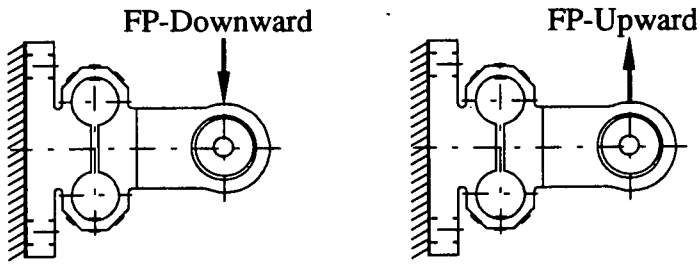

Perpendicular Force

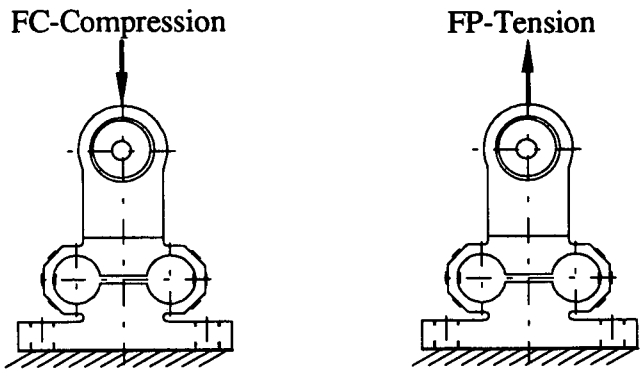

Coincident Force

a) LEORTs

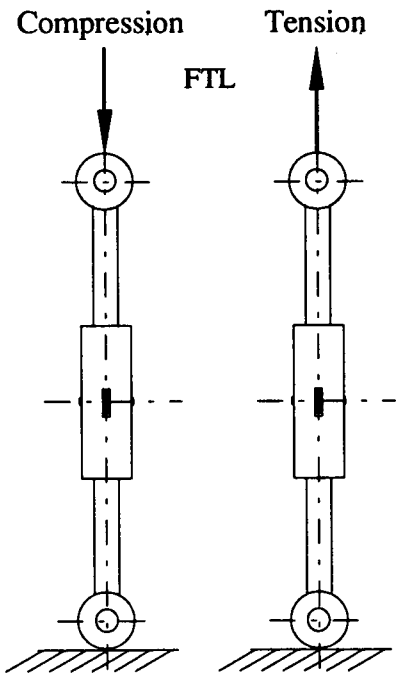

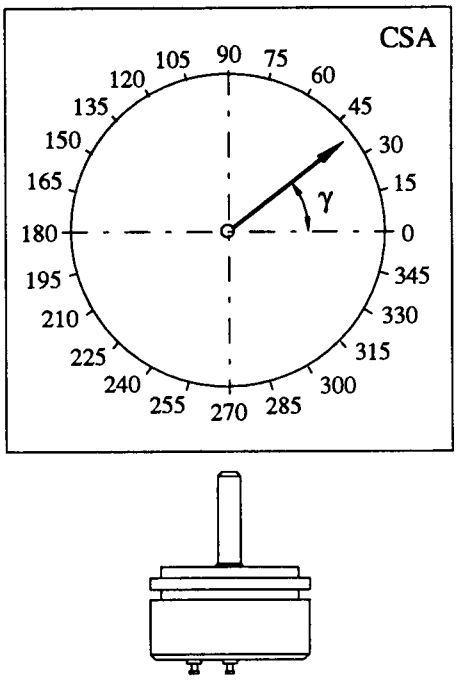

b) Top Link c) Rotary position transducer

Figure 16. Calibration procedure for transducers

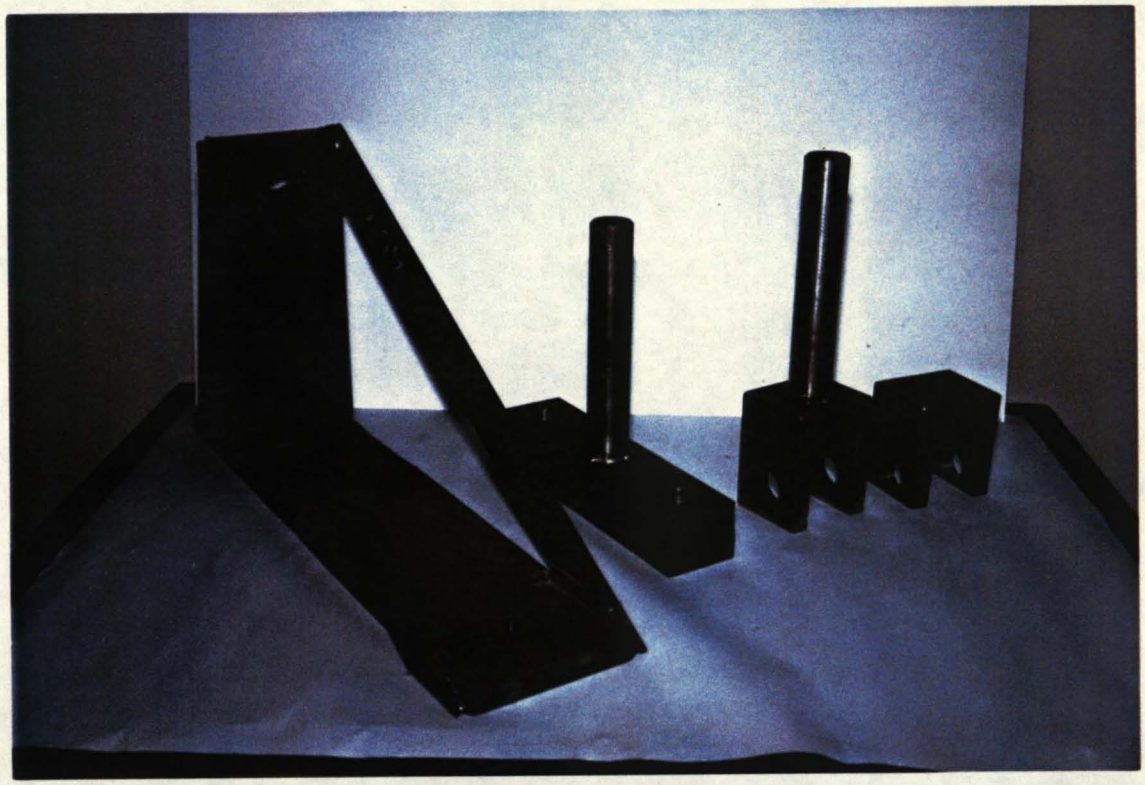

Plate 4. Support Frame and Apparatus Used with Avery Test Machine

The real tests similar to the above were conducted for the calibration of all six bridges on the four transducers, as given in Table 9, (*FCL* and *FPL* for the left lower linkage transducer; *FCR* and *FPR* for the right lower linkage transducer; *FTL* for the top link; *CSA* for the rotary position transducer) by using a datalogger. All bridges were connected in the datalogger instead of the Digital Volt Meter (DVM). LEORTs were loaded up to 18 kN in the perpendicular direction and 30 kN in the coincident direction assuming that these are actual working range expected in the tillage study. Correspondingly, the top link was calibrated in tension and in compression by using the same system and loading up to 70 kN. A Cambell Scientific 21x datalogger, as shown in Figure 17 which is the real set used for the rest of the study, was used for a variety of tasks in the system because it has a wide range of program instructions which gave it great versatility.

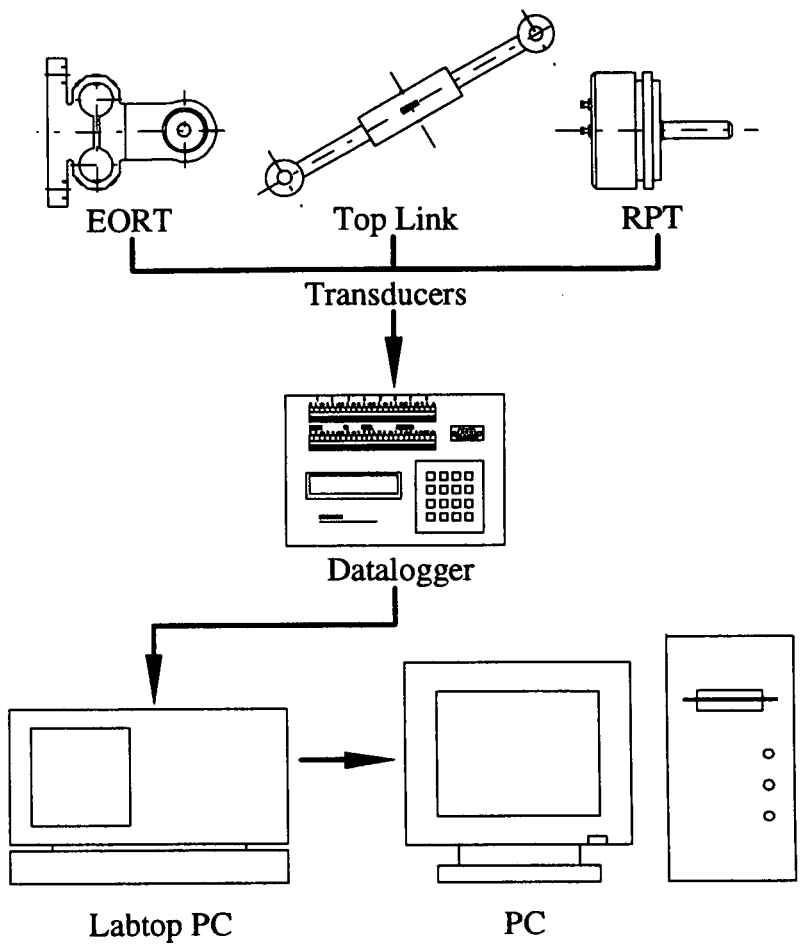

Figure 17. Instrumentation system

The excitation for the transducers was provided by the datalogger, which eliminated the need for bulky transducer amplifiers, bridge balancing equipment, and 240 V AC power supply. A program which is given in detail in Appendix 4, was developed for the datalogger which would record the data from the strain gauges. All strain gauge bridge outputs were sampled at a frequency of 1kHz using instruction "*23 Burst Measurement*", except for the CSA which was sampled at 10 Hz using instruction "*6 Full Bridge*". All bridges were zeroed with an offset command in the program itself. *23 Burst Measurement* instruction excited the bridges with 1.0 V, took an average every two seconds, recorded the data over a 1 hour time interval, and stored the output signal in milivolts. Similarly *6 Full Bridge* instruction excited the bridge with 5.0 V, took one single reading every two seconds, and stored the signal as datalogger number. Datalogger number was then converted into mV using the following equation [30]:

$$Output = \frac{DN \times Input\,Voltage}{1000} \qquad [30]$$

where

$Output$ = real output [mV]

DN = datalogger output [number]

$Input\ Voltage$ = excitation voltage [V]

After each test the average values were downloaded from the datalogger to an Amstrad PPC 640 portable computer and converted into an PRN file and manipulated as required using a PC. Calibration results for both DVM and Datalogger are presented in files on a 3 1/2" floppy disk attached, and summarised in Table 11. The results can be outlined as follows:

Rotary Position Transducer

The outputs were linear, with coefficients of determination, $R^2 > 0.999$.

The average sensitivity was 2.9350 $\mu V\ V^{-1}$ per degree while the sensitivities for clockwise and anti-clockwise directions were 2.9352 $\mu V\ V^{-1}$ per degree and 2.9349 $\mu V\ V^{-1}$ per degree, respectively.

The hysteresis error for the clockwise and anti-clockwise direction of the transducer's shaft was 0.024 % [f.s.].

The repeatability error was also small for both directions, 0.058 % [f.s.].

Modified Top Link

The outputs were linear, with coefficients of determination, $R^2 > 0.999$.

The average sensitivity was small, 0.010 $\mu V\ V^{-1}\ N^{-1}$ due to the top link material itself. However, it was independent of the direction of the load.

The hysteresis errors in compression and tension were 0.321 % [f.s.] and 1.006 % [f.s.], respectively.

The repeatability errors for both directions were 0.058 % [f.s.] and 0.668 % [f.s.], respectively.

Table 11. Transducer Calibration Results by Using Datalogger

Transducer	Sensitivity [μV V^{-1} N^{-1}]	Cross-Sensitivity [μV V^{-1} N^{-1}]	Hysteresis [% f.s.]	Linearity (R^2) [%]	Repeatability [% f.s.]
Rotary Position Transducer*					
Clockwise	2.935210**	-	-	0.999976	0.058
Anti-Clockwise	2.934852**	-	-	0.999978	0.058
Mean	2.935031**	-	0.024	0.999977	-
Top Link					
Compression	0.010354	-	0.321	0.999920	0.321
Tension	0.009964	-	1.006	0.999917	0.668
Mean	0.010159	-		0.999950	-
Left LEORT					
Perpendicular	0.075094	0.000211	-	0.999899	-
Downward	0.075470	-	0.294	0.999974	0.147
Upward	0.074717	-	0.447	0.999771	0.298
Coincident	0.063202	0.000300	-	0.999980	-
Compression	0.063201	-	0.052	0.999979	0.316
Tension	0.063204	-	0.105	0.999981	0.263
Right LEORT					
Perpendicular	0.073495	0.000305	-	0.999951	-
Downward	0.073521	-	0.529	0.999959	0.227
Upward	0.073470	-	0.757	0.999929	0.151
Coincident	0.062264	0.000991	-	0.999993	-
Compression	0.062366	-	0.053	0.999994	0.106
Tension	0.062162	-	0.107	0.999991	0.160

* It is calculated for a range of 0 ..... 330^{o}

**Sensitivity unit is [μV V^{-1} per degree]

Left-Extended Octagonal Ring Transducer (Left-LEORT)

The outputs were linear, with coefficients of determination, $R^2 > 0.999$.

The sensitivities of the perpendicular and coincident force bridges were 0.0751 $\mu V\ V^{-1}\ N^{-1}$ and 0.0632 $\mu V\ V^{-1}N^{-1}$. The effect of load direction on the coincident bridge output was ± 0.5 %.

Cross-sensitivity errors were 0.0002 $\mu V\ V^{-1}N^{-1}$ and 0.0002 $\mu V\ V^{-1}N^{-1}$ respectively for the perpendicular and coincident force bridges.

The hysteresis errors were between 0.294 and 0.447 % [f.s.], and between 0.052 and 0.105 % [f.s.] respectively for the perpendicular and coincident force bridges.

The repeatability errors on both bridge outputs were small in both directions. They were between 0.147 and 0.298 % [f.s.], and between 0.316 and 0.263 % [f.s.] respectively for the perpendicular and coincident force bridges.

Right-Extended Octagonal Ring Transducer (Right-LEORT)

The outputs were linear, with coefficients of determination, $R^2 > 0.999$.

The sensitivities of the perpendicular and coincident force bridges were 0.0735 $\mu V\ V^{-1}\ N^{-1}$ and 0.0623 $\mu V\ V^{-1}N^{-1}$. The effect of load direction on the coincident bridge output was ± 0.5 %.

Cross-sensitivity error for the coincident force bridge was high, 0.001 $\mu V\ V^{-1}N^{-1}$ due to the wrong gauge alignment while it was small for the perpendicular force bridge, 0.0003 $\mu V\ V^{-1}N^{-1}$.

The hysteresis errors were between 0.527 and 0.757 % [f.s.], and between 0.053 and 0.107 % [f.s.] respectively for the perpendicular and coincident force bridges.

The repeatability errors on both bridge outputs were small in both directions. They were between 0.227 and 0.151 % [f.s.], and between 0.106 and 0.160 % [f.s.] respectively for the perpendicular and coincident force bridges.

Figure 18, 19, 20, 21, 22 and 23 produced from the calibration results by using Digital Volt Meter (DVM) show the characteristics of bridges on the transducers.

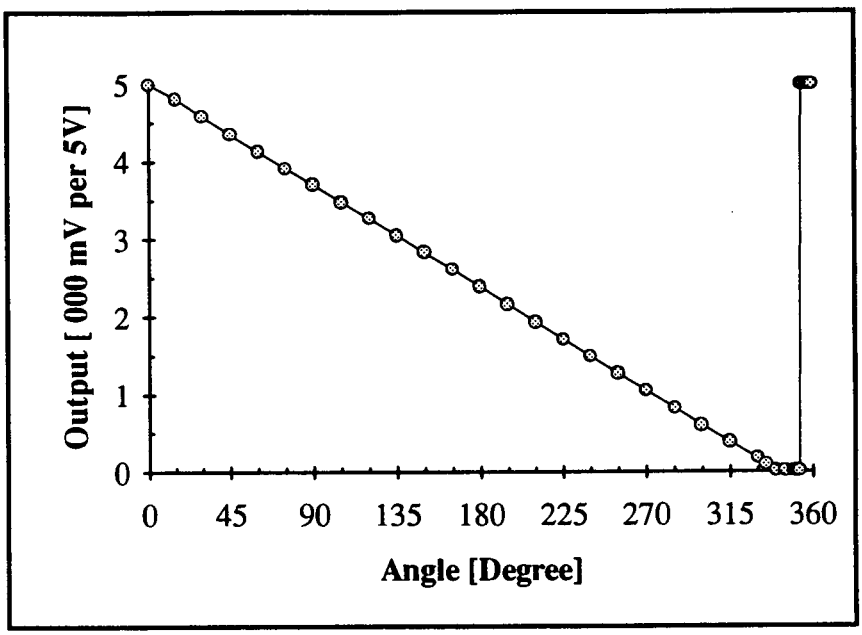

Figure 18. Characteristics of Rotary Position Transducer (RPT)

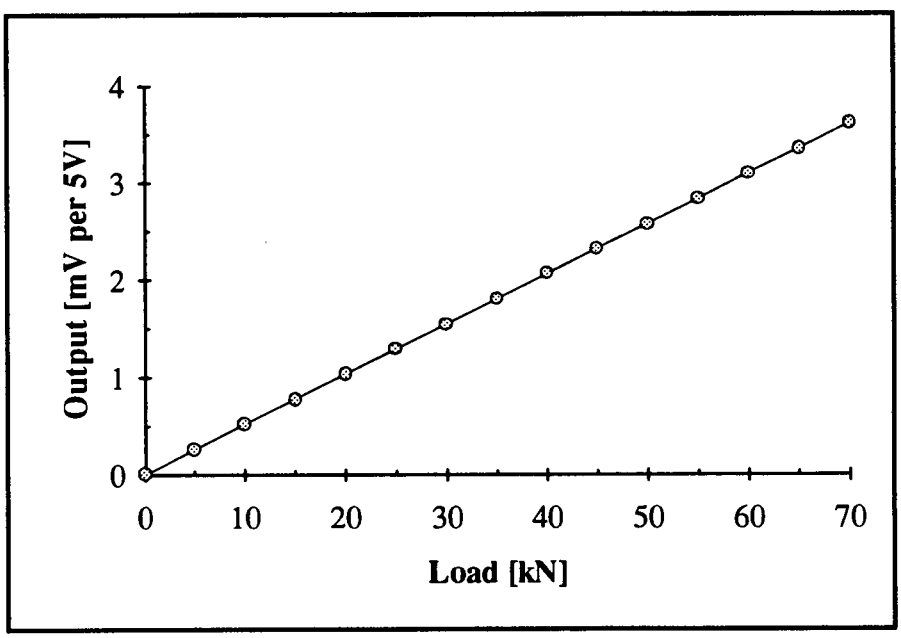

Figure 19. Characteristics of FTL bridge on Modified Top Link

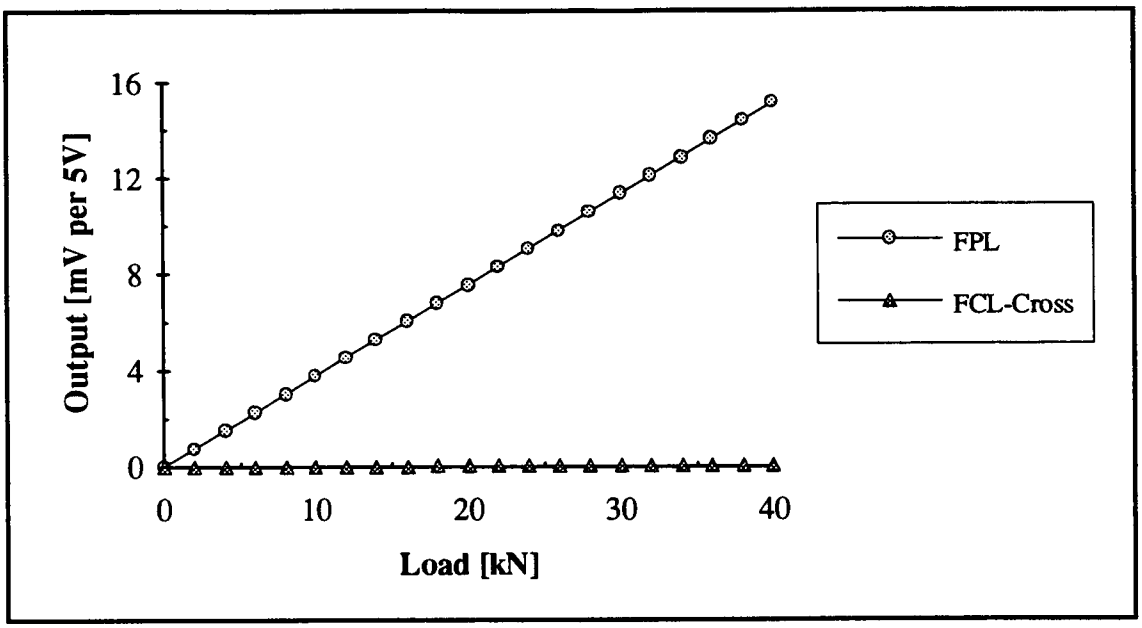

Figure 20. Characteristics of FPL bridge on Left-LEORT

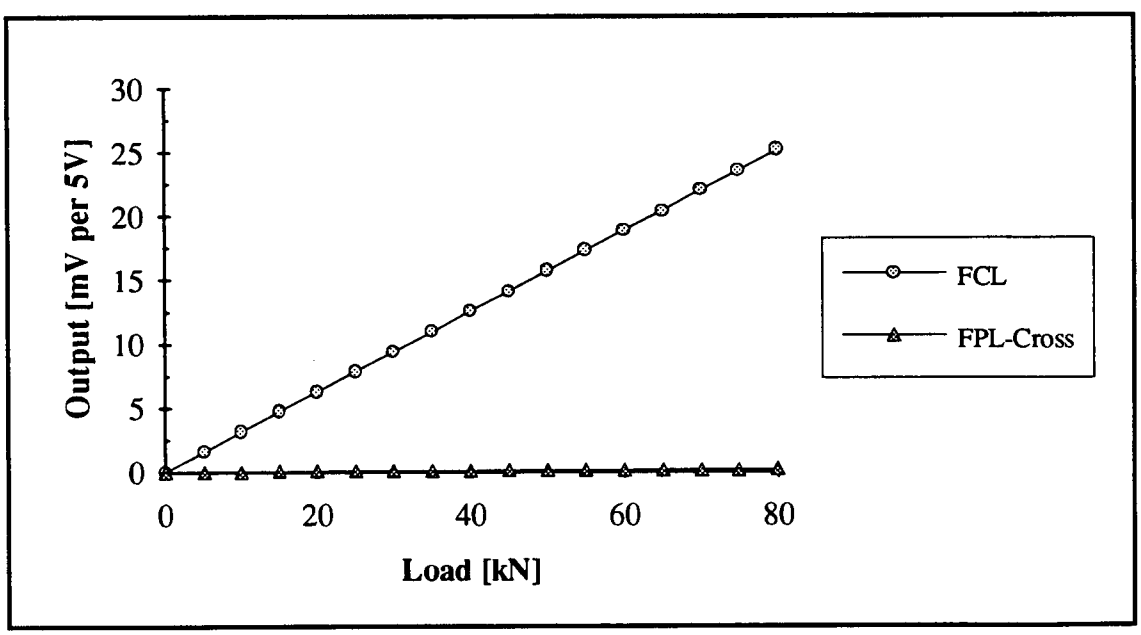

Figure 21. Characteristics of FCL bridge on Left-LEORT

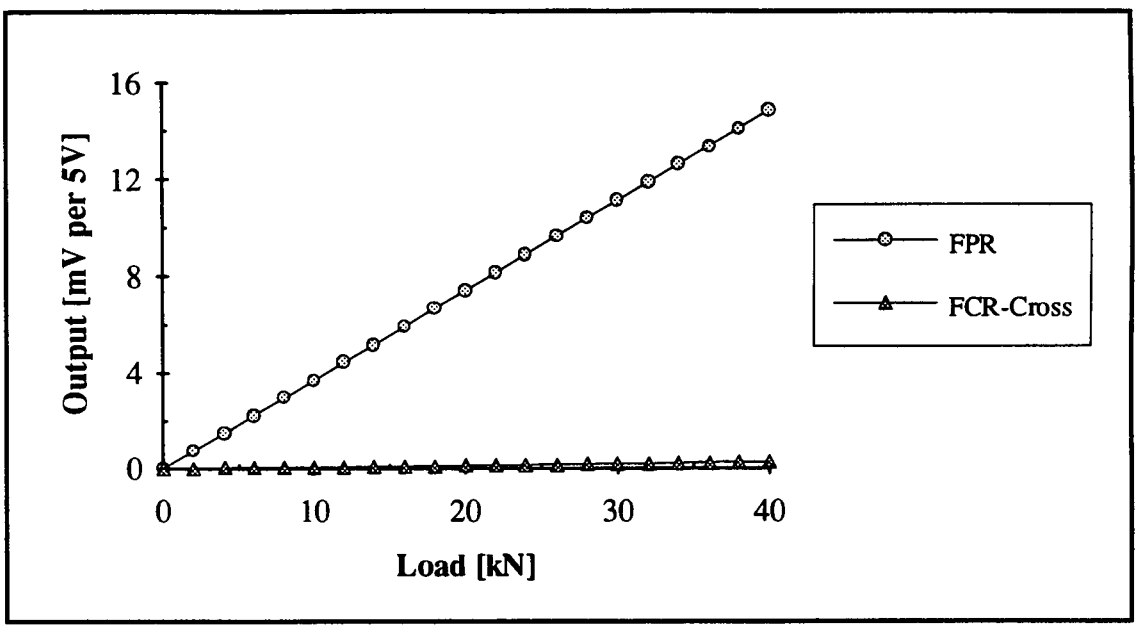

Figure 22. Characteristics of FPR bridge on Right-LEORT

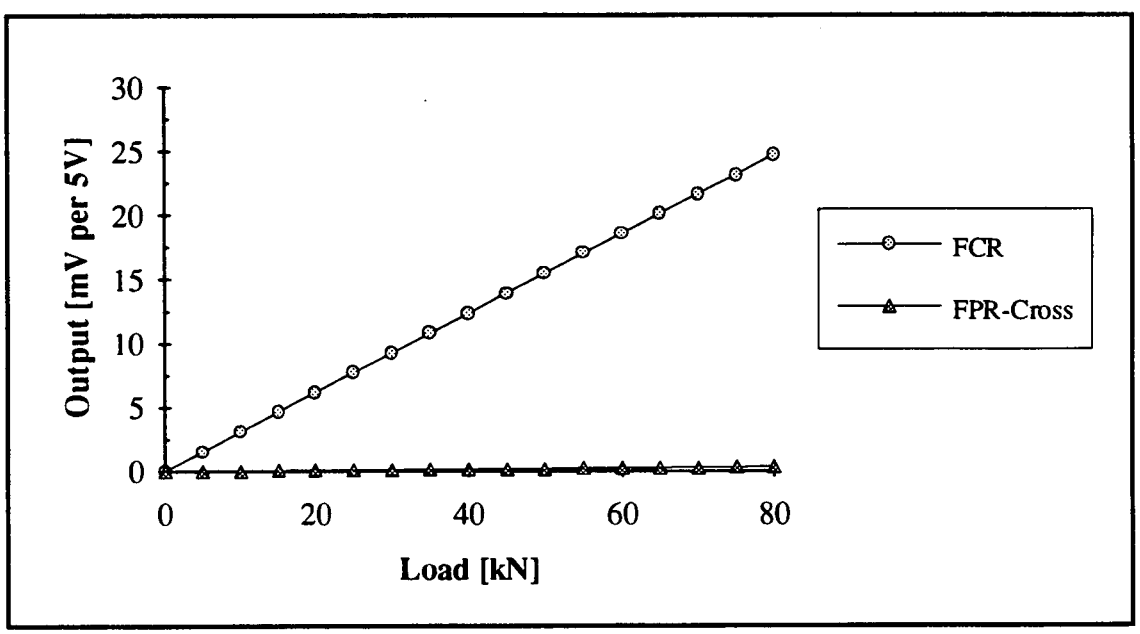

Figure 23. Characteristics of FCR bridge on Right-LEORT

Based on calibration results multipliers and offset values in datalogger software presented in Appendix 4 were calculated for all transducers (Table 12).

Table 12. Multipliers and Offset Values for Transducers

Bridge	Multiplier	Offset
CSA [Radian]	0.00595	2.6802
FTL [kN]	0.98434	13.315
FPL [kN]	0.13317	5.0572
FCL [kN]	0.15822	6.5671
FPR [kN]	0.13606	3.2609
FCR [kN]	0.16061	3.1024

Having added these figures to the software the datalogger gave the output in kN.

The same datalogger was also used for the field tests fitted into the tractor cab and connected to the portable computer. Transducers were attached on to the tractor as shown in Plate 5 and Figure 24.

Plate 5. The Dynamometer Fitted on to the Tractor

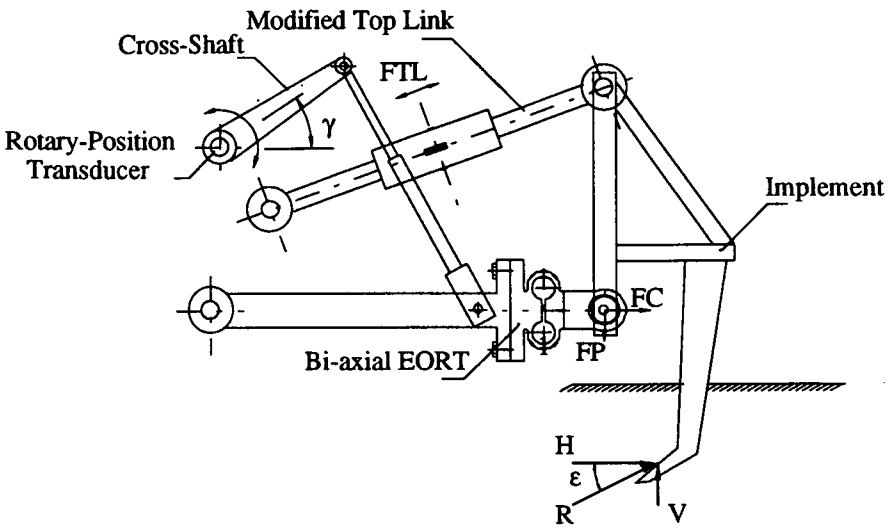

Figure 24. Three-point linkage dynamometer on the tractor

The transducers employed in the instrumentation system described earlier were donated by Silsoe College to Çukurova University through H.M. Ambassador 's Gift Scheme and left in Türkiye after field tests were completed in GAP region in 1991. Hence, when the field experiments were extended to include the application of the concept in the extreme soil conditions in UK in 1993 there was no possibility left to use the developed instrumentation system. This made it necessary to resume the tests with the system available at Silsoe College.

This system fitted on to the cab of MB trac 1 300 tractor consists of the following units: 1) Shear load cell; 2) Extended octagonal ring transducer; 3) Amplifier; 4) A/D converter; 5) Analogue data analyser; 5) Printer; 6) Batteries as power supply.

The shear load cell was used to sense either the force due to the rolling resistance only or the combined force created by the implement and towed tractor during the tillage operation (Plate 6). The capacity of the load cell is up to 500 kN. Some specifications of the load cell are presented as follows:

Make	: Transducerscel Ltd.
Type	: DC 1960
Range	: 0-500 kN
Max. Voltage	: 12 DC

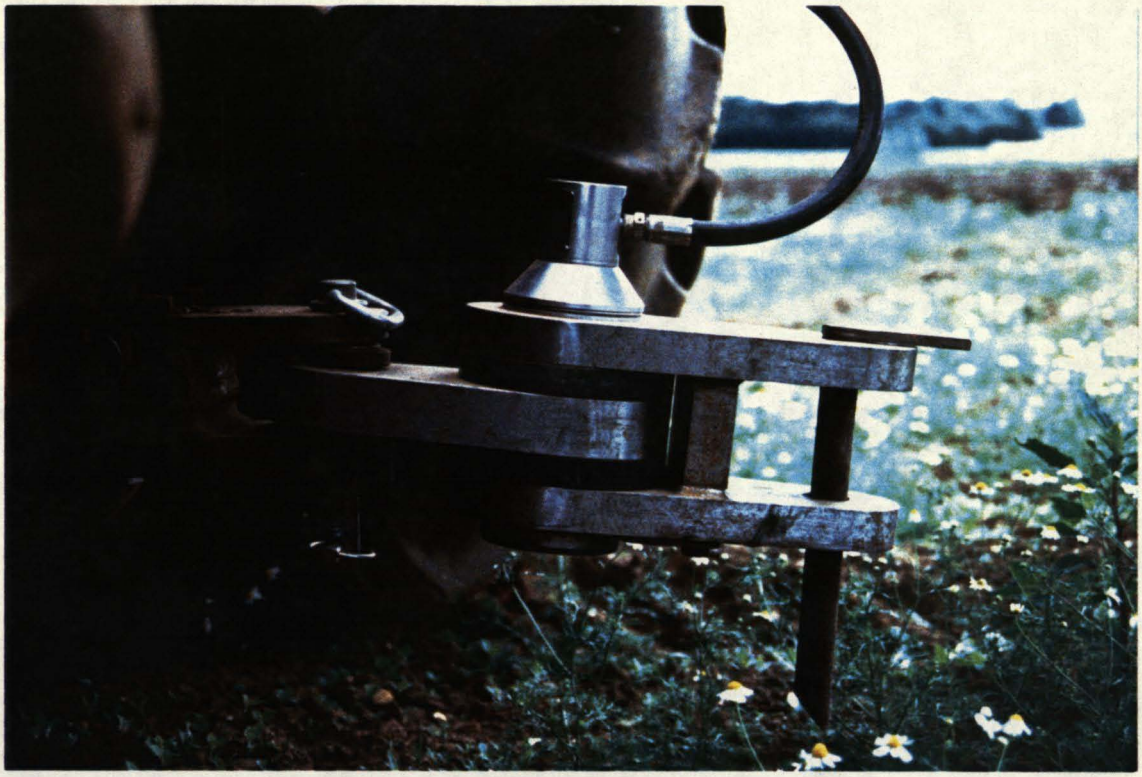

Plate 6. Shear Load Cell

The extended octagonal ring transducer was designed to carry a load of 20 kN in the perpendicular direction and 50 kN in the coincident direction and was made of an aluminium alloy described by Godwin et al. (1987) (Plate 7). The ring has three bridges to sense perpendicular force, coincident force and moment, in fact only the coincident bridge (draught) was of interest in this study. Satisfactory results for the transducer were presented Godwin et al. (1987). The bridge sensitivity was 0.05 $\mu V\ N^{-1}\ V^{-1}$ and the outputs were linear with coefficients of determination > 0.99.

With the instrumentation system, initially, the signals coming from the sensors were amplified to within 1.2 V from a selection of gain settings and transferred to a A/D converter and data analyser. The amplifier was also used to excite all the bridges with ≈ 9.3 V. The analyser, which has seven channels, sampled the signal at a fixed rate of 100 Hz, which is almost twice that expected, and produced the mean and standard deviation values. Finally, the data was sent to the printer. The energy requirement of the instrumentation system was provided by using two 12 V batteries connected in series to an DC/AC converter. Before the field tests the system was calibrated to confirm the already known characteristics of the sensors. The results are presented as given in Table 13.

Plate 7. Extended Octagonal Ring Transducer between Tine and Frame

Table 13. Calibration Results of the Transducer Used in 1993

Shear Load Cell						
Setting	30	100	300	1K	3K	10K
Resolution [N/unit]	50.6	189.83	582.9	1 934.0	5 545.0	20 791.8
Extended Octagonal Ring Transducer						
Setting	30	100	300	1K	3K	10K
Resolution [N/unit]	2.558	9.558	29.35	97.38	279.2	1 046.9

During the field tests two tractors were used, a Ford 7840 2WD and a MB trac 1 300. The Ford with the implement was towed by the MB trac to measure the force, both rolling resistance and implement draught, via the shear load cell held with chains between the tractors. Hence, the tractor with the implement was drawn twice in each run to determine firstly rolling resistance and secondly rolling resistance plus implement draught as gross draught (Plate 8 and 9).

Plate 8. The Measurement of the Rolling Resistance for the Tractor and Implement

Plate 9. The Measurement of the Draught and Rolling Resistance

The rolling resistance was subtracted from the gross draught to obtain the pure draught. MB trac was also used to pull the standard tine on a frame. The force acting upon the tine was sensed by the EORT fitted between the frame and clamp on the tine.

4.4. The Spreadsheet Model

To analyse the data provided from the field tests a template developed in Lotus by Kilgour et al. (1988) was used after some modifications for the study. Basically, the model has five main stages as given below:

- Input the known constants of the particular TPL and the implement used to the model
- Input variables from the datalogger to the model
- Calculate the unknown pin coordinates and bar length by using the cross-shaft angle *CSA* (γ)
- Calculate the relative position of the forces as well as the resultant force and angle
- Show the linkage and forces including the magnitude and position of the resultant force between the tractor and implement

A graphical plot of the linkage and forces is provided showing the magnitude and position of the resultant force between the tractor and implement as given in the floppy disk attached (see Appendix 5).

4.5. The Outline of the Study

Having designed and built an effective three-point-linkage dynamometer the second step was to set up the field experiments and to measure the forces acting upon a range of tillage implements (Figure 6). The aim was to investigate whether the concept of Desbiolles (1994) could be extended to the implement. Therefore, a plan, as shown in Figure 25, was developed and applied to the field tests which were conducted. The plan can be introduced as follows:

(a) *Geometrical Factors* for both standard tine and tillage tools such as one single tine, mouldboard body and disc determined by Desbiolles (1994) were available.

(b) Field experiments were conducted in both UK and Türkiye to measure the draught force requirements of a range of tillage implements.

(c) The geometrical factors given (a) cannot be used for a multi-tine implements such as chisel, disc plough and mouldboard plough. Therefore, these factors were corrected by multiplying by the number of units on the implement frame. In addition, the factor for the chisel which was the only multi-tine implement having interactions between tines, was revised by following the geometrical approach developed by Godwin et al. (1984). In this stage of the study *Soil Strength Factors (SSF)* for fields were also determined considering the equations [21].

(d) Finally, the draught force requirements of the implements were predicted. These forces were compared with measured draughts for the same implements used in the fields. The results were evaluated based on *Index Values* which is the ratio between either Geometrical Factors or draughts regarding the standard tine. There would be a difference between the measured and predicted draughts because of the nature of the work involved. Some error sources were taken into account.

Field experiments were conducted under the sandy loam soil condition in *Downings Field* which is one of the field of the college in UK and clay soil condition in GAP region in Türkiye in 1991. The experiments were extended to as wide a range of soil type and condition as possible in UK in 1993 in order to increase the validation of the model. For that reason, the tests were continued in two different soil types: 1-light (sandy loam); 2-heavy clay and three different moisture conditions: 1-dry; 2-normal; 3-wet. These fields are called *Showground, Millbrook* and *Copse Fields* which all belong to the College.

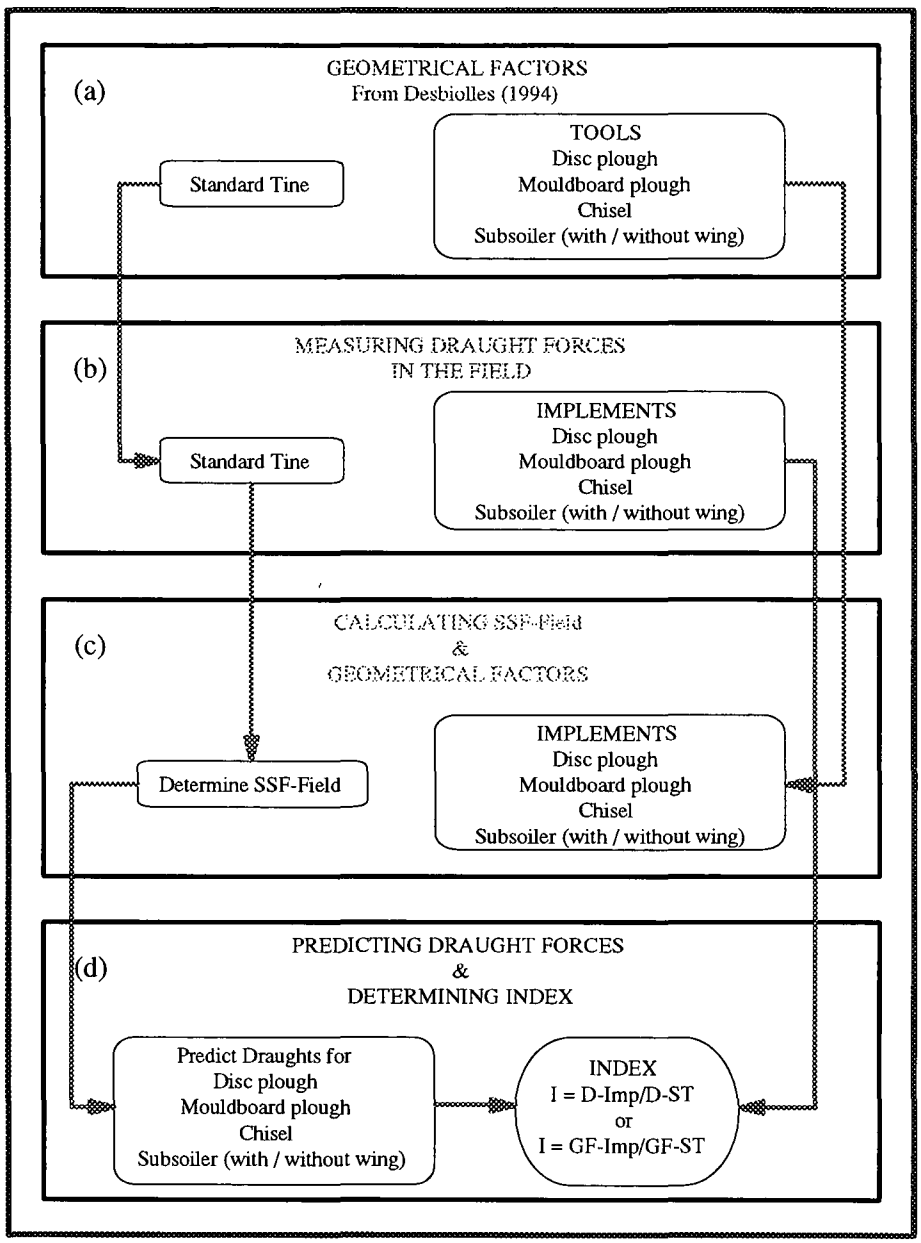

Figure 25. Block diagram of the second stage of the study conducted

During the tests treatments were randomised into plots to reduce the effect of soil heterogeneity. Due to the same reason the standard tine was run between the plots reserved for implements. A working speed of 2-4 km/h and a working depth of 0.10-0.45 m were used although they were dependent on working conditions and implement characteristics. Each run was repeated three times at least.

4.6. Soil Characteristics

The first field experiment was conducted in *Downings Field* on Silsoe College Farm in UK in 1991. The soil was mainly sand. The mechanical analysis determined by the Pipette Method is given in Table 14. The field was covered with the stubble and the moisture content was 22.1 % (d.b.).

In contrast, for the field experiments in Türkiye in 1991 the clay soil was chosen due to the dominant type in the GAP region. Thus, the tests were conducted on the farm of Çukurova University Research Station which is located in GAP region. The mechanical analysis determined by the Pipette Method is also presented in Table 15. The average moisture content was 21.4 % (d.b.).

Table 14. Mechanical Analysis of the Soil: Downings Field

Fractions [%]	Rep. I [%]	Rep. II [%]	Rep. III [%]	Average [%]
Total	60.06	57.92	59.63	59.20
Coarse sand	5.69	3.89	4.26	4.61
Sand	34.72	32.74	34.67	34.04
Fine sand	19.65	21.29	20.70	20.55
Silt	22.05	21.49	22.28	21.94
Clay	17.89	20.58	18.09	18.85

Table 15. Mechanical Analysis of the Soil: GAP in Türkiye

Fractions [%]	Rep. I [%]	Rep. II [%]	Rep. III [%]	Average [%]
Total	8.25	10.44	10.53	9.74
Coarse sand	1.54	2.32	2.02	1.96
Sand	4.75	4.93	4.63	4.77
Fine sand	1.96	3.19	3.88	3.01
Silt	32.78	32.28	32.05	32.37
Clay	58.97	57.28	57.42	57.89

In the same way, the soil characteristics of the fields used in 1993 were determined by the Pipette Method. Table 16, 17, and 18, show the soil characteristics of these fields respectively. The fields were all covered with stubble and average moisture contents were 13.7, 12.84, 33.67 % (d.b.), respectively.

Table 16. Mechanical Analysis of the Soil: Showground Field

Fractions [%]	Rep. I [%]	Rep. II [%]	Rep. III [%]	Average [%]
Total	62.05	63.06	62.05	62.39
Coarse sand	7.02	7.43	6.31	6.92
Sand	37.60	37.57	37.49	37.56
Fine sand	17.44	18.05	18.24	17.91
Silt	21.86	21.74	22.55	22.05
Clay	16.09	15.19	15.40	15.56

Table 17. Mechanical Analysis of the Soil: Millbrook Field

Fractions [%]	Rep. I [%]	Rep. II [%]	Rep. III [%]	Average [%]
Total	59.42	58.57	58.86	58.95
Coarse sand	3.30	3.10	2.64	3.01
Sand	41.26	40.27	40.55	40.69
Fine sand	14.86	15.21	15.67	15.24
Silt	25.47	25.65	25.09	25.40
Clay	15.11	15.78	16.05	15.65

Table 18. Mechanical Analysis of the Soil: Copse Field

Fractions (%)	Rep. I [%]	Rep. II [%]	Rep. III [%]	Average [%]
Total	16.04	15.86	14.40	15.43
Coarse sand	2.23	2.79	1.13	2.05
Sand	8.26	7.75	7.96	7.99
Fine sand	5.55	5.32	5.32	5.39
Silt	25.06	24.32	25.37	24.92
Clay	58.90	59.82	60.23	59.65

4.7. Standard Tine

The standard tine was extremely important in this study due to the model based on it as a reference. All field experiments were conducted with a standard tine as shown in Figure 26 which has a 45° rake angle to determine the *Soil Strength Factor (SSF)* for a particular field. Throughout the study the tine designed and built by Hall (1991) was used.

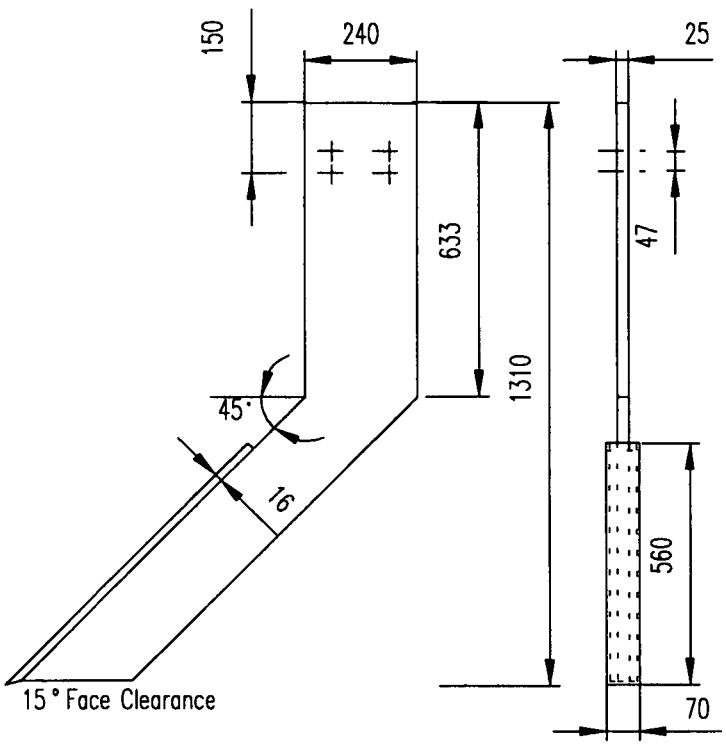

Figure 26. A simple 45° raked angle tine

The tine was made of mild steel which has relatively high strength, and is relatively cheap. It did not have a separate rake for the foot. For the tine to be classed as simple, it is then perceived as being considered as a leg rather than a tine. For the tine to operate successfully the design must provide minimum draught and optimum penetration. This can be achieved with a tine having a forward rake angle of 45° (Osman, 1964; Payne and Tanner, 1959). Minimising the draught means that the tine should be kept to as small a size as possible. The dimensions were calculated assuming the worst possible scenario which was a maximum load of 20 kN acting at the tip of the tine. This value is the greatest ever likely to be experienced, that is with the tine working to a maximum depth of 0.50 m.

The tine width is also important because the type of soil failure is dependent on the depth to width ratio. The transition between the modes of failure (Crescent and Lateral failure) takes place at a critical depth (d_c) (Godwin and Spoor, 1977). To achieve only crescent failure, the critical aspect ratio of 7 was chosen to be able to reach up to maximum depth of 0.50 m, hence a face plate with a width of 70 mm which is sufficient was attached to the tine. The plate has a 15° clearance angle on all sides of the tine to eliminate the affect of the friction.

The tine was mounted on to a frame by using special clamps and brackets which have been also designed on prior projects (Plate 10). The control of depth was monitored by depth wheels fitted to both sides of the frame. This enabled the adjustment of depth at an interval of 0.025 m.

Plate 10. Standard Tine Hitched on to the Tractor

4.8. Implement Specifications

Tillage implements can be classified as primary or secondary, although there is no clear-cut distinction. Primary tillage implements demand much more draught due to working deeper. The power selection in a farm is based on the draught required by the primary tillage implements. Therefore, the relationship between the draught force required for a range of primary tillage implements which have rigid tines and soil properties in various soil conditions was proposed.

To achieve this the implements presented in Table 19 were used for field tests in UK and in Türkiye. The concept does not require comprehensive specifications of the implements.

Table 19. Some Specifications of the Implements

Field & Implement	Make	Type	Number of Unit	Tine/unit Width [m]
Downings Field				
Disc plough	Permiter	normal	3 discs	0.650 ϕ
Mouldboard	Dowdeswell	reversible	3 bodies	0.355
Chisel	Unbranded	V-form	5 shanks	(14")
Subsoiler	Ransomes	normal	1 shank	0.080
				0.070
GAP				
Disc plough	TZDK	normal	3 discs	0.635 ϕ
Mouldboard plough	Rabe	reversible	2 bodies	0.355
Chisel	Unbranded	3 front, 3 back	6 shanks	(14")
Subsoiler	TZDK	normal	1 shank	0.065
				0.065
Tests in 1993 in UK				
Disc plough	Permiter	normal	3 discs	0.650 ϕ
Mouldboard	Dowdeswell	reversible	3 bodies	0.355
Chisel	Unbranded	V-form	5 shanks	(14")
Subsoiler	Ransomes	with wing	1 shank	0.080
				0.070

5. RESULTS AND DISCUSSIONS

5.1. Introduction

In this chapter field test results are presented both in UK and Türkiye. Draught force requirements of the implements used in the fields are also predicted. These results are compared with measured draughts and the difference between the figures is stated with the index values and error factors. The validation of the concept is also examined by the test conducted under the different soil conditions in UK in 1993. A field method for predicting the draught forces of tillage implements is presented for the mechanisation planning purpose in a particular area.

5.2. Draught Force Measurement

The results of the field tests conducted in sandy loam soil in Downings in UK in 1991 are given in detail in Appendix 6. However, based on these results regression equations and coefficient of determination (R^2) are presented in Table 20 for the individual implement and standard tine used.

Table 20. Draught Force Requirements of the Implements and Standard Tine Used under Sandy Loam Soil Condition: Downings Field-UK in 1991

Implement or tine	Regression equation	R^2 [%]*
Disc plough	$D = 230.279\ d^2$	92.3
Mouldboard plough	$D = 35.47\ d + 44.23\ d^2$	78.2
Chisel	$D = 17.062\ d + 136.17\ d^2$	98.7
Subsoiler	$D = 2.307\ d + 39.432\ d^2$	95.1
Standard tine	$D = 55.994\ d^2$	85.2

* Value determined from the regression equation with constant

Table 20 showed that depth-draught relationships for all the implements except the mouldboard plough were highly correlated with coefficients of determination (R^2) of > 0.92 although the standard tine was less than 0.92. The type of the relationships was a polynomial of the second order The mouldboard plough and standard tine also

showed a correlation with polynomial of the second order but coefficients of determination were slightly lower at 0.782 and 0.852, respectively.

The results above were also plotted in Figure 27. The variables in the Y axis of the graph are the fitted draught requirements of the implements obtained from multiple regression analysis of the measured draught given in Appendix 6.

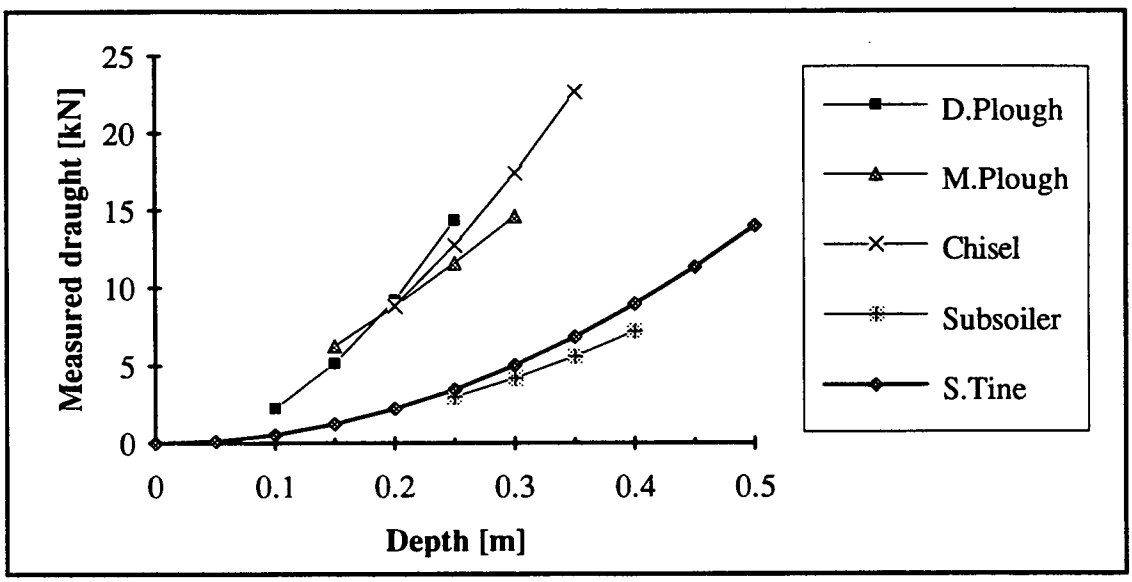

Figure 27. Measured draughts for the implements and standard tine under sandy loam soil condition: Downings field-UK in 1991

The subsoiler was similar to the standard tine in terms of the shape. This correspondingly was reflected in the depth-draught relationship of the implement in the same soil condition.

The field test results conducted under the clay soil condition in GAP-Türkiye in 1991 were presented in detail in Appendix 7. The regression equations associated with these results were given in Table 21.

All the implements and standard tine showed a high degree of correlation with polynomial relating depth and draught. The implements used under clay soil conditions required relatively much more draught in comparison with under sandy loam soil condition (Fig. 28). The chisel and subsoiler which were the closest implement to the standard tine in type also showed very similar relationships as the tine in terms of the force requirement (Fig. 28).

Table 21. Draught Force Requirements of the İmplements and Standard Tine Used under Clay Soil Condition: GAP-Türkiye in 1991

Implement or tine	Regression equation	R^2 [%]*
Disc plough	$D = 58.347\ d - 84.05\ d^2$	99.4
Mouldboard plough	$D = 5.21\ d + 200.22\ d^2$	91.6
Chisel	$D = 35.06\ d + 136.43\ d^2$	95.9
Subsoiler	$D = -0.47\ d + 73.463\ d^2$	99.3
Standard tine	$D = 84.958\ d^2$	93.2

* Value determined from the regression equation with constant

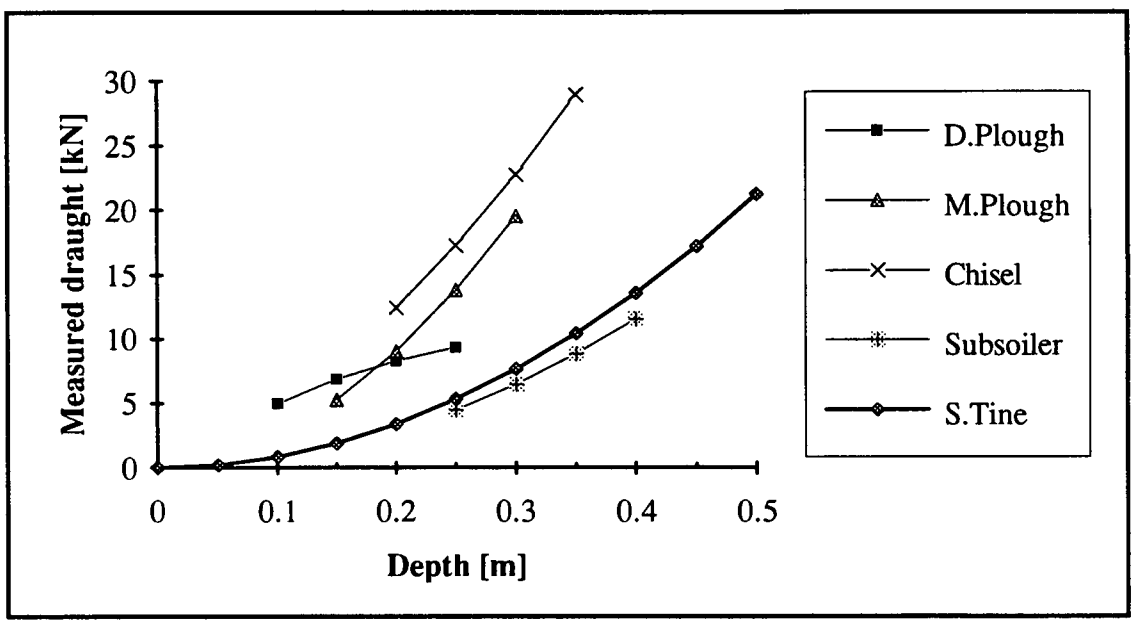

Figure 28. Measured draughts for the implements and standard tine under clay soil condition: GAP-Türkiye in 1991

5.3. Draught Force Predictions

Geometrical factors for the tools obtained from Desbiolles (1994) are given in Table 22 and the factors are plotted against the standardised depth in Figure 29. More information about these factors including the probability error bands at 95 % level of *Confidence Interval* is presented in detail in Appendix 8.

Table 22. Geometrical Factors for Tools and Standard Tine Used in 1991

Depth [m]	Geometrical Factor (GF)				
	Disc unit	Mouldboard body	Chisel (Curved)	Subsoiler No wing	Standard Tine
0.00					0.049500
0.05	0.232344		0.167653		0.110735
0.10	0.256579	0.459813	0.216080	0.162047	0.171970
0.15	0.263522	0.475668	0.253191	0.189269	0.233205
0.20	0.297973	0.480143	0.294970	0.217091	0.294440
0.25	0.404829	0.541302	0.357347	0.250431	0.355675
0.30		0.745518	0.456266	0.290670	0.416910
0.35			0.607722	0.335419	0.478145
0.40				0.378591	0.539380
0.45				0.410460	0.600615
0.50					0.661850

Source: Desbiolles (1994)

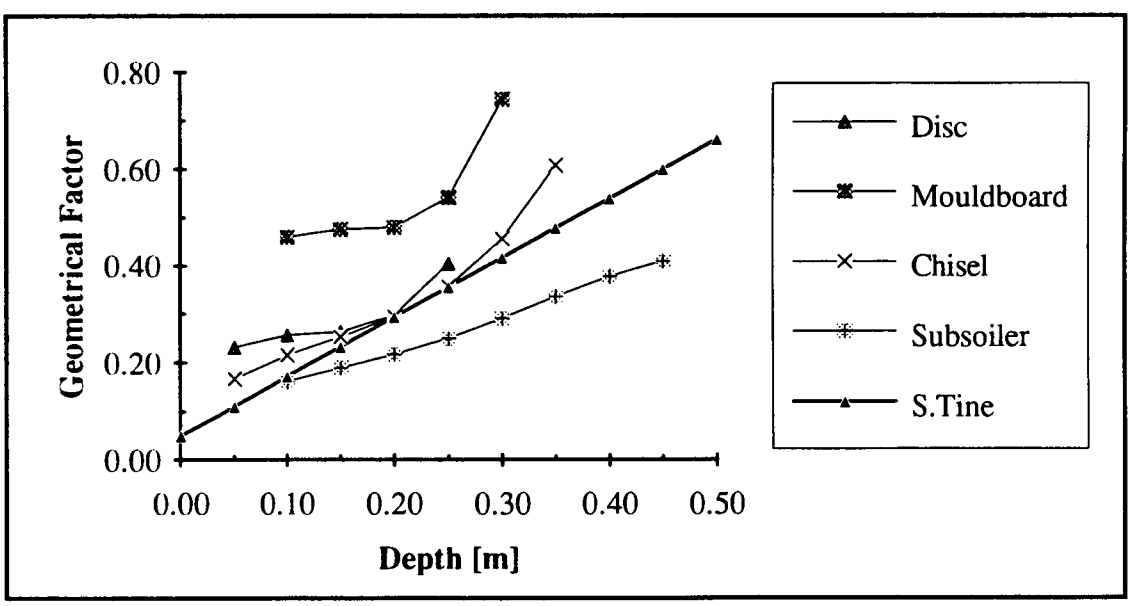

Figure 29. Geometrical factors for the tools and standard tine used in 1991

These factors were the values for a single unit called tool and the tine used in 1991. The tool factors were converted into implement geometrical factors by multiplying by the number of units on the frame i.e. 3 for disc plough with three disc units. The curves showed that the geometrical factors for a particular implement increased with the working depth but also fluctuated depending upon the area interfacing the soil.

The Geometrical factors for the tools had probability error bands. However, as the standard tine geometrical factor was a theoretical value, there was no variance for it. The changes in the geometrical factors were also expressed by the *Coefficient of Variation* (C.V.%) in Appendix 8. The coefficient of variation varied from 5 to 35 % depending on complexity and working depth of the tool. The smallest variation was recorded for the subsoiler while the worst case appeared for the disc.

The second important component of the concept was *Soil Strength Factor (SSF)* for a particular field. Therefore, the soil strength factor values were calculated from the draught requirement and geometrical factor of the tine (Table 23).

Table 23. Soil Strength Factors (SSF) for the Fields in UK and Türkiye in 1991

Depth	Soil Strength Factor (SSF)							
	Sandy Loam Soil (Downings-UK)				Clay Soil (GAP-Türkiye)			
[m]	Min	Max	Mean	C.V.%	Min	Max	Mean	C.V.%
0.00	0.000	0.000	0.000	0.00	0.000	0.000	0.000	0.00
0.05	1.128	1.399	1.264	10.71	1.616	2.220	1.913	15.80
0.10	2.907	3.605	3.256	10.71	4.157	5.727	4.942	15.88
0.15	4.817	5.979	5.400	10.75	6.891	9.493	8.194	15.87
0.20	6.788	8.424	7.606	10.76	9.705	13.375	11.538	15.91
0.25	8.782	10.900	9.843	10.76	13.122	17.306	14.933	14.01
0.30	10.787	13.384	12.084	10.75	15.422	21.252	18.336	15.90
0.35	12.800	15.884	14.341	10.75	18.301	25.219	21.759	15.90
0.40	14.821	18.391	16.606	10.75	21.190	29.203	25.196	15.90
0.45	16.848	20.907	18.877	10.75	24.088	33.195	28.642	15.90
0.50	18.877	23.427	21.151	10.76	26.992	37.196	32.094	15.90

The soil strength factor for the sandy loam soil was higher than for clay soil as the factor referred to the soil resistance per unit of the implement width. These factors naturally were dependent upon the working depth and the area of the tool interfacing the soil. The soil strength factor had certain probability error bands due to the variation in measured draught of the standard tine. This error for sandy loam soil and clay soil was about ±10.7 % and ±15.8 %, respectively.

Having obtained the geometrical factor and determined the soil strength factor the next stage was to predict the draught force requirements of the implements used. Making the prediction was very straightforward for the non-interacted implements such as the single leg subsoiler. However, multi-tined implements such as disc plough, mouldboard plough and chisel required extra calculation due to the interactions between the tines. In this study, it was assumed that of the disc plough and mouldboard plough had no interaction between the units. Therefore, the calculation was made only for the chisel and is given in detail in Appendix 9 and 10.

The predicted draughts for both sandy loam and clay soil condition are given in Appendix 11.

5.4. Comparison of Measured and Predicted Draught

One of the major concerns of the concept was to compare the predicted draught with the measured. In practice, a difference between the measured and predicted draughts is expected and inevitable. However, the magnitude of the difference exhibits how good the concept is. If the predicted value is higher than measured value this is called *Over Prediction.* If it is converse it is called *Under Prediction.* Both cases are described as *Prediction Errors.*

Overall assessment of the concept was expressed by using the ratio of the predicted implement draught to the measured which illustrates the effectiveness of the concept although each prediction result was individually evaluated in the following section. For the ideal case, this ratio equals to the index value. Inevitably, a difference exists depending upon the sensitivities of the parameters used. For this, first, the relationships between the measured and predicted draught for both conditions were plotted in Figure 30 and 31. Then the ratios were plotted against the depth in Figure 32 and 33.

The curves in Figure 30 and 31 represent the comparison for a reasonable working depth range. Under the sandy loam condition the curves were generally close to the reference line where the measured equals to predicted. The chisel showed the worst relationship, especially for the deeper working conditions. However, these relationships were closer to the equality line for all implements under the clay soil condition. The chisel showed the best relationship with the reference. In fact, sometimes it can be misleading to assess the results by giving error as a percentage especially at shallow depths i.e. require small draught forces. So, it is better to express the error as a Newton instead. However, the spread of the curves gives an overall approach to the concept.

The ratios which are another way to evaluate the results are given in Appendix 11 for both soil conditions. From Figure 32 and 33, for the best condition, it is expected that this ratio should remain at 1.0. The ratio depending upon the working depth varied from 0.689 to 1.361 for the sandy loam soil. For the clay soil condition the values varied between 0.678 and 1.313. If two cases are not taken into account in both soil conditions, the prediction errors will be around ±20 % which is reasonably well.

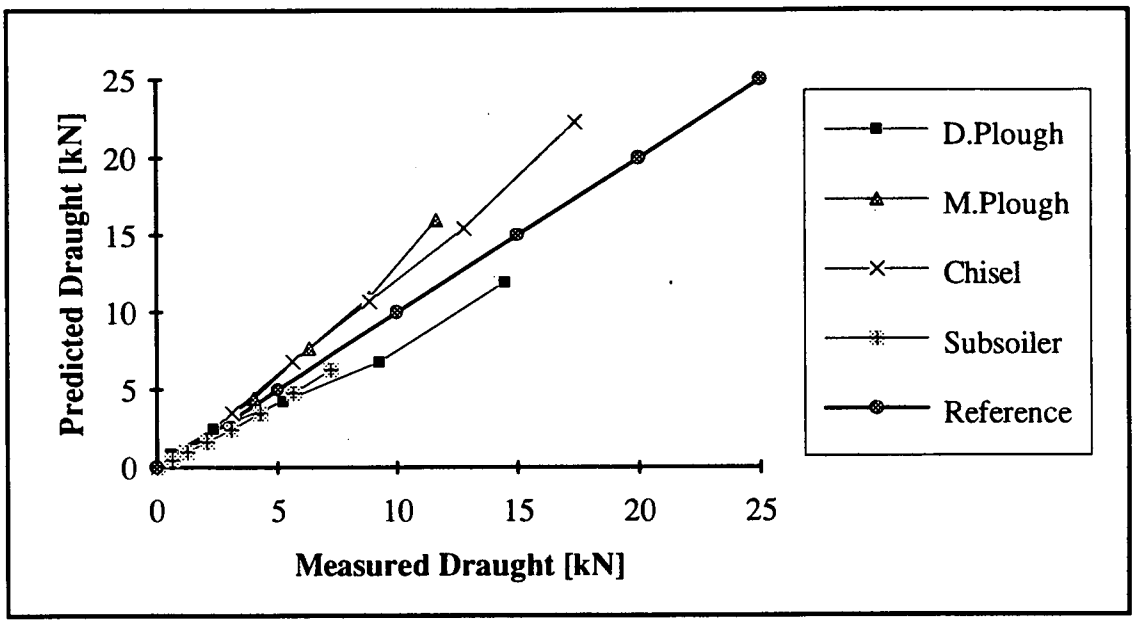

Figure 30. Predicted-Measured force relationships for the implements used in sandy loam soil: Downings-UK in 1991

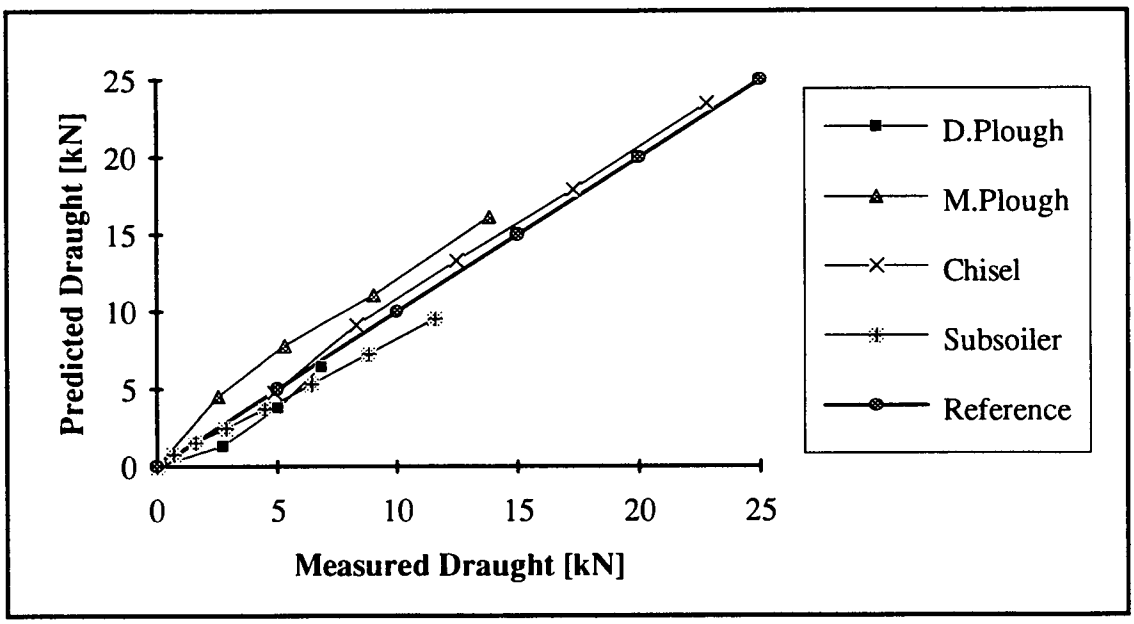

Figure 31. Predicted-Measured force relationships for the implements used in clay soil: GAP-Türkiye in 1991

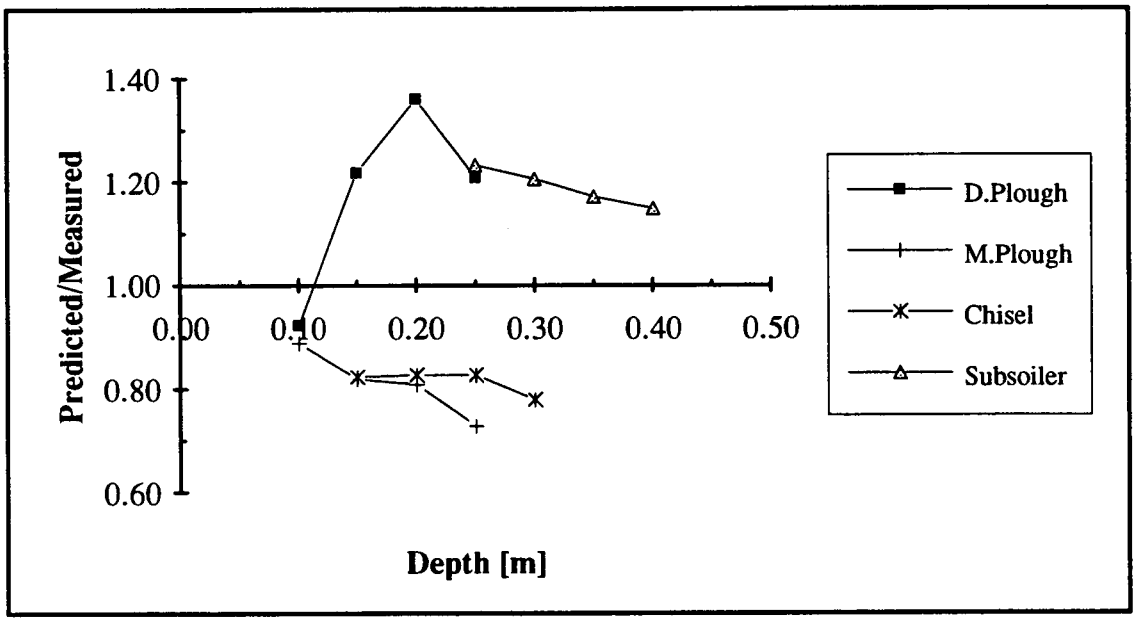

Figure 32. The ratio of predicted to measured draught for the implements used in sandy loam soil: Downings-UK in 1991

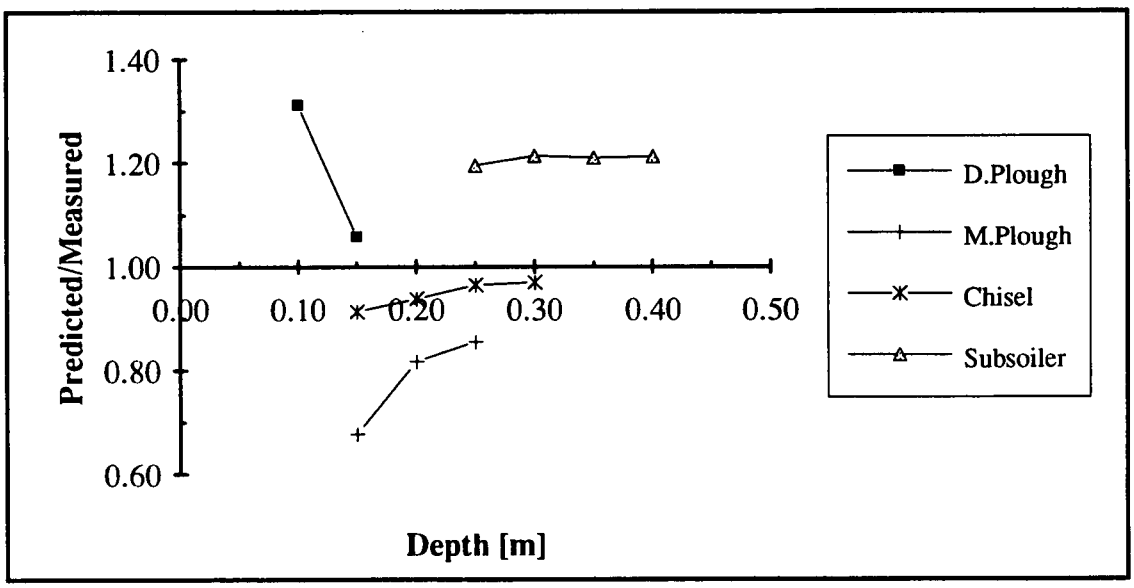

Figure 33. The ratio of predicted to measured draught for the implements used in clay soil: GAP-Türkiye in 1991

In fact, the errors in both cases can naturally raise from the following sources:

- variation in measured draught forces of the standard tine,
- variation in implement geometrical factors,
- measurement error during working depth,
- variation in soil properties and
- changes in moisture contents throughout the field tests.

Therefore, the concept works within the ±20 % error band which is reasonable when the variations especially in the geometrical factor and soil strength factor are considered. In addition, the concept eliminates the need to take specific implements to the field. Hence, the draught force requirements of the tillage implements can be predicted by the model using the standard tine only in the filed condition. The model is reliable and confident since the model uses the real data obtained from the field experiments.

The prediction results for both sandy loam and clay soil conditions are presented in detail in Appendix 11. The probability error bands and coefficient of variation are also reported for individual implements and working depth. The maximum, minimum and mean errors were calculated from the variations in predicted draughts due to changes in SSF values. On the basis of these values Figures 34, 35, 36 and 37 for the implements used in the sandy loam soil and Figures 38, 39, 40 and 41 for the implements used in the clay soil were created.

Under the sandy loam condition the draught requirements of the disc plough and subsoiler were under predicted while the mouldboard plough and chisel were over predicted. The prediction values for a particular implement at a depth varied dramatically due to the variations in the geometrical factor and soil strength factor. The lowest error was recorded in the subsoiler with an under prediction of 5.55 % the worst prediction appeared in the mouldboard plough with an under prediction of 48 %. However, the mean prediction errors for the disc plough, mouldboard plough, chisel and subsoiler were 17.30-26.50 %, 23.62-37.42 %, 20.95-28.46 % and 13.07-14.68 %, respectively. Under the clay soil condition the draught requirements of the implements were predicted with better prediction errors. The mean prediction errors were 5.58-23.83 %, 17.01-22.43 %, 3.04-3.62 % and 17.39-17.53 %. In contrast with the sandy loam soil, the lowest prediction error was obtained for the disc plough with an under prediction of 4.41 % the worst case occurred in the mouldboard plough with an under prediction of 31.30 %.

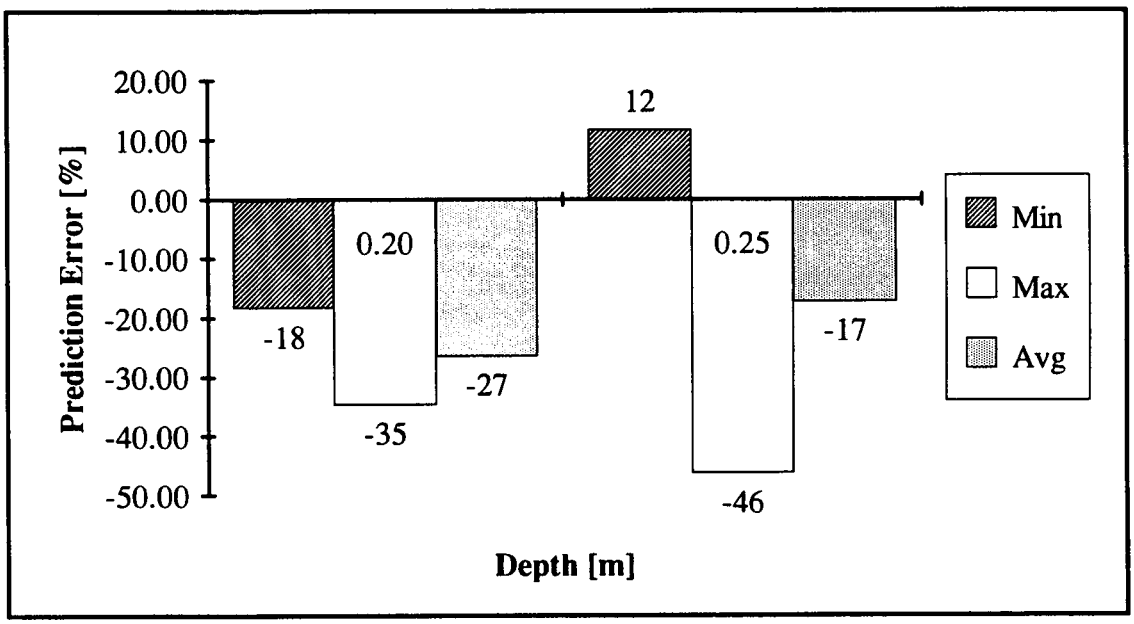

Figure 34. Prediction errors for disc plough in sandy loam soil: Downings-UK in 1991

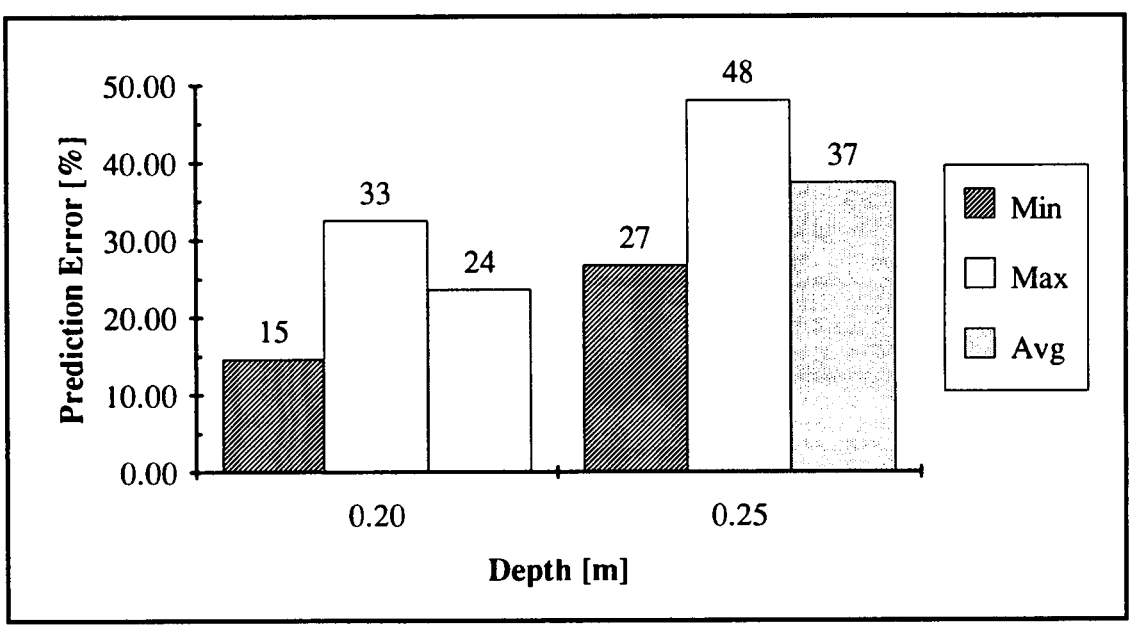

Figure 35. Prediction errors for mouldboard plough in sandy loam soil: Downings-UK in 1991

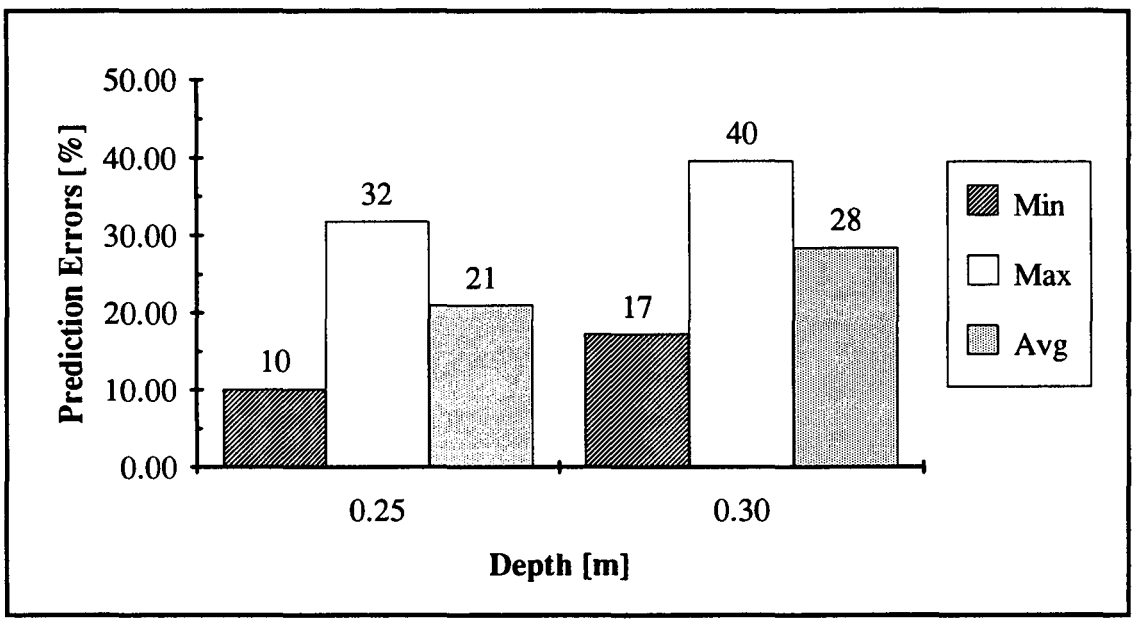

Figure 36. Prediction errors for chisel in sandy loam soil: Downings-UK in 1991

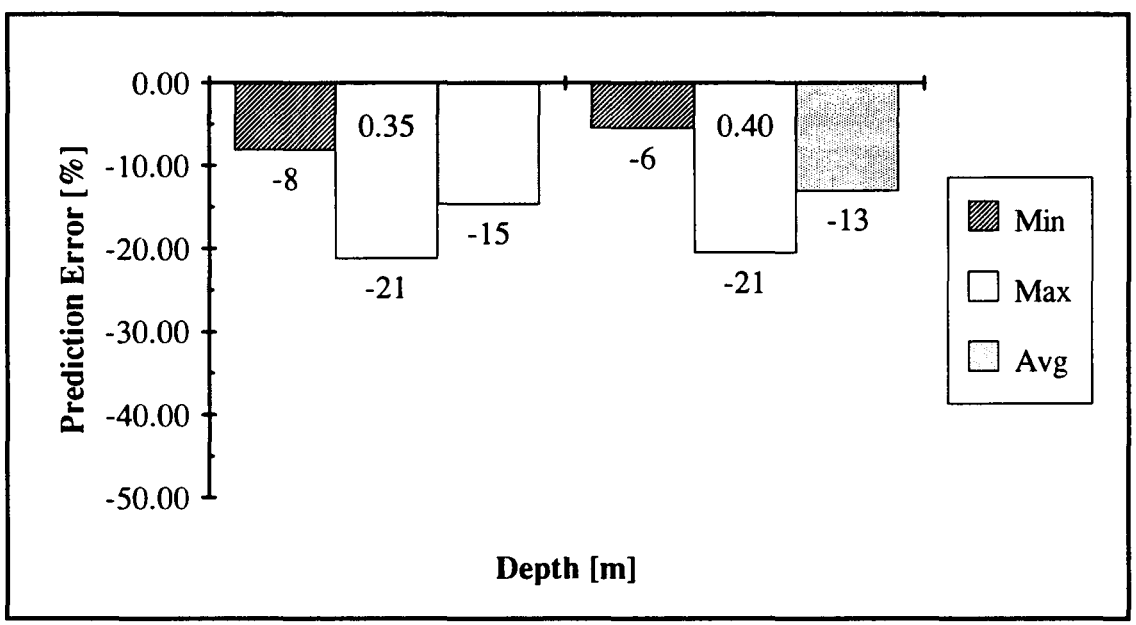

Figure 37. Prediction errors for subsoiler in sandy loam soil: Downings-UK in 1991

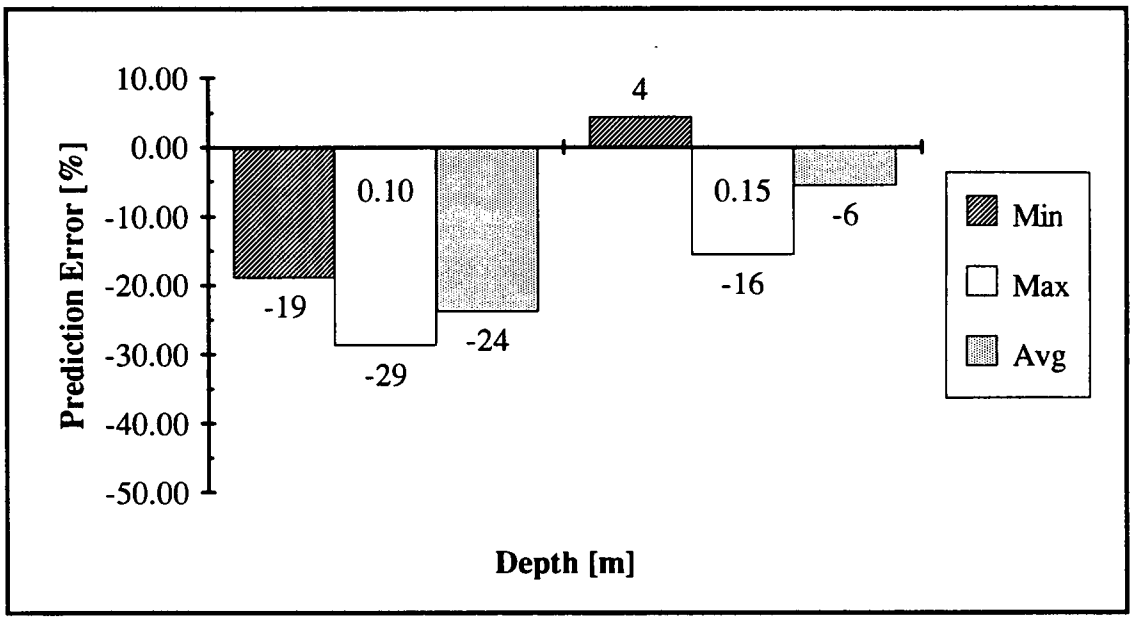

Figure 38. Prediction errors for disc plough in clay soil: GAP-Türkiye in 1991

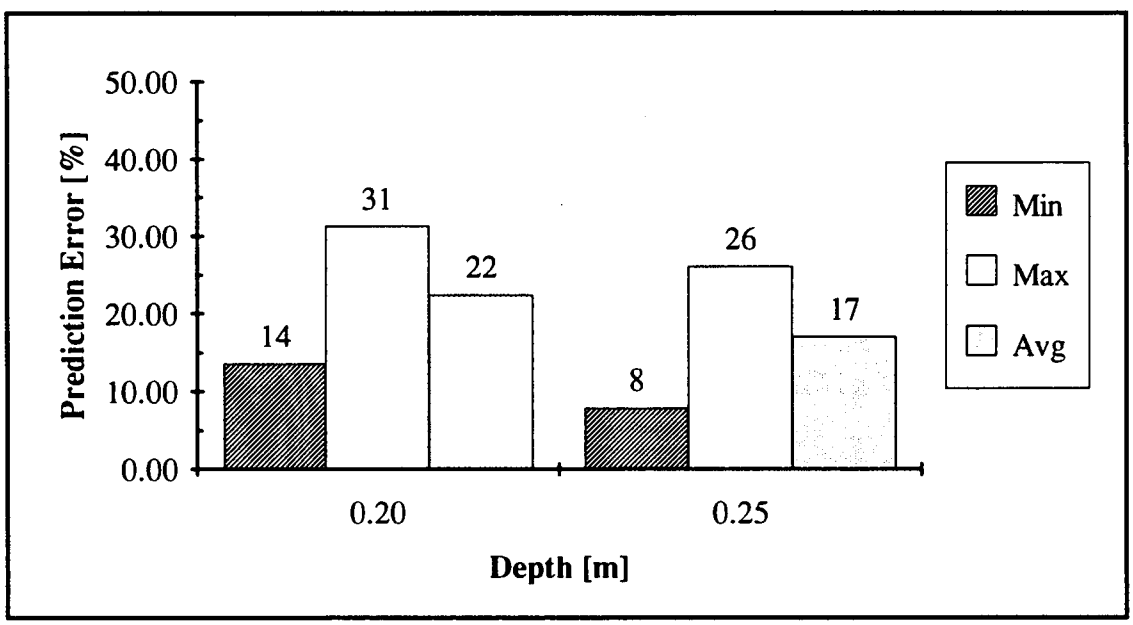

Figure 39. Prediction errors for mouldboard plough in clay soil: GAP-Türkiye in 1991

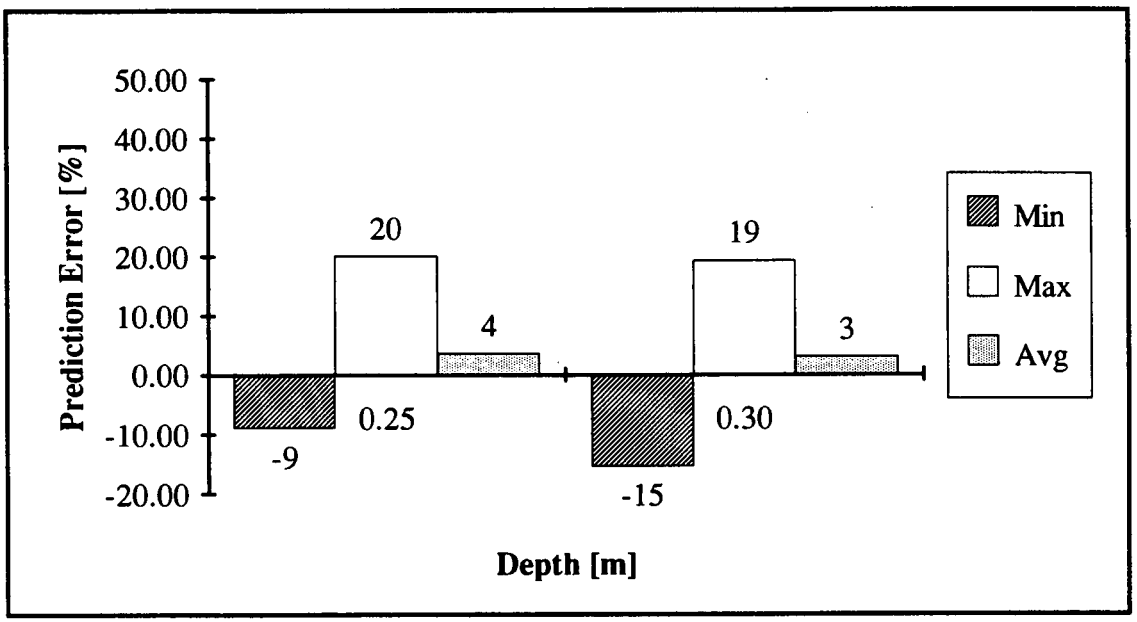

Figure 40. Prediction errors for chisel in clay soil: GAP-Türkiye in 1991

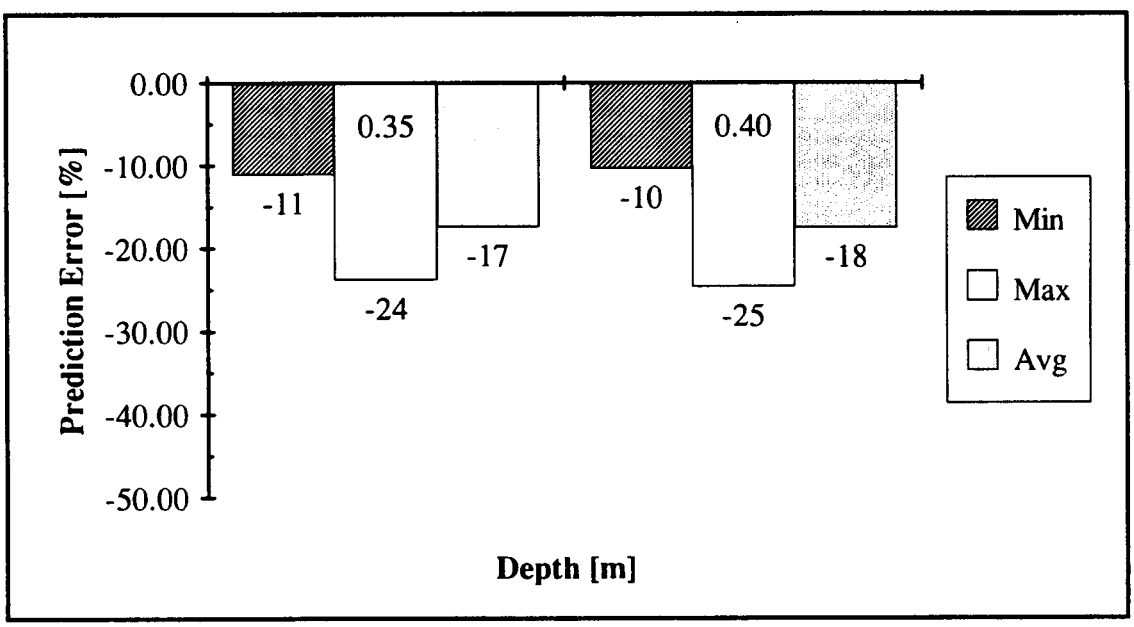

Figure 41. Prediction errors for subsoiler in clay soil: GAP-Türkiye in 1991

For both conditions the subsoiler gave the best prediction because the subsoiler had a single unit and was closest to the standard tine in terms of the geometry. Similar explanation could have been given for the chisels if they had not been multi-tined implements. Therefore, cumulatively, prediction errors for these implements were slightly higher. This indicates how important geometrical factors are.

Index values were considered as two different values viz. I_{GF} and I_D. The indexes (I_{GF}), which were based on the ratio of the tool geometrical factor to the tine, were for a particular tool and depth and were calculated in Appendix 12. The depth-index relationships were described with the regression equations as presented in Table 24 and plotted in Figure 42. The index values for all the tools except the mouldboard plough were relatively constant within the depth range of 0.15 to 0.35 m (see Appendix 12).

Table 24. Index (I_{GF}) Regression Equations of the Tools Used in 1991

Tool or tine	Regression equation	R^2 [%]
Disc	$I = 2.948 - 19.447\ d + 48.823\ d^2$	88.0
Mouldboard	$I = 4.317 - 17.434\ d + 100.047\ d^3$	83.1
Chisel	$I = 1.858 - 7.756\ d + 17.365\ d^2$	49.3
Subsoiler (without wing)	$I = 1.433 - 6.731\ d + 20.281\ d^2 - 20.050\ d^3$	60.1

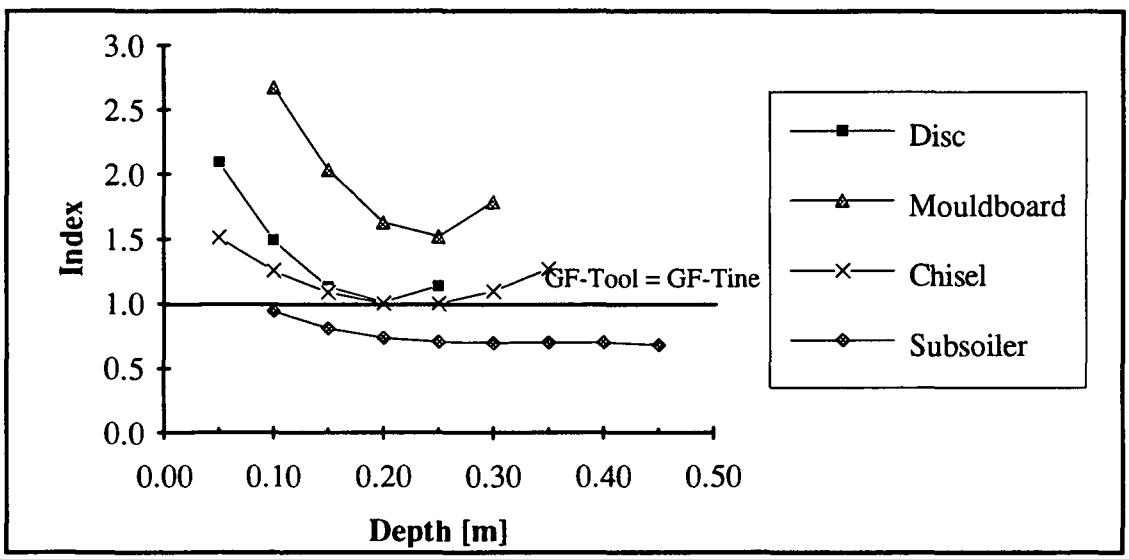

Figure 42. Index curves based on geometrical factor for the tools used in 1991

The indexes (I_D) based upon the ratio of the measured draught requirement of the tool to the standard tine were also calculated in Appendix 12 and plotted in Figure 43 and 44. It can be seen that there is a difference between the I_{GF} and I_D arising from the appropriateness of the standard tine to the implements associated with the geometry and complexity. The magnitude of the difference under the sandy loam soil condition was between 7.72 and 31.11 %. The same difference under the clay soil condition was between 5.85 and 54.83 % (Appendix 12).

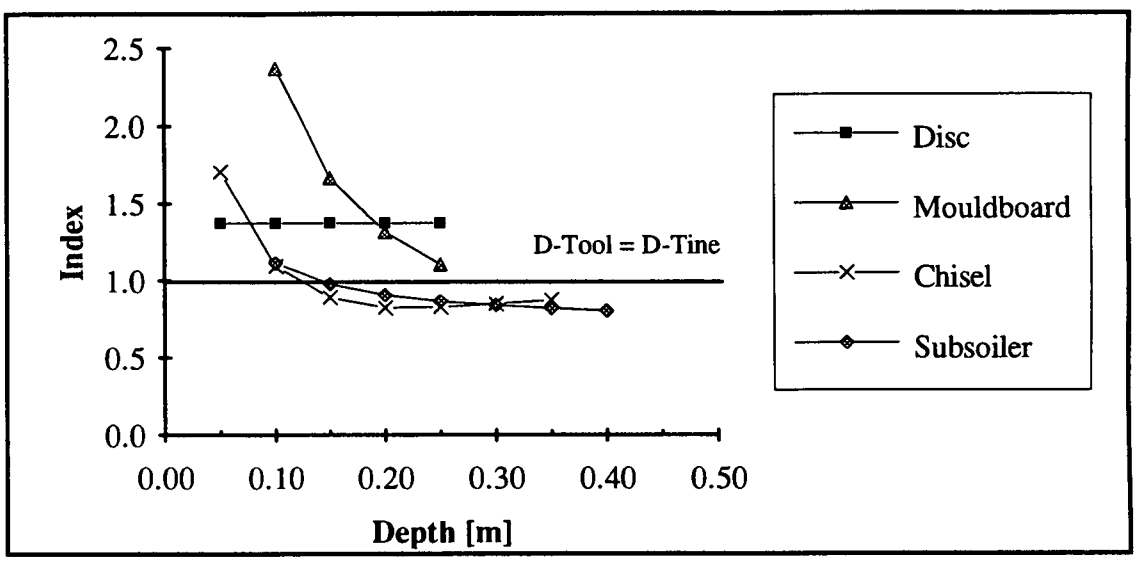

Figure 43. Index values based on the measured draught for the tools used in sandy loam soil: Downings-UK in 1991

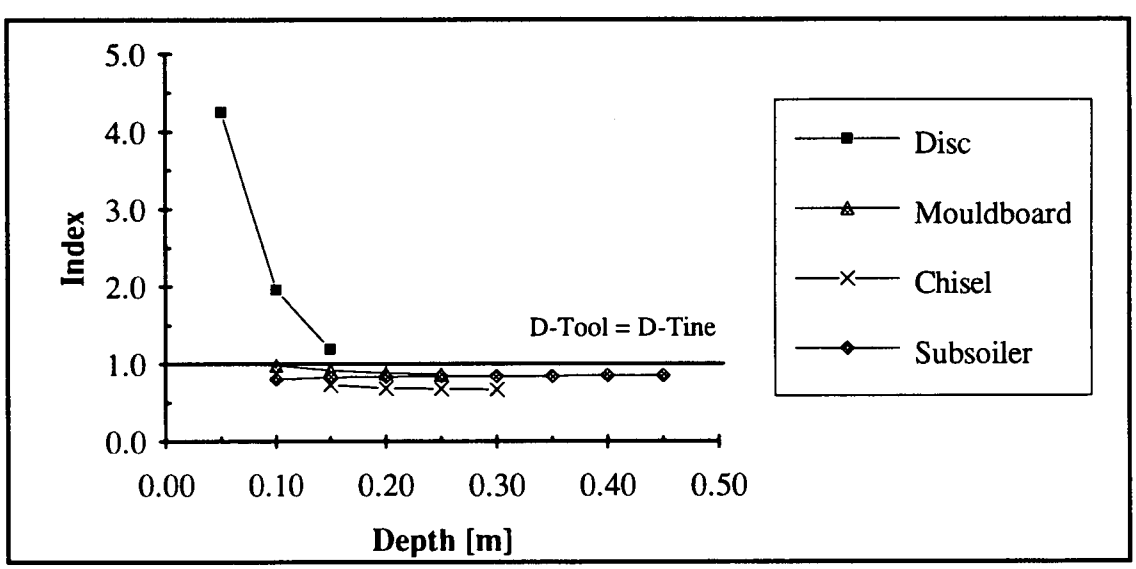

Figure 44. Index values based on the measured draught for the tools used in clay soil: GAP-Türkiye in 1991

5.5. Validation of The Concept

In 1993 the field tests were extended to a wide range of soil condition in terms of the validation of the concept. The same implements were used except for a winged type of subsoiler instead of wingless one. The draught measurement results of the standard tine are given in Table 25 in detail in Appendix 13. The draught-depth relationships given for the tine under three soil conditions were highly correlated with a coefficient of determination of > 0.988. The plot gave the best fit with the second order of the working depth (Fig. 45). The changes in the draught for a range of 0.10 to 0.40 m depth were between 3.48 % and 19.04 % at 95 % level of confidence interval on the Showground field. The same variation on Millbrook and Copse fields was 5.51 to 73.44 % and 2.95 to 12.40 %, respectively. The variation became greater at shallow depths i.e. 0.05 to 0.20 m (see Appendix 13).

Table 25. Regression Equations for Standard Tine in UK in 1993

Field	Regression equation	R^2 [%]*
Sandy Loam Soil (Showground)	$D = 12.006\ d + .25.509\ d^2$	98.8
Sandy Loam Soil (Millbrook)	$D = -0.683\ d + 64.407\ d^2$	99.4
Clay Soil (Copse)	$D = 20.645\ d + 60.181\ d^2$	99.4

* Value determined from the regression equation with constant

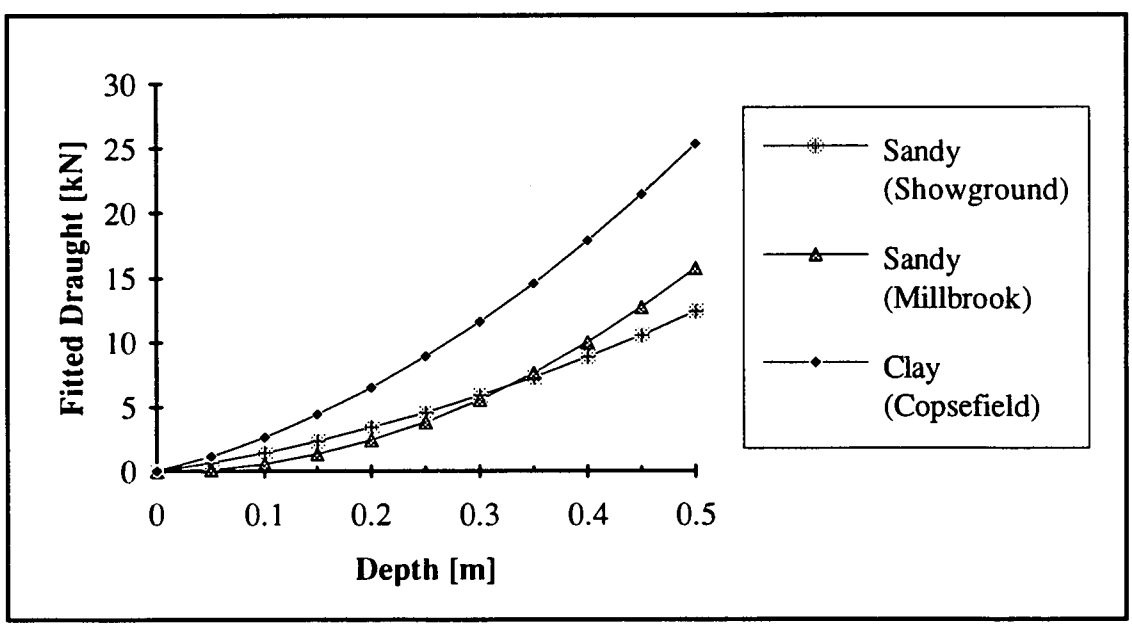

Figure 45. Draught-Depth relationship for standard tine in 1993

The geometrical factor and index values for the winged subsoiler are presented in detail in Appendix 14. Soil strength factors for the fields were also worked out by using the standard tine draught and geometrical factors and are given in Appendix 14. Considering these data, draught requirements of the implements used were predicted and compared with measured draughts (Table 26). Interactions given in Table 26 were calculated following same way expressed in Appendix 9. Based on mean values the graphs in Figure 46 were plotted.

Table 26. Comparison of Measured Draught with Predicted for Field tests in UK in 1993

Sandy Loam Soil (Showground Field)								
Implement	Depth [m] or [%]		Draught Force [kN] or [%]					
			Measured		Predicted			Prediction Error
	Mean	C.V.	Mean	C.V.	Mean	C.V.-I	C.V.-II	
D. Plough	0.174	5.75	12.902	9.97	8.948	6.20	10.88	-30.65
M. Plough	0.201	3.48	14.088	9.63	16.791	6.26	7.25	19.18
Chisel*	0.306	5.88	33.277	4.70	27.006	6.48	9.94	-18.84
W. Subsoiler	0.404	2.48	15.745	8.96	11.950	6.63	5.15	-24.11
* Tine interaction is 24.66 %								
Sandy Loam Soil (Millbrook Field)								
Implement	Depth [m] or [%]		Draught Force [kN] or [%]					
			Measured		Predicted			Prediction Error
	Mean	C.V.	Mean	C.V.	Mean	C.V.-I	C.V.-II	
D. Plough	0.147	10.20	9.481	25.54	4.432	23.78	10.22	-53.26
M. Plough	0.231	7.36	12.611	13.89	14.981	14.43	7.58	18.80
Chisel*	0.174	8.62	8.748	10.21	9.320	19.74	8.87	6.54
W. Subsoiler	0.417	5.76	12.426	15.47	14.246	7.47	5.58	14.64
* Tine interaction is 1.59 %								
Clay Soil (Copse Field)								
Implement	Depth [m] or [%]		Draught Force [kN] or [%]					
			Measured		Predicted			Prediction Error
	Mean	C.V.	Mean	C.V.	Mean	C.V.-I	C.V.-II	
D. Plough	0.144	6.94	18.717	10.33	14.689	3.74	10.48	-21.52
M. Plough	0.194	6.19	33.085	5.52	31.324	4.06	7.06	-5.32
Chisel*	0.174	8.62	39.987	6.09	27.558	3.94	8.86	-31.08
W. Subsoiler	0.334	8.08	22.845	5.85	19.546	4.73	3.75	-14.44
* Tine interaction is 1.59 %								

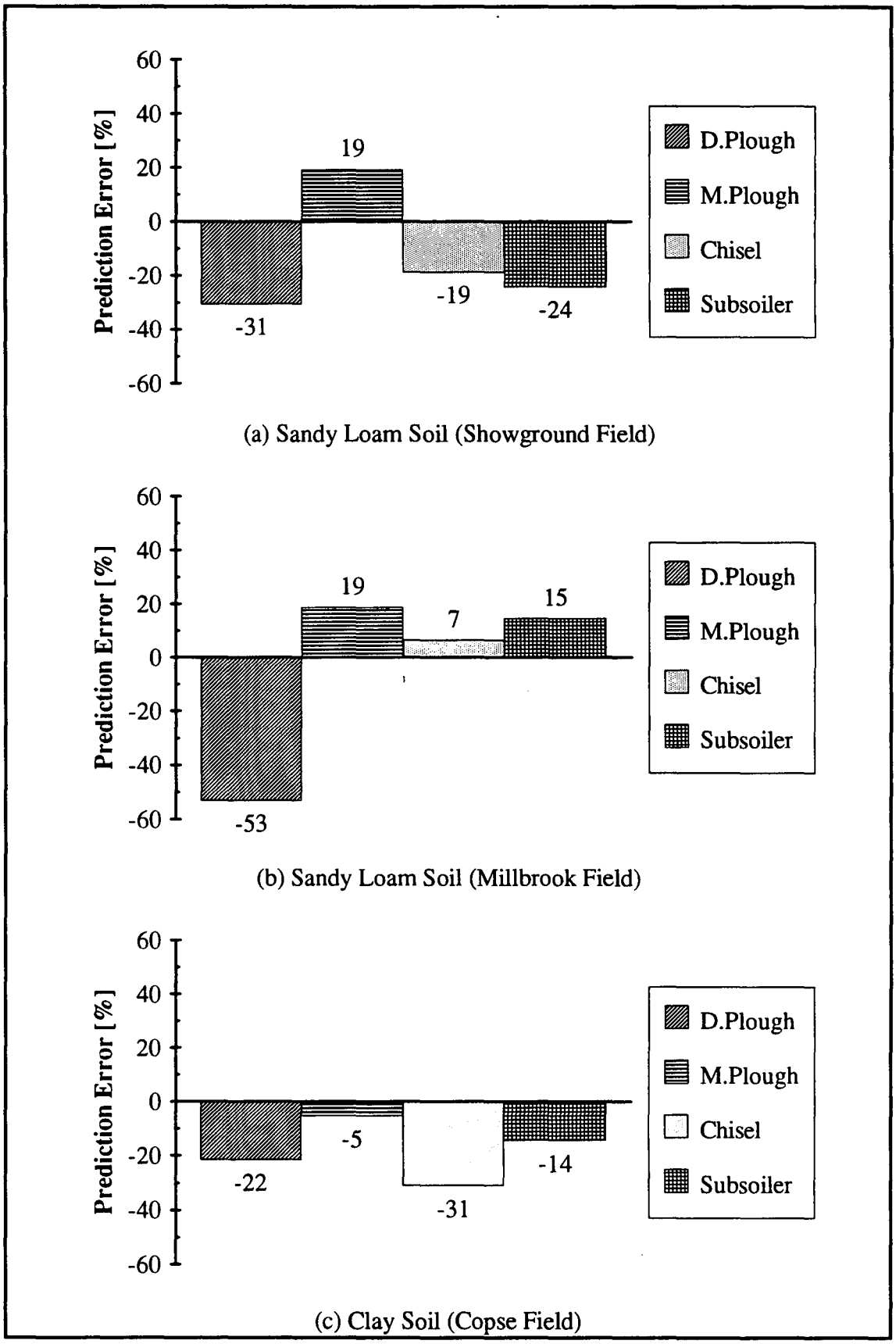

Figure 46. Prediction errors for the field tests in UK in 1993

Two coefficient of variations, C.V.-I and C.V.-II, in Table 26 were expressed to give some explanation relating prediction errors in Figure 46. C.V.-I and C.V.-II define variations in predicted draught due to the probability errors. The error band for the soil strength factor resulted in C.V.-I while the error for the geometrical factor caused C.V.-II. The magnitude of the C.V.-I for Showground, Millbrook and Copse fields varied between 6.2 to 6.63 %, 7.47 to 23.78 %, 3.74 to 4.73 %, respectively. The C.V.-II was equal to 5.15 to 10.88 %, 5.58 to 10.22 %, 3.75 to 10.48 %, respectively. In addition, the variation in the working depth during the field tests was recorded and was under ±10 % for all fields.

Prediction errors presented in Figure 46 varied between 5.32 and 53.26 % depending upon implement and soil conditions. The worst case was seen with the disc plough on Millbrook field which had gave the largest variation of 23.78 % C.V.-II in soil strength factor. The rest of the values showed reasonable agreement within ±20 % error bands.

Consequently, the results obtained in 1991 were verified with extended field work.

5.6. Comparison between the Models

Having a concept giving a novel and simple approach for predicting the draught forces acting upon tillage implements the next stage was to investigate how good the model is when it is compared with the current methods such as ASAE D497 Agricultural Machinery Management Data and Witney (1988) which have been widely used.

The draught forces were predicted for the mouldboard plough using the ASAE, Witney (1988) and the model developed in this thesis. However, for the other implements i.e. disc plough, chisel, subsoiler, only the ASAE could be compared as Witney's technique was limited to mouldboard ploughs. The predictions were made at a reasonable working depth range for both sandy loam soil and clay soil conditions. The results are presented in Appendix 15.

Figure 47, 48, 49 and 50 show the relationships between the depth and predicted draught forces of the implements under the sandy loam and clay soil conditions. For the disc plough and the chisel ASAE predictions give much larger forces (mean for the disc plough: 2.96 and 3.02 times for sandy loam and clay soils, respectively; mean for the chisel: 2.44 and 2.15 times for sandy loam and clay soils, respectively) than the predicted by Kirişci for both sandy and clay soils.. The ASAE values for disc plough and the chisel are also much larger (mean: 2.66 and 2.89 times for the disc plough in sandy loam and clay soil conditions, respectively; 3.20 and 2.22 times for the chisel in sandy loam and clay soil conditions) than measured draughts during the field tests for both sandy loam and clay soils. The results of Kirişci are close to the measured values. For the mouldboard plough in clay soil the ASAE force predictions are generally similar to these of Kirişci, but these of Witney are much lower (mean: 3.42 times) than the predicted by Kirişci and also lower (mean: 2.70) than the measured draughts. For sandy soils, however, the Witney forces are much larger (mean: 2.10 and 1.35 times, respectively) than the ASAE and the measured values, with these of Kirişci being rather lower than the Witney prediction (mean: 1.35 times). For the subsoiler the predictions of Kirişci are also lower than the ASAE values (mean: 1.36 times) for a clay soil but for a sandy soil the results are comparable.

Overall, the ASAE values give draught force predictions which are much greater than these observed in this work. The results of Witney for a mouldboard plough seem anomalous in that the predicted draught for a sandy soil is very much greater than for a clay soil as shown by the experimental work of this program and results of this program and results of Rogers and Hawkins (1956).

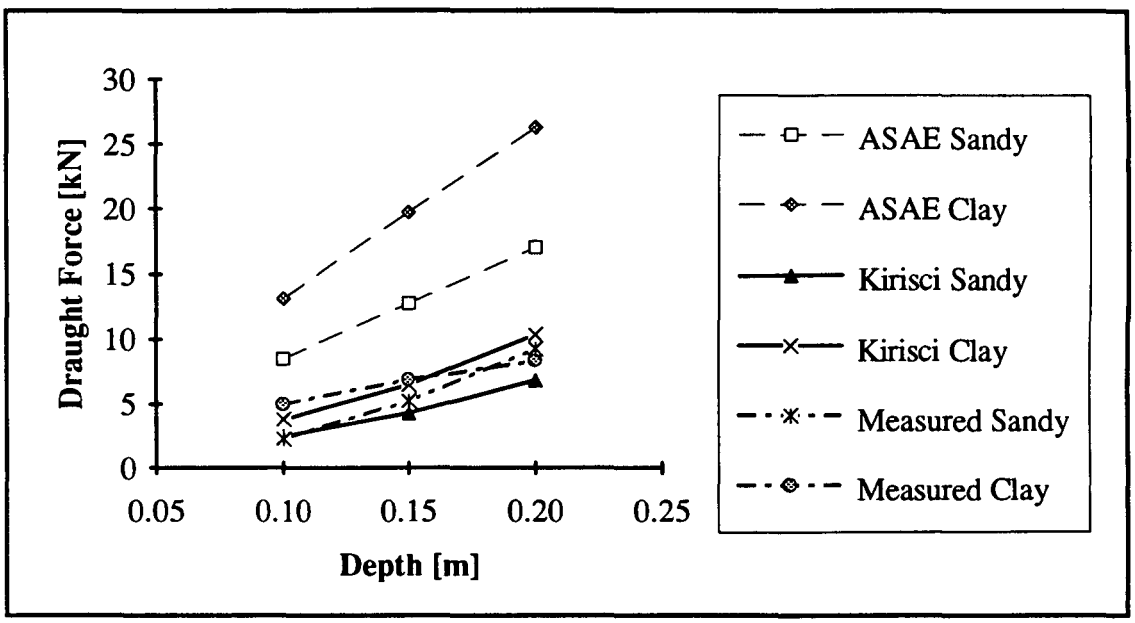

Figure 47. Comparison between draught forces predicted by different methods for disc plough

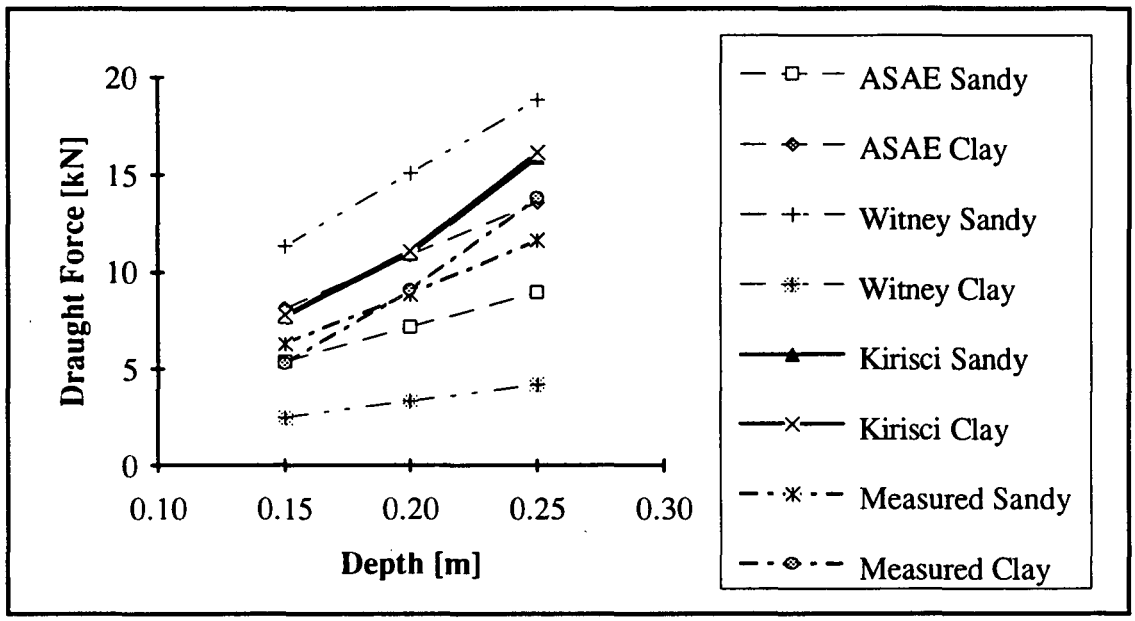

Figure 48. Comparison between draught forces predicted by different methods for mouldboard plough

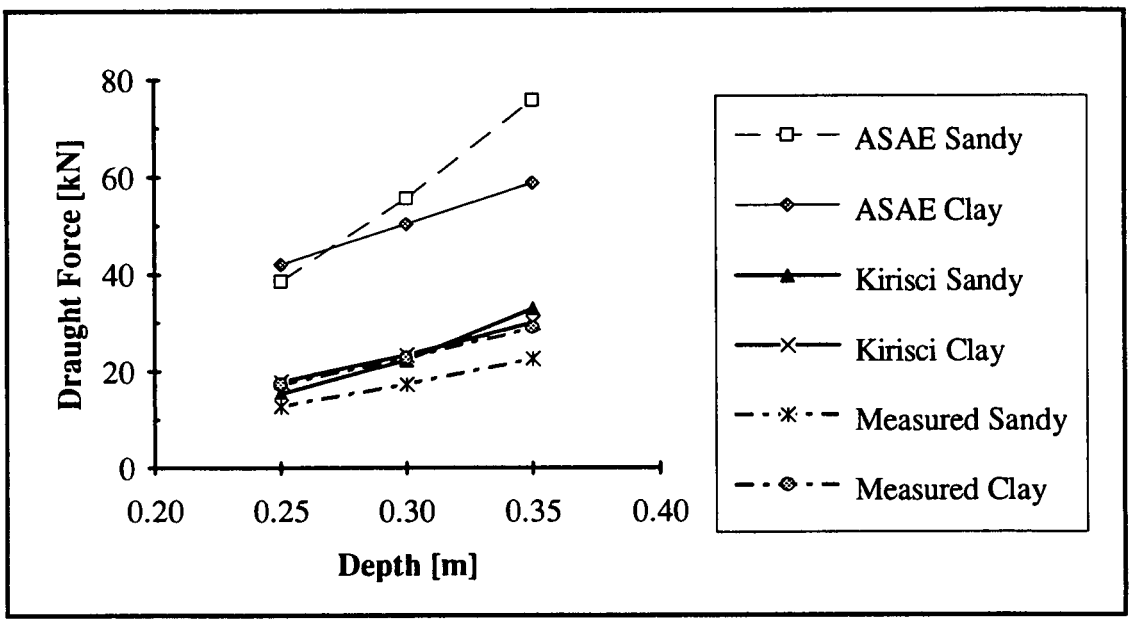

Figure 49. Comparison between draught forces predicted by different methods for chisel

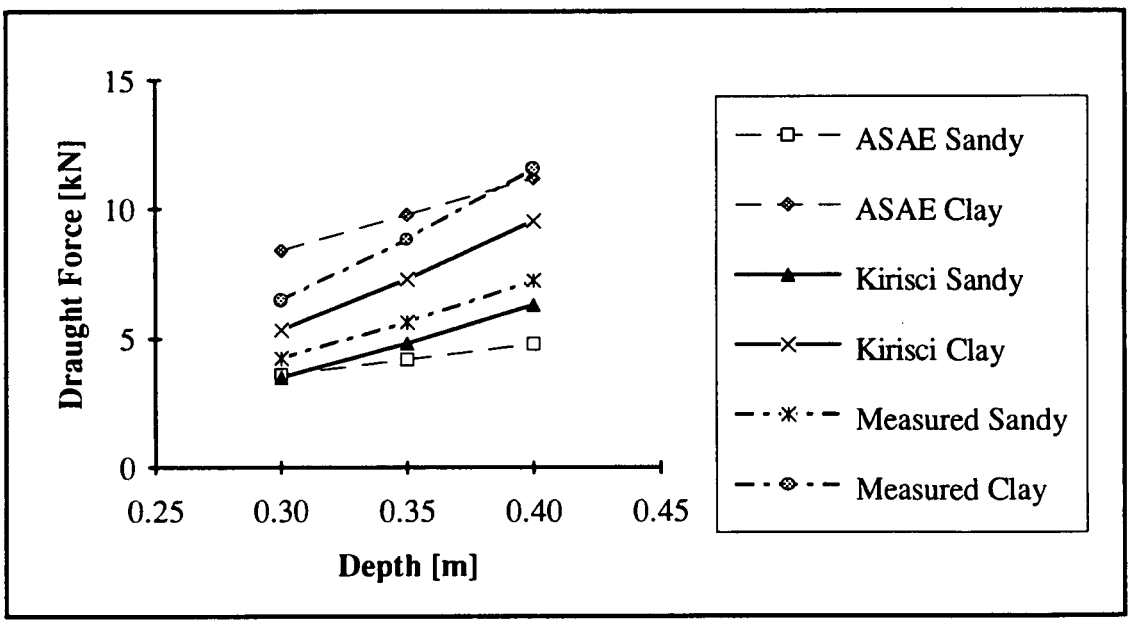

Figure 50. Comparison between draught forces predicted by different methods for subsoiler

In fact, comparing Kirişci's results with others can be misleading since Kirişci's method takes the implement and soil characteristics into account directly in a particular field and are much more representative. The ASAE and Witney models give a global figure for the draught of the implement which cannot therefore be used for specific work. ASAE data are limited to soil type, implement type, speed and working depth. Furthermore, the data have a wider variation so that the ratio of the lower to the upper draught limits for the chisel is approximately five.

ASAE data and Witney systems cannot be used for a mechanisation planning in a particular area since they have a wide range and have limited applications to specific implements and soil conditions. However, Kirişci's model which eliminates the need to take the implements to the field is practical and provides more realistic values for mechanisation planning in specific areas, i.e. GAP region although the model still needs to take the standard tine to the field.

6. CONCLUSIONS AND RECOMMENDATIONS

6.1. Conclusions

1. An effective a three-point linkage dynamometer system was designed and built as a research tool to measure draught and vertical forces. The system was compact and eliminated the need for bulky transducer amplifiers, bridge balancing equipment, and 240 V AC power supply by using a datalogger. All transducers outputs were linear with a coefficient of determination, $R^2 > 0.999$ and were also repeatable. The hysteresis errors were less than 1.00 % [f.s.] and within acceptable limits.

2. Bi-axial linkage extended octagonal rings were the most sensitive transducers. The sensitivities of the perpendicular and coincident bridges for the left ring were 0.075 $\mu V\ V^{-1}\ N^{-1}$ and 0.063 $\mu V\ V^{-1}N^{-1}$, respectively. The right ring had similar sensitivities. The effect of load direction on the output was negligible. The cross sensitivity errors were less than 0.0003 $\mu V\ V^{-1}N^{-1}$. The rotary position transducer was successful in sensing the angle of cross-shaft. It was the simplest and cheapest transducer in the system. The average sensitivity of the top link transducer was small at 0.010 $\mu V\ V^{-1}\ N^{-1}$ due to the top link strain values being small. However, it gave satisfactory results and was an important part of the system.

3. Generally, the system can be used as a reliable tool to describe the draught force acting upon a tillage implement. The system has all advantages of an integrated linkage dynamometer. However, it requires high level of workshop and instrumentation skill for manufacture and calibration. A disadvantage of the system is that cannot be moved easily between tractors. The spreadsheet model was versatile and easy to use for plotting the forces as well as for calculations on the three-point linkage.

4. Field experiments were conducted to determine draught force requirements of tillage implements such as disc plough, mouldboard plough, chisel and subsoiler both under sandy loam soil condition at a reasonable depth range in UK and clay soil condition in Türkiye. The standard tine which has a 45^o rake angle was used together with the implements as a reference tine. The field tests were continued to examine the validation of a predictive model for different soil conditions in UK such as dry, wet, light and heavy soil conditions.

5. A simple method was developed to predict tillage forces for a range of implements so that it was not necessary to measure individual Mohr-Coulomb soil properties, such as cohesion (c) and angle of internal shearing resistance (ϕ), which are not easy to obtain in remote areas under field conditions. The method eliminates the need to use implements in the field for future studies such as mechanisation planning. The standard tine should be taken to the field to measure the soil strength factor under the field condition.

6. The model is adequate for predicting the draught requirements of a tillage implement within a ± 20 % error if two extreme cases are ignored, although the predictions gave a varying agreement with the measured draughts of the implements depending particularly on soil conditions and working depth. This range is still valid when the variation in the geometrical factor and soil strength factor are considered. Furthermore, the variations in soil characteristics in a same field represents a variation contribution of ±10 %. The probability error bands for the geometrical factor and soil strength factor were important factors in causing the largest prediction errors. The geometrical factor was momentous particularly for the multi-tined implements such as disc plough, mouldboard plough and chisel.

7. The model was also compared with other current prediction approaches such as ASAE D497 Agricultural Machinery Management Data and Witney (1988). The model of Kirişci showed a closer prediction than the others and are much more reliable since the model is based on experimental data including both soil and implement characteristics. The model needs to take the standard tine to the field site. Predictions due to Witney (1988) for a mouldboard plough seem anomalous and cannot be explained. The ASAE data are not specific for a mechanisation planning in a particular area.

8. The model is valuable for areas like the GAP region where the forces on a simple tine can be used to predict the draught requirement for the region and a large sample of soil conditions can be evaluated.

6.2. Recommendations

The following recommendations for further work arise from the study.

1. The geometrical factors should be determined for a wider range of implements having different geometries. This could reduce the error bands of the factor itself. The concept should be extended to the other primary and secondary tillage implements.

2. It would be of value to study different standard tines having a foot, wing and bottom to be able reduce the prediction errors for a wider range of tillage implements.

3. Variations in the soil strength factor should be minimised by conducting more field experiments under different conditions.

4. The working depth is a crucial parameter which the researchers requires and the measurement in the field should be made more accurately.

5. The top link sensitivity should be increased by replacing the turnbuckle with different material. In addition, the strain gauge application could be applied to the existing links on a three-point linkage system.

6. During ploughing the lower links were not at the same level. Therefore, only one rotary position transducers on each cross-shaft can be mounted although the angle is not important for the horizontal (draught) force rather than vertical due to being small. This will enable the angle of the lower links to be sensed independently.

REFERENCES

AMA, 1990. *General and Statistical Data Catalogue on the Turkish Automotive Industry*.İstanbul-Türkiye: Automotive Manufacturers Association (AMA).

Bandy, S.M., W.A. Babacz, J. Grogan, S.W. Searcy and B.A. Stout. 1985. Monitoring tractor performance with three-point hitch dynamometer and an on-board microcomputer. ASAE Paper No. 85-1078. St. Joseph, MI: ASAE.

Barker, G.L., L.A. Smithand R.F. Colwick. 1981. Three-point hitch dynamometer for directional force measurement. ASAE Paper No. 81-1044. St. Joseph, MI: ASAE.

Chaplin, J., M. Leuders and Y. Zhao. 1987. Three-point hitch dynamometer design and calibration. *Applied Engineering in Agriculture* 3(1):10-13.

Chi, L. and R.L. Kushwaha. 1989. Finite element analysis of forces on a plane soil blade. *Canadian Agricultural Engineering* 31(2):135-140.

Chung, Y.G., S.J. Marley and W.F. Buchele. 1983. Development of a three-point hitch dynamometer. ASAE Paper No. 83-1035. St. Joseph, MI: ASAE.

Cook, N.H., E.G. Loewen and M.C. Shaw. 1954. Machine-tool dynamometers. *American Machinist* 98 (May):125-129.

Cook, N.H. and E. Rabinowicz. 1963. *Physical Measurements and Analysis*. New York: Addison-Wesley.

Cox, S.W.R. 1988. *Farm Electronics*. Oxford: BSP Professional Books.

Culpin , C. 1986. *Farm Machinery*. Oxford: BSP Professional Books.

Desbiolles, J. 1994. Tillage force models for mechanisation planning. Ph.D. thesis (Unpublished), Cranfield University, Silsoe College, Silsoe, Bedford.

Dransfield, P., S.T. Willatt and A.H. Willis. 1964. Soil-to-implement reaction experienced with simple tines at various angles of attack. *J. Agric. Eng. Res.* 9(3):220-224.

Dwyer, M.J. and P. Febo. 1987. Handbook of agricultural tyre performance. AFRC Institute of Engineering Research-47, Silsoe.

Garner, T.H., R.B. and D. Dodd. 1985. Application of a three-point hitch dynamometer. ASAE Paper No. 85-1077. St. Joseph, MI: ASAE.

Garner, T.H., R.B. Dodd, D. Wolf and U.M. Peiper. 1988. Force analysis and application of a three-point hitch dynamometer. *Transactions of the ASAE* 31(4):1047-1053.

Gee-Clough, D. 1980. Selection of tyre sizes for agricultural vehicles. *J. Agric. Eng. Res.* 25:261-278.

Gill, W.R. and G.E. Vanden Berg. 1968. *Soil Dynamics in Tillage and Traction.* Washington, D.C.: U.S. Agricultural Research Service USDA.

Godwin, R.J. 1974. An investigation into the mechanics of narrow tines in frictional soils. Ph.D. thesis, National College of Agricultural Engineering, Silsoe, Bedford.

Godwin, R.J. 1975. An extended octagonal ring transducer for use in tillage studies. *J. Agric. Eng. Res.* 20:347-352.

Godwin, R.J. 1982. Force measurement on tillage tools. In. *Proc. 9th Conference of the International Soil Tillage Research Organisation.* Osijeck, Yugoslavia.

Godwin, R.J., A.J. Reynolds, M.J. O'Dogherty and A.A. Al-Ghazal. 1993. A triaxial dynamometer for force and moment measurements on tillage implements. *J. Agric. Eng. Res.* 55:189-205.

Godwin, R.J. and G. Spoor. 1977. Soil failure with narrow tines. *J. Agric. Eng. Res.* 22(3):213-228.

Godwin, R.J., G. Spoor, M.S. Soomro. 1984. The effect of tine arrangement on soil forces and disturbance. *J. Agric. Eng. Res.* 30:47-56.

Godwin, R.J., P.S.G. Magalhaes, S.M. Miller and R.K. Fry. 1987. Instrumentation to study the force systems and vertical dynamic behaviour of soil-engaging implements. *J. Agric. Eng. Res.* 36:301-310.

Grisso, R.D. and J.V. Perumpral. 1985. Review of models for predicting performance of narrow tillage tool. *Transactions of the ASAE* 28(4):1062-1067.

Grisso, R.D., S.A. Al-Hamed, R.K. Taylor and F.M. Zoz. 1992. Demonstrating tractor performance trends using Lotus templates. *Applied Engineering in Agriculture* 8(6):733-738.

Hall, D.M. 1991. Soil management information system: data collection and analysis for use in an expert system for compaction alleviation. B.Sc. thesis (Unpublished), Cranfield Institute of Technology, Silsoe College, Silsoe, Bedford.

Hanna, H.M., G.C. Erbach, S.J. Marley, S.W. Merlin. 1993. Comparison of the Goryachkin theory to soil flow on a sweep. *Transactions of the ASAE* 36(2):293-299.

Hettiaratchi, D.R.P. and A.R. Reece. 1967. Symmetrical three-dimensional soil failure. *J. Terramechanics*. 4(3):45-67.

Hettiaratchi, D.R.P. and A.R. Reece. 1974. The calculation of passive soil resistance. *Geotechnique*. 24(3):289-310.

Hettiaratchi, D.R.P., B.D. Witney and A.R. Reece. 1966. The calculation of passive pressure in two-dimensional soil failure. *J. Agric. Eng. Res.* 11(2):89-107.

Hunt, D.R. 1983. *Farm Power and Machinery Management (Eighth Edition)*. Iowa: The Iowa State University.

Jensen, J.K. 1954. Experimental stress analysis. *Agricultural Engineering* 35(9):625-629, 634.

Johnson, C.E. and W.B. Voorhees. 1979. A force dynamometer for three-point hitches. *Transactions of the ASAE* 22(2):226-228, 232.

Kawamura, N. 1985. Soil dynamics and its application to tillage machineries. *Research Report on Agricultural Mechanisation* 15:1-22. Kyoto, Japan.

Kepner, R.A., R. Bainer and E.L. Barger. 1982. *Principles of Farm Machinery*. Connecticut: AVI Publ. Company Inc.

Kilgour, J., S.A. Al-Suhaibani and B.S. Blackmore. 1988. Three-point linkage dynamometer for Cat.II and Cat.III tractors. Unpublished Project Report, Silsoe.

Kirişci, V. and İ. Akıncı. 1992. Force system for a tractor three-point linkage. In *Proc. 14th National Conference on Agricultural Mechanisation* 346-354. Samsun, Türkiye 14-16 Oct.

Kirişci, V., B.S. Blackmore, R.J. Godwin and J. Blake. 1993. Design and calibration of three different three-point linkage dynamometers. ASAE Paper No. 93-1009. St. Joseph, MI: ASAE.

Kirişci, V., B.S. Blackmore, J. Kilgour, R.J. Godwin and A.S. Babier. 1992. A three-point linkage dynamometer system. In *Proc. Int. Conference on Agricultural Engineering*. Uppsala, Sweden, 1-4 June.

Kostritsyn, A.K. 1956. Cutting of a cohesive soil medium with knives and cores. Translation 58, NIAE, Silsoe, Bedford.

Lal, R. 1959. Measurement of forces on mounted implements. *Transactions of the ASAE* 2(1):109-111.

Lowen, E.G. and N.H. Cook. 1956. Metal cutting measurements and their interpretation. In *Proc. Soc. Exp. Stress Analysis.* 13(2):57-62.

Luth, H.J. and R.D. Wismer. 1971. Performance of plane soil cutting blades in sand. *Transactions of the ASAE* 14(2):255-259, 262.

McKyes, E. and O.S. Ali. 1977. The cutting of soil by narrow blades. *J. Terramechanics* 14(2):43-58.

McLaughlin, N.B., L.C. Heslop, D.J. Buckley, G.R.St. Amour, B.A. Compton, A.M. Jones, P.Van Bodegom. 1993. A general purpose tractor instrumentation and data logging system. *Transactions of the ASAE* 36(2):265-273.

Miller, P.C.H. 1971. Soil failure and the nature of the force system with very narrow tines. Unpublished B.Sc. thesis, National College of Agricultural Engineering, Silsoe, Bedford.

O'Callaghan, J.R. and K.M. Farrelly. 1964. Cleavage of soil by tined implements. *J. Agric. Eng. Res.* 9(3):259-270.

O'Callaghan, J.R. and P.J. McCullen. 1965. Cleavage of soil by inclined and wedge-shaped tines. *J. Agric. Eng. Res.* 10(3):248-254.

O'Dogherty, M.J. 1975. A dynamometer to measure the forces on a sugar beet topping knife. *J. Agric. Eng. Res.* 20:339-345.

O'Dogherty, M.J. 1986. A tri-axial dynamometer for soil trough measurements of forces on soil working components. *J. Agric. Eng. Res.* 34:141-147.

Osman, M.S. 1964. The mechanics of soil cutting blades. *J. Agric. Eng. Res.* 9:313-328.

Payne P.C.J. 1956. The relationship between the mechanical properties of soil and the performance of simple cultivation implements. *J. Agric. Eng. Res.* 1(1):23-50.

Payne P.C.J. and D.W. Tanner 1959. The relationship between rake angle and the performance of simple cultivation implements. *J. Agric. Eng. Res.* 4(4):312-325.

Perry, C.C. and H.R. Lissner. 1962. *The Strain Gauge Primer (Second Edition).* New York: McGraw-Hill Book Company.

Perumpral, J.V., R.D. Grisso and C.S. Desai. 1983. A soil-tool model based on limit equilibrium analysis. *Transactions of the ASAE* 26(4):991-995.

Plasse, R., G.S.V. Raghavan and E. McKyes. 1985. Simulation of narrow blade performance in different soils. *Transactions of the ASAE* 28(4):1007-1012.

Reece, A.R. 1961. A three-point linkage dynamometer. *J. Agric. Eng. Res.* 6(1):45-50.

Reece, A.R. 1965. The fundamental equation of earth-moving mechanics. In *Proc. Symposium on Earth-Moving Machinery,* 16-22. London: The Automobile Division, The Institution of Mechanical Engineers.

Reece, A.R. and D.R.P. Hettiaratchi. 1989. A slip line method for estimating passive earth pressure. *J. Agric. Eng. Res.* 42:27-41.

Reid, J.T., L.M. Carter and R.L. Clark. 1985. Draft measurements with a three-point hitch dynamometer. *Transactions of the ASAE* 28(1):89-93.

Reid, J.T., L.M. Carter and R.L. Clark. 1983. Draft requirements with a three-point dynamometer. ASAE Paper No. 83-1036. St. Joseph, MI: ASAE.

Rogers, O.J.J. and J.C. Hawkins. 1956. Soil loads on plough bodies, Parts I and II. Tech. Memo. 105. Silsoe: NIAE.

Rogers, I.C. and C.N. Johnston. 1953. Measuring the forces in tractor linkage. *Agricultural Engineering* 34(8):542-545.

Sağlam, R. 1987. A research on planning and determining the present situation of agricultural mechanisation in the Harran Plain. M.Sc. thesis, Çukurova University, Adana, Türkiye.

Scholtz, D.C. 1964. A three point linkage dynamometer for mounted implements. *J. Agric. Eng. Res.* 9(3):252-258.

Scholtz, D.C. 1966. A three point linkage dynamometer for restrained linkages. *J. Agric. Eng. Res.* 11:33-37.

Schuring, D.J. and R.I. Emori. 1965. Soil deforming processes and dimensional analysis. *Transactions of the ASAE* 485.

Sındır, K.O. 1992. Agricultural mechanisation systems planning for the irrigated GAP region. Ph.D. thesis, Cranfield Institute of Technology, Silsoe College, Silsoe, Bedford.

Siemens, J.C., J.A. Weber and T.H. Thornburn. 1965. Mechanics of soil as influenced by model tillage tools. *Transactions of the ASAE* 8(1):1-7.

SIS, 1988. *The Summary of Agricultural Statistics,* 1988. Ankara-Türkiye: State Institute of Statistics (SIS).

SIS, 1993. *Statistical Year Book of Türkiye,* 1991. Ankara-Türkiye: State Institute of Statistics (SIS).

Smith, D.L.O., R.J. Godwin and G. Spoor. 1989. Modelling soil disturbance due to tillage and traffic. *Mechanics and Related Processes in Structured Agricultural Soils 121-136.*

Smith, L.A. and G.L. Barker. 1982. Equipment to monitor field energy requirements. *Transactions of the ASAE* 25(6):1556-1559.

Sokolovski, V.V. 1960. *Statistics of Soil Media.* London: Butterworth.

Söhne, W. 1956. Some basic considerations of soil mechanics as applied to agricultural engineering. National. Institute of Agricultural. Engineering. Translation No. 53. Grundlagen der Landtechnik 7:11-27.

SPO, 1989. *GAP The South-eastern Anatolia Project Master Plan Study, Final Master Plan Report, 4 Volumes.* Ankara-Türkiye: State Planning Organisation (SPO).

Spoor, G. and R.J. Godwin. 1978. An experimental investigation into the deep loosening of soil by rigid tines. *J. Agric. Eng. Res.* 23(3):243-258.

Stafford, J.V. 1979a. The performance of rigid tine in relation to soil properties and speed. *J. Agric. Eng. Res.* 24:41-56.

Stafford, J.V. 1979b. Force prediction models for brittle and flow failure of soil by draught tillage tools. *J. Agric. Eng. Res.* 29:51-60.

Stafford, J.V. 1981. An application of critical state soil mechanics: the performance of rigid tines. *J. Agric. Eng. Res.* 26:387-401.

Stafford, J.V. 1984. Force prediction models for brittle and flow failure of soil by draught tillage tools. *J. Agric. Eng. Res.* 29:51-60.

Steel, R.G.D. and J.H. Torrie. 1980. *Principles and Procedures of Statistics: Biometrical Approach (Second Edition).* Kogagusha: McGraw-Hill Book Co. Inc.

Swick, W.C. and J.V. Perumpral. 1988. A model for predicting soil-tool interaction. *Terramechanics 25(1):43-66.*

Terzaghi, K. 1962. *Theoretical Soil Mechanics.* Newyork: John Wiley and Sons, Inc.

Thomson, N.P. and K.J. Shinners. 1989. A portable instrumentation system for measuring draft and speed. *Applied Engineering in Agriculture* 5(2):133-137.

Upadhyaya, S.K., L.J. Kemble, N.E. Collins and F.A. Camargo, Jr. 1985. Accuracy of mounted implement draft prediction using strain gages mounted directly on three-point hitch linkage system. *Transactions of the ASAE* 28(1):40-46, 50.

Vanden Berg, G.E. 1966. Analysis of forces on tillage tools. *J. Agric. Eng. Res.* 11(3):201-205.

Wang, J.K. and T. Liang. 1970. A new technique for draft prediction. *J. Agric. Eng. Res.* 15(2):111-116.

Willatt, S.T. and A.H. Willis. 1965. A study of the trough formed by the passage of tines through soil. *J. Agric. Eng. Res.* 10(1):1-4.

Witney, B.D. 1988. *Choosing and Using Farm Machines*. London: Longman, Scientific and Technical Publ.

Witney, B.D. and K.E. Oskoui. 1982. The basis of tractor power selection on arable farms. *J. Agric. Eng. Res.* 27:513-527.

Yong, R.N. and A.W. Hanna. 1977. Finite element analysis of plane soil cutting. *Journal of Terramechanics* 14(3):103-125.

Zelenin, A.N. 1950. Fizicheski osmovie teorii rezaniye gruntow (Basic physics of the theory of soil cuttings), Akademia Newk USSR, Moscow-Leningrad (NIAE Translation).

Zoerb, G.C. 1963. A strain gage dynamometer for direct horsepower indication. *Agricultural Engineering* 44(8):434-435, 437.

Zoz, F.M. 1972. Predicting tractor field performance. *Transactions of the ASAE* 15(2):249-255.

Zoz, F.M. 1987. Predicting tractor field performance. ASAE Paper No. 87-1623. St. Joseph, MI: ASAE.

APPENDIX 1

Tractor Force System for Mounted Implements

In operation at a depth and constant speed a simple tillage tool or implement, as shown in Figure A1.1, is subjected to soil forces. The resultant of soil forces has two major components *H* and *V* in XY-plane. The power unit should produce enough force which is equal and opposite to the resultant of soil forces so as to be able to pull the implement.

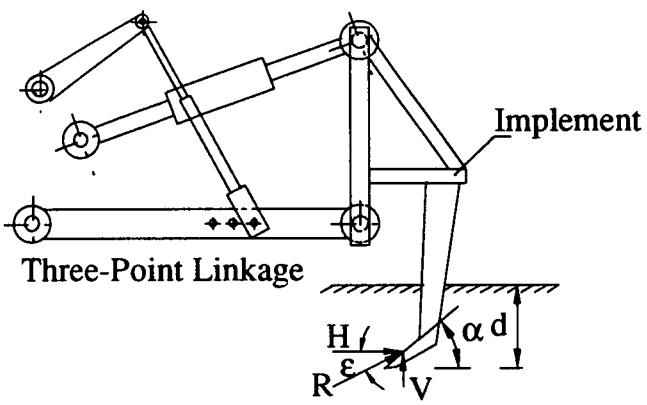

Figure A1.1. The forces acting upon a tillage implement

The force system between a tractor and mounted implement is much more complex than between a tractor and trailed implements due to the nature of the attachment system. Figure A1.2. shows the resultant exerted by a mounted implement on a conventional three-point linkage system.

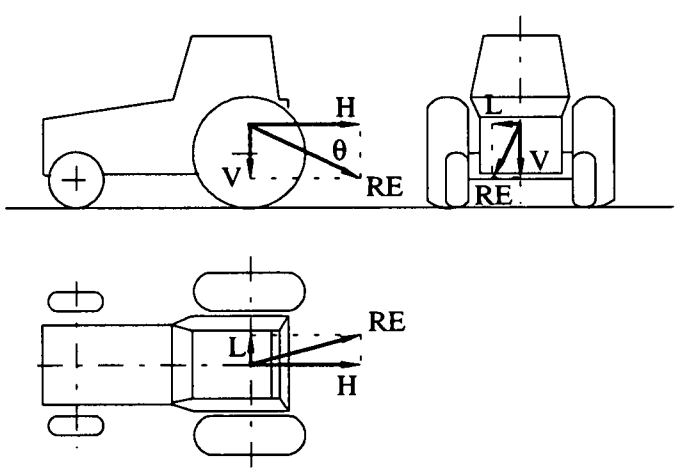

Figure A1.2. Forces acting between a tractor and mounted implement.

This force has components in all the major planes of the tractor assuming that the tractor is working along a horizontal plane surface. Therefore, the force can be resolved into three components *H*, *V*, and *L*, which are parallel to the major axes of the tractor.

The component *H* is the main component of the resultant which is parallel to the direction of travel, and generally this is assumed as the draught of implement. This force should be measured to determine the traction required from the tractor. The vertical component, *V*, is the second important part of the resultant. It has the effect of adding load to the tractor rear wheels, and removing load from the front wheels. It also determines the implement penetration ability, and maintains depth as well as having the effect on the draught of the implement because of the friction forces associated with this force. Finally, the side force, *L*, exists only in the case of using asymmetrical implements. It causes some stability problems for either or both tractor and implement, and increases the draught of the implement because of the friction produced. However, this force is non-existent for symmetrical implements which are much more common, and can be neglected as it is small (Lal, 1959; Kilgour et al., 1988).

The forces system between a tractor and implement can be also given as a resultant of the sub-component forces acting upon the two tractor lower links and top link (Fig. A1.3).

The resolution followed is based on three angles which are the angle of the lower links in the XY- plane (α), the angle of the top link (β), and the angle of the lower links in the XZ-plane (ψ). Numbers 1, 2 and 6 refer to pin joints to attach to the tractor and 5 and 6 to the implement.

The relative position of all the pin joints and angles can be calculated by using the cross-shaft angle (Kilgour et al., 1988). The tractor rear axle and centre line are main references to define each joint position. The forces on the links are either compressive or tensile depending on the position of the three-point linkage. Both the angle of the lower links in the XY-plane (α) and the top link angle (β) play the greatest role while the angle of lower links in the XZ-plane is less important. This angle remains constant when a quick-attach coupler is used. Normally, it varies between 10-15^{o} (Bandy et al., 1985).

To make the force system simpler and understandable Kirişci and Akıncı (1992) took the pin joints *5R*, *5L*, and *6* for the implement into account individually, and resolved the forces into components which are shown in Figure A1.4. The definitions used and assumptions made are presented in Table A1.1.

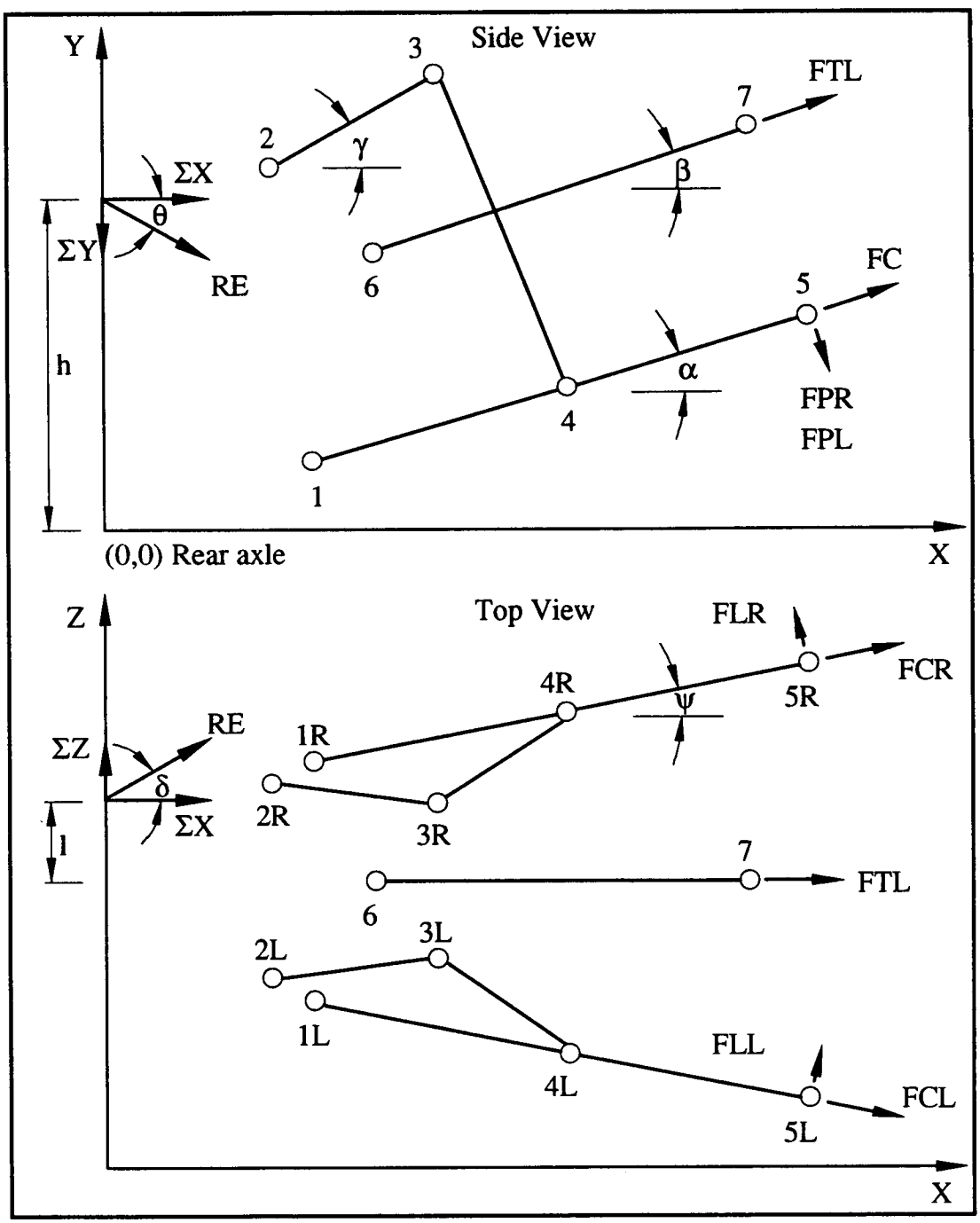

Figure A1.3. Force system for a three-point linkage system in XY and XZ-Planes

The resultant (*RE*) is the vector summation of its major components which are ΣX, ΣY and ΣZ which must be known. However, ΣX and ΣY include the total forces of *FX* or *FY* in lower links and *FTL*'s component in the top link with a mounted implement on a three-point linkage system.

Therefore, *FX* can be expressed as:

$$FX = FXR + FXL \qquad [A1.1]$$

where

$$FXR = FPR\sin\alpha\cos\psi + FCR\cos\alpha\cos\psi - FLR\sin\psi$$
$$FXL = FPL\sin\alpha\cos\psi + FCL\cos\alpha\cos\psi + FLL\sin\psi$$

Similarly, *FY* and *FZ* can be also determined as:

$$FY = FYR + FYL \qquad [A1.2]$$

$$FZ = FZR + FZL \qquad [A1.3]$$

where

$$FYR = FPR\cos\alpha - FCR\sin\alpha$$
$$FYR = FPL\cos\alpha - FCL\sin\alpha$$

and

$$FZR = FPR\sin\alpha\sin\psi + FCR\cos\alpha\sin\psi + FLR\cos\psi$$
$$FZL = FPL\sin\alpha\sin\psi + FCL\cos\alpha\sin\psi + FLL\cos\psi$$

The major components of the resultant can be rewritten as:

$$\Sigma X = FX + FTL\sin\beta \qquad [A1.4]$$

$$\Sigma Y = FY - FTL\sin\beta \qquad [A1.5]$$

$$\Sigma Z = FZ \qquad [A1.6]$$

From the above equations the resultant (*RE*) can be calculated as:

$$RE = \sqrt{\left[\left(\Sigma X^2\right) + \left(\Sigma Y^2\right) + \left(\Sigma Z^2\right)\right]} \qquad [A1.7]$$

Also, the angles (θ and δ) of the resultant in the XY and XZ-planes can be given as:

$$\theta = \arctan\left(\frac{\Sigma Y}{\Sigma X}\right) \qquad [A1.8]$$

$$\delta = \arctan\left(\frac{\Sigma Z}{\Sigma X}\right) \qquad [A1.9]$$

XY-PLANE		XZ-PLANE	
FPR	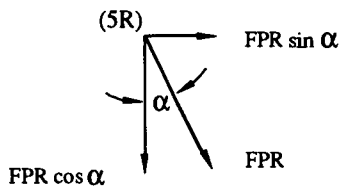	FPR	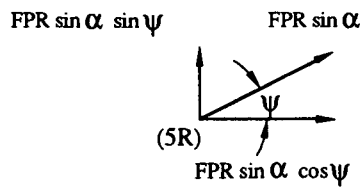
FPL	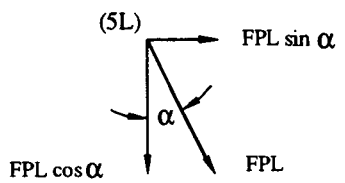	FPL	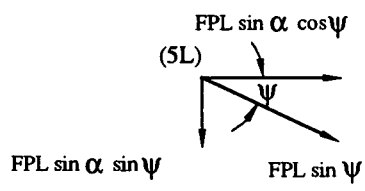
FCR	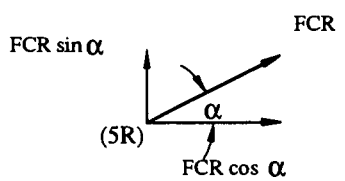	FCR	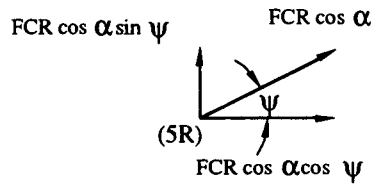
FCL	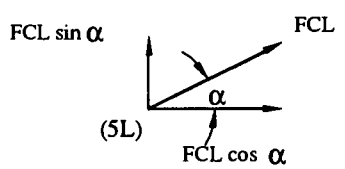	FCL	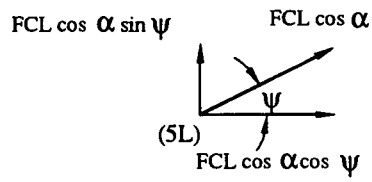
FLR	None	FLR	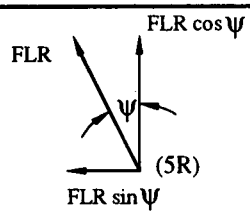
FLL	None	FLL	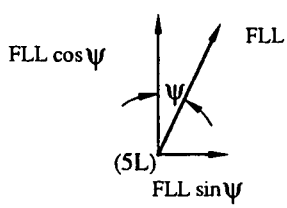
FTL	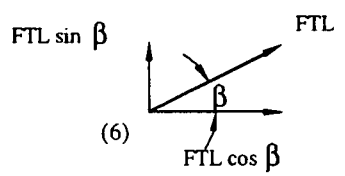	FTL	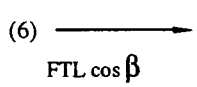

Figure A1.4. Force components in the XY and XZ-planes

Table A1.1. Variables Used and Assumptions Made in Force Resolution Procedure

α	Angle of lower links with respect to horizontal plane in XY-plane
β	Angle of top link with respect to horizontal plane in XY-plane
ψ	Angle of lower links with respect to the tractor centre line in XY-plane
θ	Angle of resultant in XY-plane
δ	Angle of resultant in XZ-plane
γ	Angle of cross shaft with respect to horizontal plane in XY-plane
RE	Magnitude of resultant in XYZ-planes
ΣX	Total forces in X-direction (Draught force)
ΣY	Total forces in Y-direction (Vertical force)
ΣZ	Total forces in Z-direction (Lateral force)
FX	Total forces on lower links in X-direction
FY	Total forces on lower links in Y-direction
FZ	Total forces on lower links in Z- direction
FXR	Total forces on right lower link in X-direction
FXL	Total forces on left lower link in X-direction
FYR	Total forces on right lower link in Y-direction
FYL	Total forces on left lower link in Y-direction
FZR	Total forces on right lower link in Z-direction
FZL	Total forces on left lower link in Z-direction
FCR	Coincident force to right lower link in XY-plane (tension = +)
FCL	Coincident force to left lower link in XY-plane (tension = +)
FPR	Perpendicular force to right lower link in XY-plane (down = +)
FPL	Perpendicular force to left lower link in XY-plane (down = +)
FLR	Lateral force to right lower link in XZ-plane (right = +)
FLL	Lateral force to right lower link in XZ-plane (right = +)
FTL	Top link force (tension = +)
h	Height of resultant in XY-plane (right = +)
l	Lateral distance of resultant from tractor centre line
a	Moment arm which is a distance from tractor rear axle

The resultant found in Equation [A1.7] represents the resolution of all components exerted on the three-point linkage into one single force, oriented at angle θ, and acting at a distance (*a*) from the rear axle (Fig. A1.5).

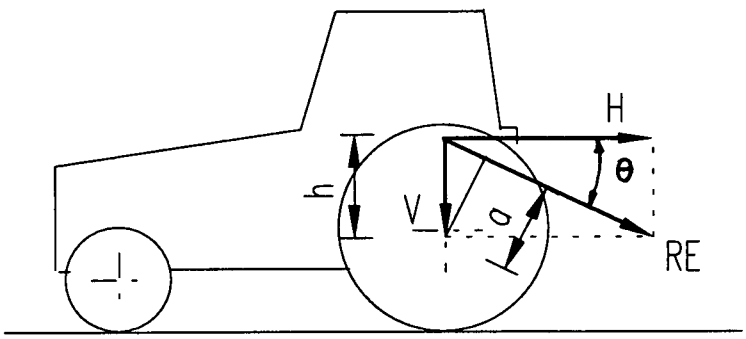

Figure A1.5. The position of resultant about rear axle

If the resultant (*RE*) is resolved into its horizontal and vertical components in the XY-plane, the horizontal component acts at a distance (*h*) above the tractor rear axle, while the vertical component passes through the axle. Therefore,

$$RE \times a = \sum X \times h \qquad [A1.10]$$

or to solve for *h*,

$$h = RE \times \frac{a}{\sum X} \qquad [A1.11]$$

and *h* can be also expressed as:

$$h = \frac{a}{\cos\theta} \qquad [A1.12]$$

As mentioned earlier, the magnitude of the lateral force exerted by asymmetrical implements on the three-point linkage has been neglected as being small. In this case, the equations given above might be re-expressed without lateral force components in a two-dimensional system instead of a three-dimensional system.

APPENDIX 2

Ring Theory (from Cook and Rabinowicz (1963))

Circular Ring

Rings have been used as springs for many years. There is a linear relationships between the load and deflection (Fig. A2.1)

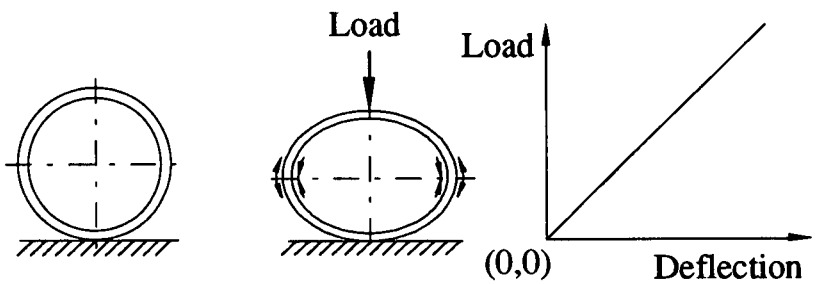

Figure A2.1. The force-deflection relationship for springs

Rings, (Fig. A2.2) have been also used as transducers in various force measuring system since the full potential of a ring was discovered in 1951.

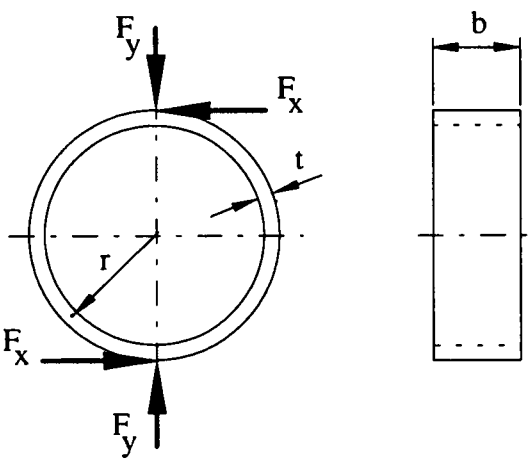

Figure A2.2. A circular ring used to measure force

If one-half of a ring, as shown in Figure A2.3 is considered, the case where the top and bottom of the ring are restrained from rotation; then M_0 is the moment required to satisfy this condition.

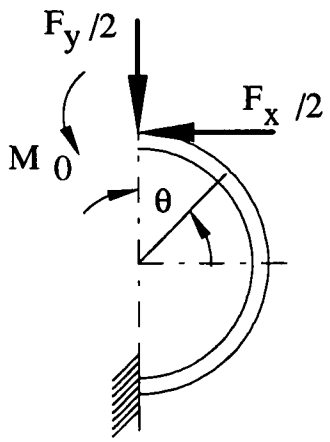

Figure A2.3. Half ring for strain analysis

The bending moment M_θ at any point in the ring is

$$M_\theta = M_0 + \frac{F_y r}{2}\sin\theta + \frac{F_z r}{2}(1-\cos\theta) \qquad [A2.1]$$

The total strain energy in the ring is

$$U = \frac{1}{2EI}\int_0^\pi M_\theta^2 r\, d\theta \qquad [A2.2]$$

The angular rotation ϕ of the ring at $\theta = 0$ is 0; thus

$$\left(\frac{\partial U}{\partial M_0}\right)_{\theta=0} = 0 = \frac{1}{EI}\int_0^\pi M_\theta \frac{M_\theta}{M_0} r\, d\theta \qquad [A2.3]$$

or from Equation [A2.1]

$$0 = \int_0^\pi \left[M_0 + \frac{F_y \sin\theta}{2} + \frac{F_x}{2}(1-\cos\theta) \right] d\theta \qquad [A2.4]$$

when integrated this gives

$$M_0\pi + F_y r + \frac{F_x r\pi}{2} = 0 \qquad [A2.5]$$

$$M_0 = -\frac{F_y r}{\pi} - \frac{F_x r}{2} \qquad [A2.6]$$

So, Equation [A2.1] can be rewritten as

$$M_\theta = \frac{F_y r}{2}\left(\sin\theta - \frac{2}{\pi}\right) - \frac{F_x r}{2}\cos\theta \qquad [A2.7]$$

The moment due to $F_y/2$ is zero when

$$\sin\theta = \frac{2}{\pi} \qquad \theta = 39.6^\circ \qquad \text{[A2.8]}$$

and the moment due to $F_x/2$ is zero when

$$\cos\theta = 0 \qquad \theta = 90^\circ \qquad \text{[A2.9]}$$

Therefore, the two positions $\theta = 39.6^o$ and $\theta = 90^o$ are the positions of the strain nodes to sense each force.

$$M_{39.6^\circ} = -\frac{F_x r}{2}\cos 39.6^2 = -0.385 F_x r \qquad \text{[A2.10]}$$

$$M_{90^\circ} = \frac{F_y r}{2}\left(\sin 90^0 - \frac{2}{\pi}\right) = 0.181 F_y r \qquad \text{[A2.11]}$$

The strain ε in a ring is

$$\varepsilon = \frac{6M}{Ebt^2} \qquad \text{[A2.12]}$$

So,

$$\varepsilon_{39.6^\circ} = 2.31\frac{F_x r}{Ebt^2} \qquad \text{[A2.13]}$$

$$\varepsilon_{90^\circ} = 1.09\frac{F_y r}{Ebt^2} \qquad \text{[A2.14]}$$

Hence the ring can measure either or both forces F_x and F_y independently of each other.

The horizontal (δ_x) and vertical (δ_y) deflections of the ring can be also computed.

$$\delta_x = \frac{\partial U}{\partial\left(\frac{F_x}{2}\right)} = \frac{1}{EI}\int_0^\pi M_\theta \frac{\partial M_\theta}{\partial\left(\frac{F_x}{2}\right)} r\, d\theta \qquad \text{[A2.15]}$$

$$\delta_y = \frac{1}{EI}\int_0^\pi \left[\frac{F_y r}{2}\left(\sin\theta - \frac{2}{\pi}\right) - \frac{F_y r}{2}\cos\theta\right](-r\cos\theta) r\, d\theta \qquad \text{[A2.16]}$$

Therefore

$$\delta_x = 9.42\frac{F_x r^3}{Ebt^3} \qquad \text{[A2.17]}$$

In a similar way

$$\delta_y = 1.79\frac{F_y r^3}{Ebt^3} \qquad \text{[A2.18]}$$

Octagonal Ring

When maximum horizontal stiffness is not required (F_x, not large), round rings attached to the system frame by screws through holes at $\theta = 0^o$ and $\theta = 180^o$ are satisfactory. However, there is a tendency for the ring to roll due to F_x. This is avoided by using an octagonal ring as shown in Figure A2.4.

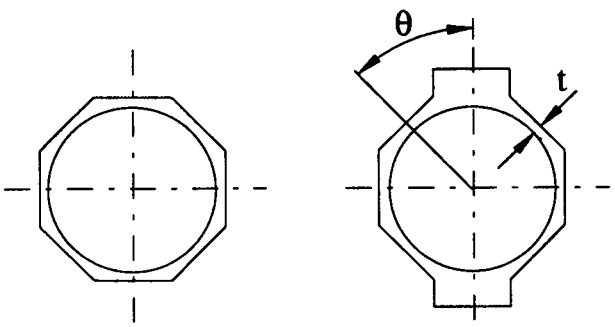

Figure A2.4. Octagonal ring

The upper and lower faces of the octagon are extended for mounting to the frame. In this case, there is no satisfactory mathematical model. However, Cook and Rabinowicz (1963) reported that the strain nodes, which were determined by photoelastic analyse occur at $\theta = 50^o$ and $\theta = 90^o$. They gave the following approximate equations for strain and deflections:

$$\varepsilon_{50^o} \approx 1.4\frac{F_x r}{Ebt^2} \qquad [A2.19]$$

$$\varepsilon_{90^o} \approx 0.7\frac{F_y r}{Ebt^2} \qquad [A2.20]$$

$$\delta_x = 3.7\frac{F_x r^3}{Ebt^3} \qquad [A2.21]$$

$$\delta_y = 1.0\frac{F_y r^3}{Ebt^3} \qquad [A2.22]$$

Godwin (1974) considered stress nodes and gave the following equations to find the position of stress nodes for an octagonal ring with the limits of integration for the ring section reduced to $\theta = \pi/8$ to $7\pi/8$.

Substituting $\theta = \pi/8$ to $7\pi/8$ in Equation [A2.4] above gives

$$0 = \int_{\pi/8}^{7\pi/8}\left[M_0 + \frac{F_y \sin\theta}{2} + \frac{F_x}{2}(1-\cos\theta)\right]d\theta \qquad [A2.23]$$

integrating gives

$$0 = M_0 \frac{6\pi}{8} + F_y r\, 0.9239 + F_x r \frac{6\pi}{16} \qquad [A2.24]$$

$$M_0 = -\frac{4F_y r\, 0.9239}{3\pi} - \frac{F_x r}{2} \qquad [A2.25]$$

Substituting into Equation [A2.1] gives

$$M_\theta = -\frac{4F_y r\, 0.9239}{3\pi} - \frac{F_x r}{2} + \frac{F_y r \sin\theta}{2} + \frac{F_x r(1-\cos\theta)}{2} \qquad [A2.26]$$

$$M_\theta = F_y r\left(\frac{\sin\theta}{2} - \frac{4\times 0.9239}{3\pi}\right) - \frac{F_x r}{2}\cos\theta \qquad [A2.27]$$

The moment due to $F_y/2$ is zero when

$$\sin\theta = \frac{8\times 0.9239}{3\pi} = 0.784 \qquad \theta = 51^0 36' \qquad [A2.28]$$

and the moment due to $F_x/2$ is zero when

$$\cos\theta = 0 \qquad \theta = 90^\circ \qquad [A2.29]$$

Therefore, the two positions θ = 51°36' and θ = 90° are the positions of the strain nodes for each force.

Circular or octagonal rings have been used in a different ways for force measurement. The extended octagonal ring is a common application. Figure A2.5 shows an octagonal ring extended by *2L* to gain stability and approximately meet the requirement of zero rotation of the top surface.

Godwin (1974) conducted a series of tests to enable the position of the nodes to be located. He placed strain gauges at a different angular locations, θ, along the face AB of the transducer , Figure A2.5. The position of the node was found to be at an angle of θ = 34°. He also reported that to prevent dependency in the position of F_x for an octagonal ring without side plates, the insertion of a plate of length less than the distance between the ring centres (*2L*) was needed between the mounting and the transducer and a second between the transducer and the tine clamp. A suitable plate length is $P = 0.85 \times 2L$ (Fig. A2.5).

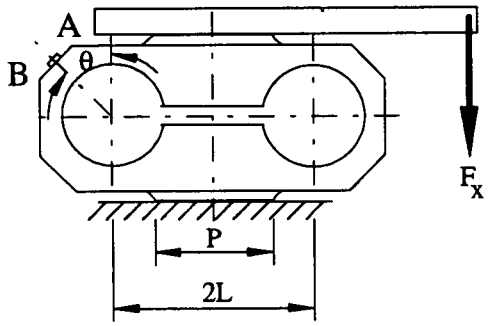

Figure A2.5. The position of strain nodes and the plate on an extended octagonal ring

When using an extended circular ring to measure a moment (M) (Fig. A2.6), there will be rotation ϕ of the upper face. For this case Cook and Rabinowicz (1963) introduced the following equations.

$$\frac{\varepsilon E b t^2}{M} = 0.4 \text{ when } k = 1.6\left(=\frac{L}{r}\right) \qquad \text{[A2.30]}$$

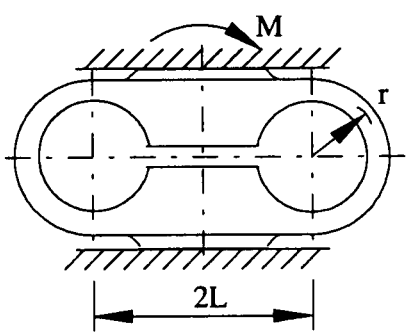

Figure A2.6. Moment effecting on an extended circular ring

Unfortunately, for an extended octagonal ring transducer there are no equations available similar to the above.

APPENDIX 3

Lower Link Transducer Design

The design was proposed for an MB-trac 1 300 tractor which has Cat. II and III linkage. The tractor weight is approximately 70 kN.

Design specification

The maximum force through the lower link arms is assumed as the maximum pull exerted by the tractor which is 75 % of the tractor weight multiplied by a safety factor of three.

So, the design specification is as follows:

$$\begin{aligned} \text{Weight} &= 70 \text{ kN} \\ \text{Max. pull} &= 70 \times 0.75 \\ \text{Safety factor} &= 3 \\ \text{Design force} &= (70 \times 0.75) \times 3 \\ &= 157.5 \text{ kN} \end{aligned}$$

This force will be acting through two lower links and hence two Extended Octagonal Rings (EORs) are required. Thus, each ring should be designed to carry approximately a half of the design force (Fig. A3.1).

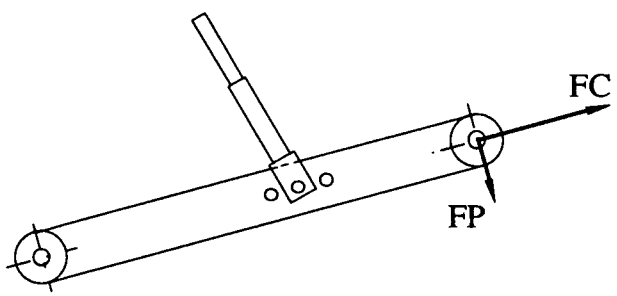

Figure A3.1. Forces exerted on a lower link

However, another assumption is made that the forces on each link are:

$$\begin{aligned} \text{Max. coincident force } (FC) &\cong 80 \text{ kN} \\ \text{Max. perpendicular force } (FP) &\cong 40 \text{ kN} \end{aligned}$$

So, the resultant (RE) is going to be:

$$RE = \sqrt{(FC)^2 + (FP)^2}$$
$$= \sqrt{(80)^2 + (40)^2}$$
$$= 89.4 \text{ kN}$$

The transducers were constructed from a solid block of pre hardened alloy mould steel that can be machined by normal workshop techniques. General specifications of the material used are shown in Table A3.1.

Table A3.1. Some Specifications of the Material Used for EOR

General							
Approximate analysis [%]	C	Si	Mn	Cr	Ni	Mo	S
	0.33	0.3	0.8	1.8	0.9	0.2	0.008
Standard specification	AISI P20 Modified						
Delivery condition	Hardened and tempered to 290-330 HB						
Testing temperature	20°C						
Tensile strength [N/mm^2]	1 010						
Yield strength [N/mm^2]	800						
Reduction of area Z [%]	60						
Elongation as [%]	20						
Impact strength [kJ]	50						
Density [kg/m^3]	7 800						
Modulus of elasticity [N/mm^2]	205 000						
Material manufacturer	Uddeholm Impax Supreme						

(Source: Uddeholm catalogue)

To make fewer modification to the lower links themselves, original swivel sets were used at the ball end of the rings (Figure A3.2).

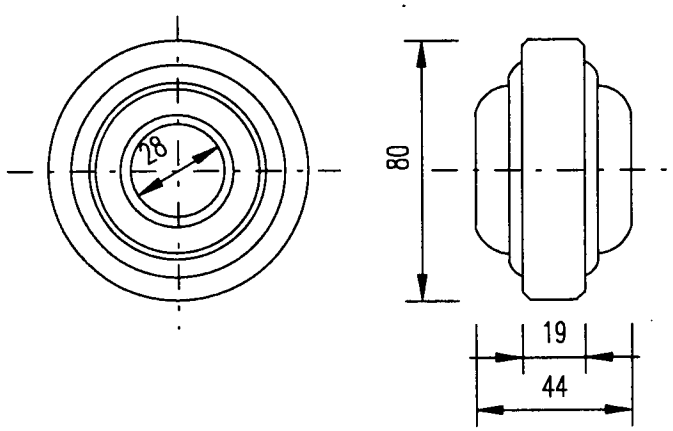

Figure A3.2. Swivel set for rings instead of the lower link ball end

Housing for Swivel Set

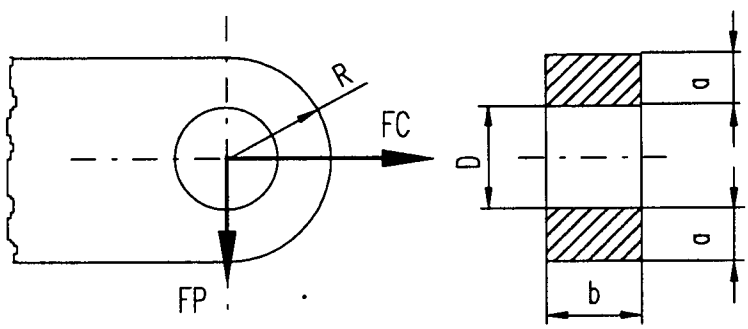

Figure A3.3. The effect of the shearing and tensile forces on the link

<u>40 000 N Shear Force</u>

Critical force (F) = 40 kN

Lower link width (b) = 38 mm (for MB-trac 1 300)

Shear strength (τ) $\approx 0.6 \times UTS$ (Ultimate Tensile Strength)

$$\tau = \frac{F \times SF}{A} \qquad A = 2 \times a \times b$$

Therefore, the thickness of the housing is:

$$0.6 \times 1\,010 = \frac{40\,000 \times 3.0}{2 \times a \times 38} = \frac{40\,000 \times 3.0}{2 \times 38 \times 0.6 \times 1\,010} \Rightarrow a_{min} = 2.61 \text{ mm}$$

<u>80 000 N Tensile Force</u>

$$\sigma_{yield} = \frac{F \times SF}{A} \Rightarrow 800 = \frac{80\,000 \times 3.0}{2 \times a \times 38} \Rightarrow a_{min} = 3.95 \text{ mm}$$

Physical R_{max} = 55 mm (to clear implement superstructure)

when R = 55 mm:

$$a_{max} = R_{max} - \frac{D}{2}$$

where

D = outside diameter of swivel set [mm]

$$a_{max} = 55 - \frac{80}{2} \Rightarrow a_{max} = 15 \text{ mm}$$

This is the value taken for the design, thus increasing the safety factor of the housing.

Side Force on Swivel Set Housing

The lip on swivel set housing is necessary since the swivel set is used. The side force effected on the lip is shown in Figure A3.4.

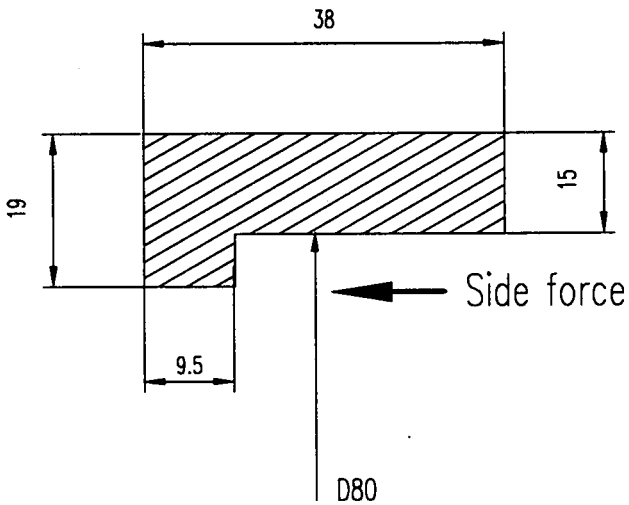

Figure A3.4. Side force on swivel set housing

If the outside diameter of the swivel set D = 80 mm and the lip is 9.5 mm wide area,

Side force area $(A) = 9.5 \times \pi \times D$

Maximum side force $(S) = \frac{\sigma_{yield} \times A}{SF} = \frac{800 \times 9.5 \times \pi \times 80}{3.0} \Rightarrow S = 636\ 696 \text{ N}$

In practice, it is likely to be about a maximum of 1 400 N (Kilgour et al., 1988).

Design of Extended Octagonal Ring

General Dimensions

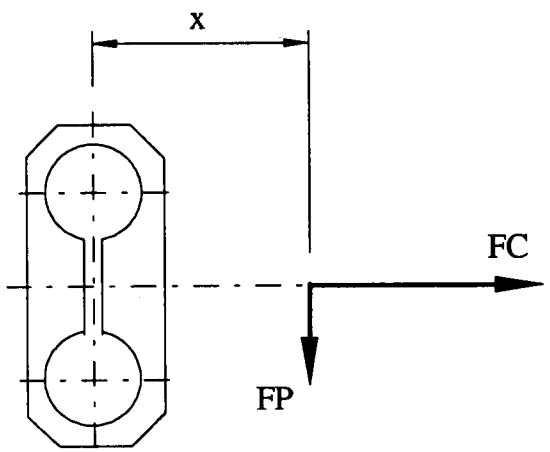

Figure A3.5. Forces on an EOR

Let x = 160 mm. In this case, bending moment (M) is:

$$M = FP \times x \times SF = 40\ 000 \times 160 \times 3.0 \Rightarrow M = 19.2 \text{ MNm}$$

It is also assumed that b = 60 mm as ring width.

From Cook and Rabinowicz (1963) $\frac{\varepsilon E b t^2}{M} = 0.4$ when $k = 1.6\left(=\frac{L}{r}\right)$

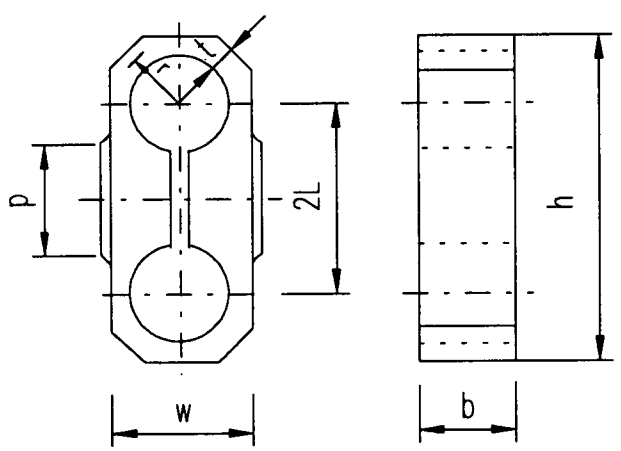

ε = strain
E = modulus of elasticity
b = width of ring
t = ring thickness
M = applied moment
$2L$ = distance between ring centres
r = mean radius of ring

Figure A3.6. Major dimensions of extended octagonal ring

Ring thickness (t) is:

$$t = \sqrt{\frac{0.4M}{\varepsilon E b}} \qquad (\varepsilon E = \sigma) \ \therefore\ t = \sqrt{\frac{0.4 \times 19.2 \times 10^6}{800 \times 60}} \Rightarrow t = 12.65 \text{ mm}$$

For gauging purposes the hole in octagonal ring needs to be 60 mm diameter (ϕ). Therefore, mean radius of ring (r) is calculated from:

$$r = \frac{D}{2} + \frac{t}{2} = \frac{60}{2} + \frac{12.65}{2} \Rightarrow r = 36.33 \text{ mm}$$

$$\frac{L}{r} = 1.6 \Rightarrow L = 1.6 \times r$$

$$2L = 1.6 \times r \times 2 = 1.6 \times 36.33 \times 2 \Rightarrow 2L = 116.26 \text{ mm}$$

In this case, overall width of extended octagonal ring (w) is going to be:

$$w = 2r + t = 2 \times 36.33 \times 12.65 \Rightarrow w = 85.31 \text{ mm}$$

Similar way, overall length of the ring (h) can be given as:

$$h = 2L + 2r + t = 116.26 + 2 \times 36.33 + 12.65 \Rightarrow h = 201.57 \text{ mm}$$

Size of Plate (land)

Size of plate (land), which should be considered for the case that without plates the coincident force (FC) output is not independent of the position of the force (Godwin, 1975), the effective plate length can be expressed as (Godwin, 1990):

$$p = 1.7 \times L = 1.7 \times \frac{116.26}{2} \Rightarrow p = 98.82 \text{ mm}$$

Plate strength can be checked as follows:

$$A = p \times b = 98.82 \times 60 \Rightarrow A = 5\ 929.2 \text{ mm}^2$$

Hence maximum force before yield is:

$$F_{max} = \sigma_{yield} \times A = 800 \times 5\ 929.2 \Rightarrow F_{max} = 4.74 \text{ MN}$$

Design Flange for EOR

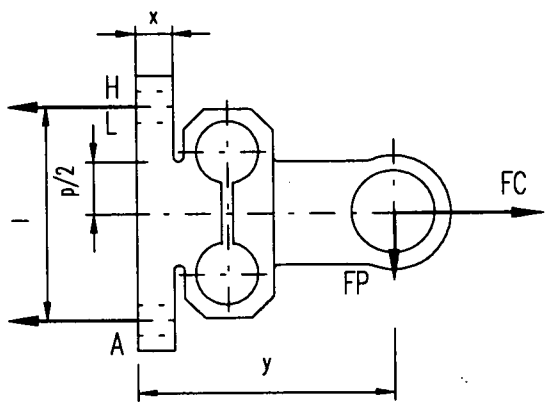

Figure A3.7. The effect of forces on the flange and bolts

Direct Shear

Shear strength (τ) is:

$$\tau = 0.6 \times UTS = 0.6 \times 1\,010 \Rightarrow \tau = 606 \text{ Nmm}^{-2}$$

Area under shear stress (A) is:

$$A = b \times x \times 2 = 60 \times x \times 2 \Rightarrow A = 120 \times x \text{ mm}^2$$

Flange width (x_{min}) is:

$$\tau = \frac{F \times SF}{A} \Rightarrow A = \frac{F \times SF}{\tau}$$

$$120x = \frac{80\,000 \times 3.0}{606} \Rightarrow x_{min} = 3.30 \text{ mm}$$

Bending

If x = 20 mm, l =205 mm and y = 232.7 mm (=160+42.7+10+20) from Figure A3.7.

$$\sigma = \frac{M \times SF}{Z}$$

where

σ = working stress in bending

M = bending moment

Z = section modulus $\left(\frac{bx^2}{6}\right)$

$$\sigma = \frac{40\,000 \times \left(\frac{232.7}{205}\right) \times 52.6 \times 3.0}{\frac{60 \times 20^2}{6}}$$

$\sigma = 1\,791.2 \text{ Nmm}^{-2} \rangle 800 \text{ Nmm}^{-2}$

Hence the size chosen is not sufficient.

If $x = 35$ mm, $l = 205$ mm and $y = 247.7$ mm (=160+42.7+10+35)

$$\sigma = \frac{40\,000 \times \left(\frac{247.7}{205}\right) \times 52.6 \times 3.0}{\frac{60 \times 35^2}{6}}$$

Hence $\sigma = 622.6 \text{ Nmm}^{-2} (\langle 800 \text{ Nmm}^{-2})$ and is, therefore, adequate.

Choosing Bolts for Flange

Proof load = 201 kN for 8.8 grade M24 bolt

Proof load = 321 kN for 8.8 grade M30 bolt

Moment about *A* in Figure A3.7:

$$(FP \times y) + \left(FC \times \frac{l}{2}\right) = L \times 205$$

$$(40\,000 \times 247.7) + \left(80\,000 \times \frac{205}{2}\right) = L \times 205$$

$$L = 88\,331.7 \text{ N}$$

$$L \times SF = 88\,331.7 \times 3.0 = 264\,995 \text{ N}$$

In this case, M30 must be chosen.

Area (A) in shear of bolts is: $A = 2\pi r^2$

Shear stress due to tension is: $\sigma = \frac{F \times SF}{A} = \frac{40\,000 \times 3.0}{2 \times \pi \times 15^2} \Rightarrow \sigma = 84.9 \text{ Nmm}^{-2}$

Yield stress for 8.8 grade steel = 627.8 Nmm^{-2}

Hence 84.9 Nmm^{-2} ($\langle$ 627.8 Nmm^{-2}) is suitable.

Shear stress due to bending

$$FP \times y \times SF = H \times l$$

$$40\,000 \times 247.7 \times 3.0 = H \times 205 \Rightarrow H = 144\,936.6 \text{ N}$$

$$\tau = \frac{H}{2\pi r^2} = \frac{144\,936.6}{2 \times \pi \times 15^2} \Rightarrow \tau = 102.5 \text{ Nmm}^{-2}$$

UTS for 8.8 grade steel = 784.8 Nmm^{-2}

Shear strength = $0.6 \times 784.8 = 470.9 \text{ Nmm}^{-2}$

Hence 102.5 Nmm^{-2} ($\langle$ 470.9 Nmm^{-2}) is suitable.

Figure A3.8 shows all dimensions of the linkage type extended octagonal ring

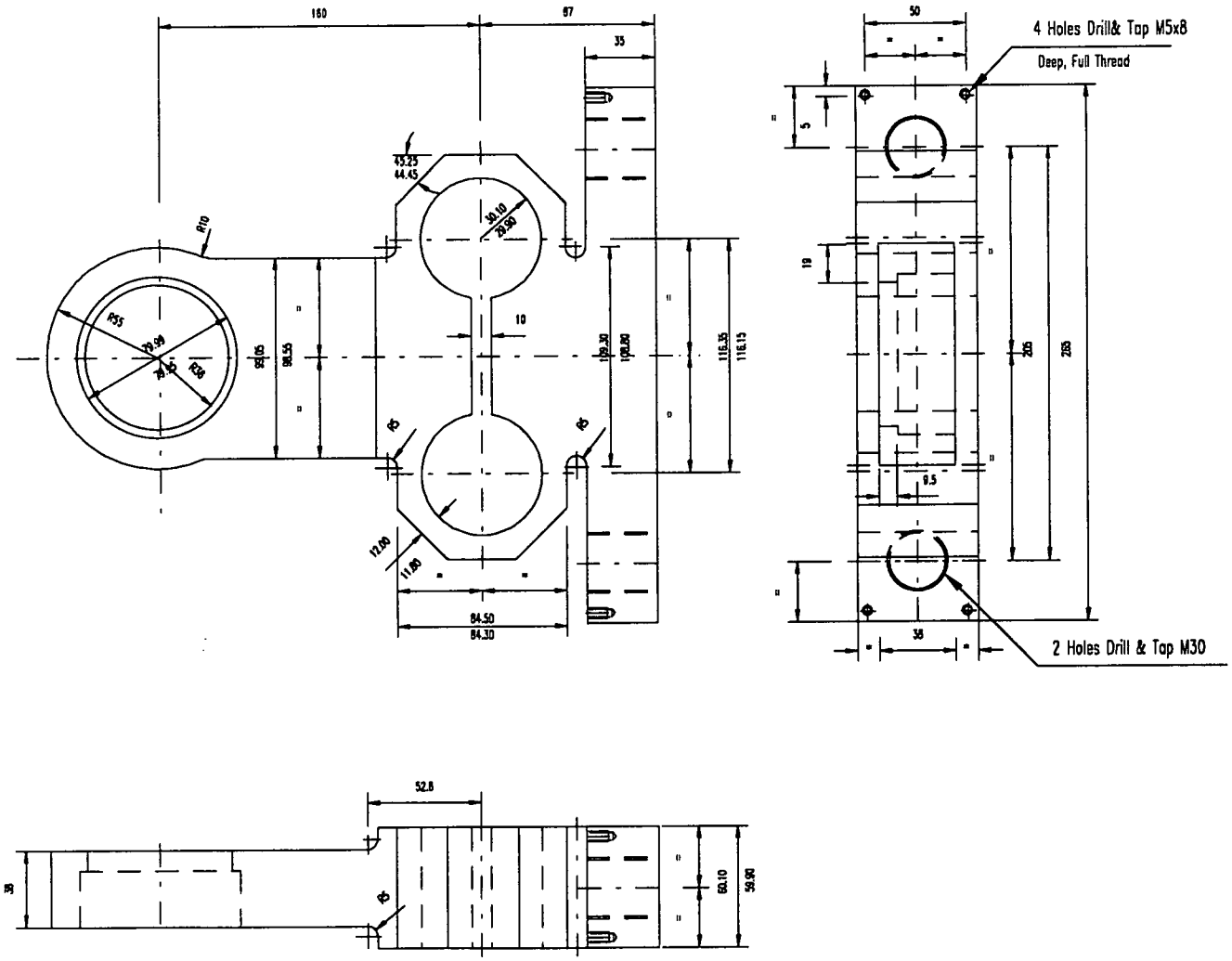

Figure A3.8. Linkage type extended octagonal ring

Design of Flange for the Lower Link

After designing EOR for the MB trac 1 300 tractor it is decided to attach it to the Ford 6410 2WD tractor instead due to availability. Therefore, further calculations were made for the Ford 6410 2WD tractor.

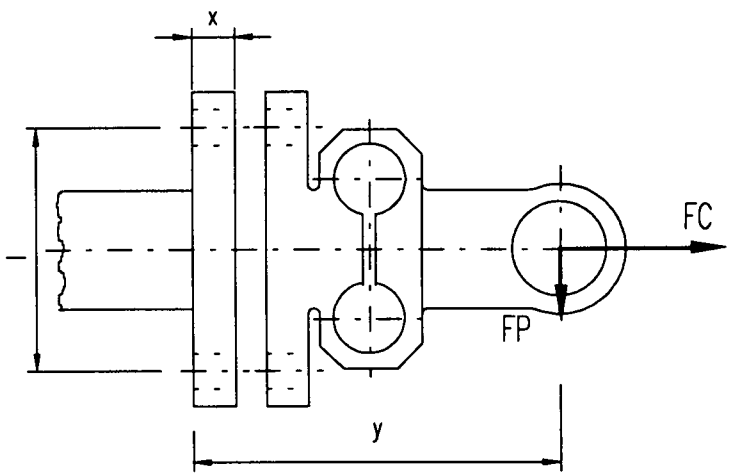

Figure A3.9. Dimension of the flange on the link for Linkage EOR

Let $x = 30$ mm

$$\sigma = \frac{FP \times \frac{y}{l} \times \times FS}{\frac{bx^2}{6}} = \frac{40\,000 \times \frac{277.7}{205} \times 52.6 \times 3.0}{\frac{60 \times 30^2}{6}} \Rightarrow \sigma = 950 \text{ Nmm}^{-2}$$

$\sigma = 950 \text{ Nmm}^{-2} \rangle 800 \text{ Nmm}^{-2}$

Let $x = 35$ mm

$$\sigma = \frac{40\,000 \times \frac{282.7}{205} \times 52.6 \times 3.0}{\frac{60 \times 35^2}{6}} \Rightarrow \sigma = 710.6 \text{ Nmm}^{-2}$$

Hence $\sigma = 710.6 \text{ Nmm}^{-2}$ ($\langle 800 \text{ Nmm}^{-2}$) and dimension is suitable.

The implement ends of the bottom links were cut off, and a pad welded on the links in such a way that the overall lengths and angles were not changed from the original dimensions (Fig. A3.10).

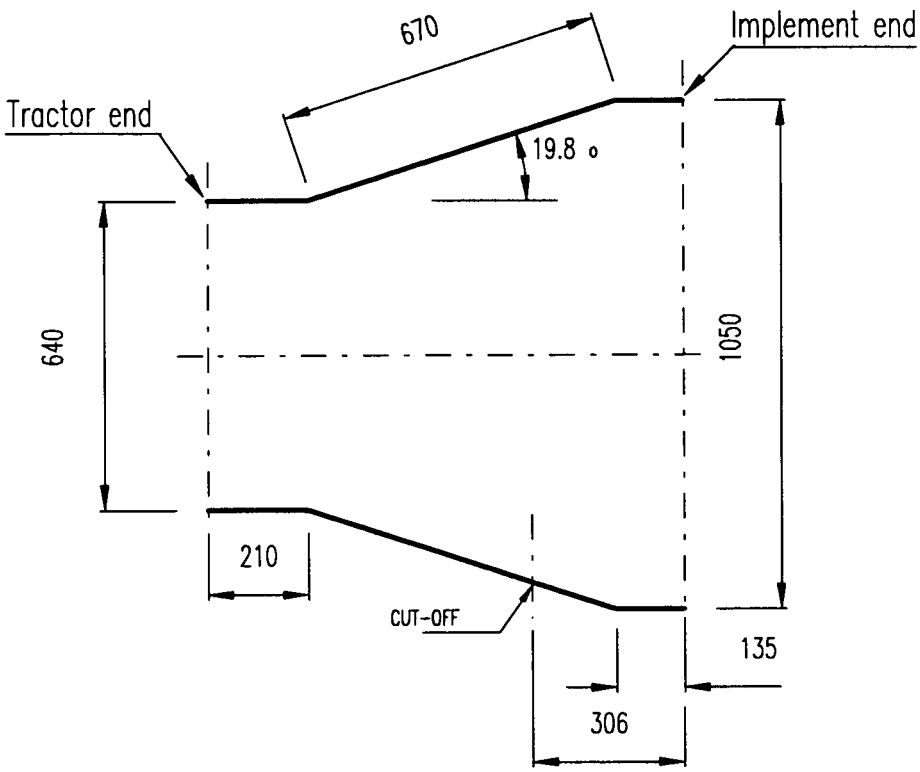

Figure A3.10. Overall dimensions of lower links for Ford 6410 tractor

APPENDIX 4

Datalogger Program

The program below was developed for the datalogger. The program had two versions: 1) for calibration test i.e. multiplier is one and offset is zero for all bridges; 2) for real tests i.e. multiplier and offset has an individual value for each bridge. Both versions had the following stages:

- Switch
- Full Bridge (Instruction 6) for Rotary Position Transducer
- Burst Measurement (Instruction 23) for Top Link and EORTs
- Loop for Input Location
- Loop for Summation
- Multipliers & Offsets
- Output Location
- Saving Datalogger Time for Every Switch Press
- Switch Toggle

The multiplier and offset values derived from the calibration tests were added to the following program for the calibration purposes.

Program: Full Bridge & Burst Measurement Average Test
Date:26/9/1991
Flag Usage:1
Input Channel Usage:1:CSA, 2:FTL, 3:FPL, 4:FCL, 5:FPR, 6:FCR
Excitation Channel Usage:1:Full Bridge, 2:Burst Measurement
Continuous Analog Usage: None
Control Port Usage: None
Pulse Input Channel Usage: Switch on 1
Output Array Definitions:1:Switch, 2:CSA, 3:FTL, 4:FPL, 5:FCL, 6:FPR, 7:FCR

*	1	Table 1 Programs
01:	2	Sec. Execution Interval
01:	P3	Pulse
01:	1	Rep
02:	1	Pulse Input Chan
03:	2	Switch Closure
04:	1	Loc [:Switch]
05:	1	Mult
06:	0	Offset
02:	P89	If X<=>F
01:	1	X Loc Switch
02:	2	<>
03:	0	F
04:	1	Call Subroutine 1
03:	P91	If Flag
01:	21	1 is Reset
02:	0	Go to end of Program Table

Start Instructions here

04:	P6	Full Bridge
01:	1	Rep
02:	5	5000 mV slow Range
03:	1	IN Chan
04:	2	Excite all reps w/EXchan 2
05:	5000	mV Excitation
06:	2	Loc [:CSA]
07:	1	Mult
08:	0	Offset

05:	P23	Burst Meas. (Extended)
01:	5	Reps
02:	13	50 mV fast Range
03:	2	IN Chan
04:	0000	Trig/Trig/Dest/Meas Options
05:	5	Time per Scan (msec.)
06:	.1	Scans (in thousands)
07:	0000	Samples before Trigger
08:	0.0000	mV Limit
09:	1000	mV Excitation
10:	8	Loc [:BFTL]
11:	1	Mult
12:	0	Offset

End Instructions here

06:	P87	Beginning of Loop
01:	00	Delay
02:	5	Loop Count

07:	P30	Z=F
01:	0	F
02:	3--	Z Loc [:FTL]

```
08:     P95    End

09:     P87    Beginning of Loop
 01:    00     Delay
 02:    100    Loop Count

10:     P33    Z=X+Y
 01:    3      X Loc FTL
 02:    8--    Y Loc BFTL
 03:    3      Z Loc [:FTL]

11:     P33    Z=X+Y
 01:    4      X Loc FPL
 02:    108--  Y Loc
 03:    4      Z Loc [:FPL]

12:     P33    Z=X+Y
 01:    5      X Loc FCL
 02:    208--  Y Loc
 03:    5      Z Loc [:FCL]

13:     P33    Z=X+Y
 01:    6      X Loc FPR
 02:    308--  Y Loc
 03:    6      Z Loc [:FPR]

14:     P33    Z=X+Y
 01:    7      Y Loc
 03:    7      Z Loc [:FCR]

15:     P95    End

16:     P37    Z=X*F
 01:    3      X Loc FTL
 02:    1      F
 03:    3      Z Loc [:FTL]
```

```
17:     P34   Z=X+F
 01:    3     X Loc FTL
 02:    0     F
 03:    3     Z Loc [:FTL]

18:     P37   Z=X*F
 01:    4     X Loc FPL
 02:    1     F
 03:    4     Z Loc [:FPL]

19:     P34   Z=X+F
 01:    4     X Loc FPL
 02:    0     F
 03:    4     Z Loc [:FPL]

20:     P37   Z=X*F
 01:    5     X Loc FCL
 02:    1     F
 03:    5     Z Loc [:FCL]

21:     P34   Z=X+F
 01:    5     X Loc FCL
 02:    0     F
 03:    5     Z Loc [:FCL]

22:     P37   Z=X*F
 01:    6     X Loc FPR
 02:    1     F
 03:    6     Z Loc [:FPR]

23:     P34   Z=X+F
 01:    6     X Loc FPR
 02:    0     F
 03:    6     Z Loc [:FPR]
```

```
24:     P37   Z=X*F
 01:    7     X Loc FCR
 02:    1     F
 03:    7     Z Loc [:FCR]

25:     P34   Z=X+F
 01:    7     X Loc FCR
 02:    0     F
 03:    7     Z Loc [:FCR]

26:     P86   Do
 01:    10    Set flag 0 (output)

27:     P70   Sample
 01:    6     Reps
 02:    2     Loc CSA

28:     P     End Table 1


*       2     Table 2 Programs
 01:    0.0000 Sec. Execution Interval

01:     P     End Table 2


*       3     Table 3 Subroutines

01:     P85   Beginning of Subroutine
 01:    1     Subroutine Number

02:     P86   Do
 01:    10    Set flag 0 (output)

03:     P77   Real Time
 01:    111   Day, Hour-Minute, Second
```

04:	P86	Do
01:	20	Reset flag 0 (output)
05:	P91	If Flag
01:	11	1 is set
02:	30	Then Do
06:	P86	Do
01:	21	Reset flag 1
07:	P94	Else
08:	P86	Do
01:	11	Set flag 1
09:	P95	End
10:	P95	End
11:	P	End Table 3
*	4	Mode 4 Output Options
01:	0	(Tape OFF) (Printer OFF)
02:	0	Printer 300 Baud
*	A	Mode 10 Memory Allocation
01:	512	Input Locations
02:	64	Intermediate Locations
*	C	Mode 12 Security
01:	00	Security Option
02:	0000	Security Code

Input Location Assignments (with comments)

Key:
T=Table Number
E=Entry Number
L=Location Number

T:	E:	L:	
1:	1:	1:	Loc [:Switch]
1:	4:	2:	Loc [:CSA]
1:	7:	3:	Z Loc [:FTL]
1:	10:	3:	Z Loc [:FTL]
1:	16:	3:	Z Loc [:FTL]
1:	17:	3:	Z Loc [:FTL]
1:	11:	4:	Z Loc [:FPL]
1:	18:	4:	Z Loc [:FPL]
1:	19:	4:	Z Loc [:FPL]
1:	12:	5:	Z Loc [:FCL]
1:	20:	5:	Z Loc [:FCL]
1:	21:	5:	Z Loc [:FCL]
1:	13:	6:	Z Loc [:FPR]
1:	22:	6:	Z Loc [:FPR]
1:	23:	6:	Z Loc [:FPR]
1:	14:	7:	Z Loc [:FCR]
1:	24:	7:	Z Loc [:FCR]
1:	25:	7:	Z Loc [:FCR]
1:	5:	8:	Loc [:BFTL]
1:	8:	8:	Z Loc [:BFTL]

Input Location Labels

1:Switch	3:FTL	5:FCL	7:FCR
2:CSA	4:FPL	6:FPR	8:BFTL

APPENDIX 5

Three-Point Linkage Model

Once the five forces *FCL, FPL, FCR, FPR, FTL* and one angle can be ascertained from the instrumentation the process of computing the resultant is fairly straightforward.

The model assumes that the three-point linkage (TPL) mechanism consists entirely of bars (ties) and pin joints for simplification. The TPL stands in three-dimensional space but assuming side forces are zero when the linkage is unrestrained laterally, this can be modelled in two dimensions (Fig. A5.1).

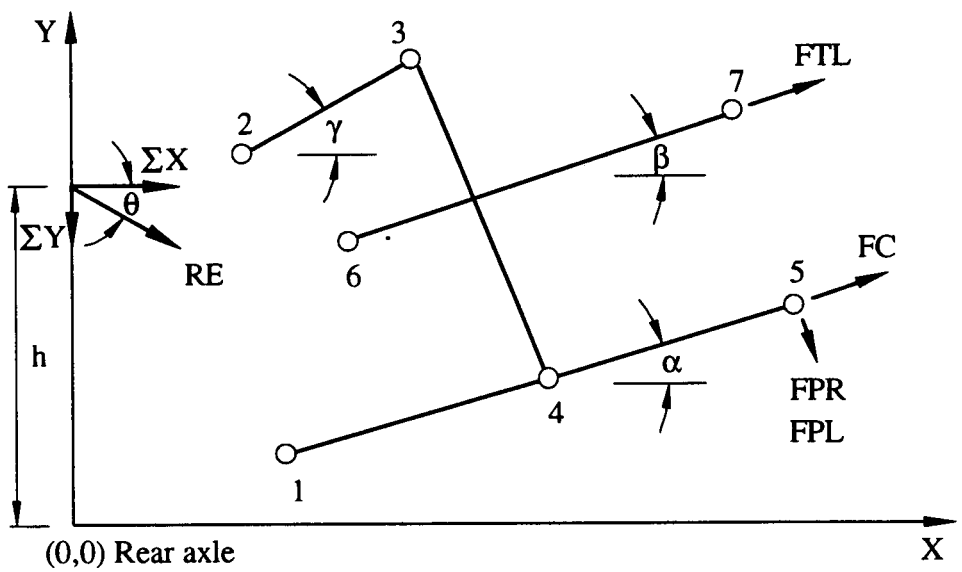

Figure A5.1. Three-point linkage system in XY-Plane

Basically, the model can be analysed in five main stages as given below:

- Input the known constants of the particular TPL and the implement used to the model
- Input variables from the datalogger to the model
- Calculate the unknown pin coordinates and bar (tie) length by using the cross-shaft angle *CSA* (γ)

- Calculate the relative position of the forces as well as the resultant force and angle
- Show the linkage and forces including the magnitude and position of the resultant force between the tractor and implement

Constants Used in Calculations

The constants used in calculations for Ford 6410 2WD tractor is given as follows:

Three Point Linkage Geometry (0,0) = Rear Axle

Positive X = Rearwards, Positive Y = Upwards

Mounting Lower Link	[mm]	PINX1	98
Mounting Lower Link	[mm]	PINY1	-236
Mounting Cross-Shaft	[mm]	PINX2	-98
Mounting Cross-Shaft	[mm]	PINY2	327
Mounting Top Link	[mm]	PINX6	322
Mounting Top Link	[mm]	PINY6	210
Inner Lower Link	[mm]	TIE14	457
Lower Link	[mm]	TIE15	924
Cross-Shaft Arm	[mm]	TIE23	230
Lift Rod	[mm]	TIE34	774
Mass Height	[mm]	TIE57	515
Top Link	[mm]	TIE67	774

N.B. The mast height and top link length are variables depending on the working conditions of the implement used.

Inputs to the Model from the Datalogger

After each test the following outcomes are stored by the instrumentation system:

Cross-Shaft Angle (*CSA*, γ) [Radians]:

this is the angle of the cross-shaft arm with respect to the horizontal plane in the XY-Plane, anti-clockwise

Force-Top Link (*FTL*) [Newton]:

this is the force sensed in the top link, rearwards = +.

Force-Perpendicular Left (*FPL*) [Newton]:

this is the force perpendicular to the left lower link, downwards = +.

Force-Perpendicular Left (*FCL*) [Newton]:

this is the force coincident with the left lower link, rearwards = +.

Force-Perpendicular Right (*FPR*) [Newton]:

this is the force perpendicular to the right lower link, downwards = +.

Force-Perpendicular Right (*FCR*) [Newton]:

this is the force coincident with the right lower link, rearwards = +.

Calculating the Pin Coordinates

There are some calculations which must be done by using the cross-shaft angle. These are given in the following equations:

The coordinates of *PIN3* [mm]

$$PINX3 = PINX2 + TIE23 \times \cos\gamma$$
$$PINY3 = PINY2 + TIE23 \times \sin\gamma$$

Tie length [mm]

$$TIE13 = \sqrt{(PINX3 - PINX1)^2 + (PINY3 - PINY1)^2}$$

The angle of lower link (α) [Radians]

$$\alpha = \arctan\left(\frac{PINY3 - PINY1}{PINX3 - PINX1}\right) - \cos\left[\frac{(TIE13)^2 + (TIE14)^2 - (TIE34)^2}{2 \times TIE13 \times TIE14}\right]$$

The coordinates of *PIN5* [mm]

$$PINX5 = PINX1 + TIE15 \times \cos\alpha$$
$$PINY5 = PINY1 + TIE15 \times \sin\alpha$$

Tie length [mm]

$$TIE56 = \sqrt{(PINX5 - PINX7)^2 + (PINY6 - PINY5)^2}$$

The angle of the top link (β) [Radians]

$$\beta = \arccos\left[\frac{(TIE67)^2 + (TIE56)^2 - (TIE57)^2}{2 \times TIE67 \times TIE56}\right] - \arctan\left(\frac{PINY6 - PINY5}{PINX5 - PINX6}\right)$$

The coordinates of *PIN7* [mm]

$$PINX7 = PINX6 + TIE67 \times \cos\beta$$
$$PINY7 = PINY6 + TIE67 \times \sin\beta$$

Calculating the Forces

Sum of the horizontal forces [kN]

$$\Sigma FX = (FCL + FCR)\cos\alpha + (FPL + FPR)\sin\alpha + FTL\cos\beta$$

Sum of the vertical forces [kN]

$$\Sigma FX = (FPL + FPR)\cos\alpha - (FCL + FCR)\sin\alpha - FTL\sin\beta$$

Resultant force [kN]

$$RE = \sqrt{(\Sigma X)^2 + (\Sigma Y)^2}$$

Resultant angle [Radians]

$$\theta = \arctan\left(\frac{\Sigma Y}{\Sigma X}\right)$$

Showing the Linkage and Forces

This stage is ready to use in the floppy diskette attached

APPENDIX 6

Field Test Results

(Sandy Loam Soil: Downings Field in UK-1991)

Table A6.1. Measured and Resolved Forces for Disc Plough

Depth [m]		FX [kN]		FY [kN]		RE [kN]		θ [Radians]	
Mean	Stdev	Mean	Stdev	Mean	Stdev	Mean	Stdev	Mean	Stdev
0.000	0.000	0.000	0.000	4.541	0.000	4.541	0.000	1.570	0.000
0.169	0.024	7.019	1.521	1.054	0.673	7.129	1.523	0.151	0.095
0.176	0.019	5.554	0.958	1.670	0.717	5.874	0.752	0.307	0.170
0.178	0.016	6.757	2.709	0.614	1.033	6.916	2.570	0.136	0.236
0.208	0.006	12.080	1.430	0.131	0.589	12.096	1.423	0.015	0.051
0.220	0.015	12.941	1.317	-0.493	0.354	12.956	1.317	-0.038	0.027
0.229	0.023	12.358	1.969	-0.155	0.490	12.370	1.959	-0.011	0.048
0.235	0.040	12.748	1.800	0.540	1.400	12.855	1.656	0.054	0.131
0.239	0.026	12.597	2.149	0.156	0.728	12.625	2.115	0.021	0.073
0.243	0.006	12.069	1.816	0.318	1.418	12.178	1.658	0.041	0.144

Table A6.2. Measured and Resolved Forces for Mouldboard Plough

Depth [m]		FX [kN]		FY [kN]		RE [kN]		θ [Radians]	
Mean	Stdev	Mean	Stdev	Mean	Stdev	Mean	Stdev	Mean	Stdev
0.000	0.000	0.000	0.000	6.082	0.000	6.082	0.000	1.570	0.000
0.190	0.017	8.198	0.590	8.328	0.272	11.696	0.445	0.794	0.040
0.203	0.006	9.528	1.037	5.856	0.387	11.194	0.999	0.554	0.043
0.207	0.006	8.182	0.998	7.590	0.380	11.170	0.954	0.751	0.042
0.217	0.012	11.832	0.791	5.463	0.230	13.036	0.762	0.434	0.024
0.220	0.010	10.396	1.078	5.833	0.204	11.926	0.905	0.513	0.053
0.220	0.010	8.844	0.812	7.789	0.329	11.801	0.807	0.726	0.029
0.223	0.006	8.578	0.554	8.148	0.219	11.836	0.468	0.761	0.031
0.223	0.006	8.069	0.936	7.584	0.238	11.088	0.790	0.758	0.050
0.225	0.013	11.756	0.965	6.183	0.313	13.286	0.973	0.485	0.021
0.230	0.017	12.236	1.255	6.441	0.426	13.834	1.258	0.486	0.030
0.233	0.010	12.772	1.208	5.909	0.349	14.077	1.215	0.435	0.023
0.237	0.015	11.585	1.153	5.831	0.385	12.973	1.179	0.468	0.023
0.240	0.010	8.182	0.765	8.324	0.346	11.681	0.705	0.796	0.040
0.262	0.023	10.680	1.083	6.159	0.304	12.335	1.053	0.525	0.032
0.262	0.010	10.945	1.078	6.230	0.474	12.600	1.108	0.519	0.033
0.267	0.018	13.768	0.601	4.304	0.371	14.430	0.594	0.303	0.026
0.273	0.006	14.878	1.247	4.873	0.418	15.661	1.248	0.317	0.027
0.293	0.015	13.827	1.262	5.071	0.565	14.739	1.249	0.353	0.041

Table A6.3. Measured and Resolved Forces Depending for Chisel

Depth [m]		FX [kN]		FY [kN]		RE [kN]		θ [Radians]	
Mean	Stdev	Mean	Stdev	Mean	Stdev	Mean	Stdev	Mean	Stdev
0.000	0.000	0.000	0.000	2.786	0.000	2.786	0.000	1.570	0.000
0.076	0.021	2.260	0.929	3.207	0.289	3.987	0.667	0.983	0.179
0.086	0.021	2.582	1.320	3.316	0.318	4.301	1.004	0.952	0.214
0.088	0.023	2.717	1.250	3.291	0.344	4.331	1.065	0.916	0.163
0.089	0.025	2.691	0.878	3.216	0.284	4.231	0.727	0.893	0.132
0.102	0.027	2.987	1.150	3.165	0.217	4.426	0.848	0.847	0.186
0.104	0.019	2.310	1.023	3.324	0.244	4.118	0.732	0.993	0.180
0.155	0.048	6.114	2.017	4.118	0.320	7.435	1.799	0.624	0.132
0.165	0.027	6.527	1.682	3.743	0.221	7.583	1.408	0.545	0.132
0.168	0.045	6.719	1.336	3.946	0.246	7.818	1.200	0.542	0.078
0.173	0.050	8.494	1.575	4.288	0.245	9.547	1.392	0.479	0.080
0.202	0.028	8.369	2.147	3.678	0.203	9.189	1.944	0.435	0.101
0.207	0.040	8.691	2.661	3.818	0.372	9.559	2.442	0.444	0.122
0.226	0.028	10.633	1.443	3.942	0.279	11.351	1.383	0.360	0.045
0.231	0.025	11.151	1.377	4.221	0.226	11.930	1.336	0.365	0.035
0.232	0.032	11.087	1.522	4.476	0.327	11.964	1.502	0.387	0.034
0.240	0.026	12.383	1.607	3.915	0.223	12.994	1.565	0.310	0.033
0.254	0.026	13.239	1.207	4.222	0.307	13.905	1.130	0.311	0.038
0.256	0.025	13.344	1.432	4.408	0.333	14.066	1.341	0.322	0.044

Table A6.4. Measured and Resolved Forces for Subsoiler

Depth [m]		FX [kN]		FY [kN]		RE [kN]		θ [Radians]	
Mean	Stdev	Mean	Stdev	Mean	Stdev	Mean	Stdev	Mean	Stdev
0.000	0.000	0.000	0.000	1.696	0.000	1.696	0.000	1.570	0.000
0.158	0.025	1.269	0.477	1.975	0.281	2.401	0.235	1.011	0.219
0.173	0.025	1.549	0.479	2.015	0.148	2.578	0.253	0.930	0.172
0.192	0.014	1.579	0.418	2.002	0.147	2.577	0.238	0.914	0.146
0.217	0.006	3.016	0.737	2.288	0.393	3.848	0.467	0.666	0.173
0.233	0.035	2.988	0.563	2.316	0.283	3.808	0.430	0.668	0.119
0.243	0.030	2.863	0.569	2.312	0.230	3.709	0.404	0.691	0.125
0.285	0.018	3.826	0.853	2.730	0.311	4.733	0.716	0.632	0.116
0.323	0.025	4.233	0.874	2.866	0.337	5.147	0.720	0.607	0.110
0.330	0.045	5.562	0.398	3.148	0.204	6.409	0.387	0.523	0.042
0.333	0.012	4.551	0.979	2.976	0.460	5.442	0.789	0.581	0.116
0.333	0.010	5.366	0.907	2.871	0.262	6.130	0.812	0.503	0.074
0.360	0.020	5.325	0.724	2.954	0.375	6.104	0.697	0.511	0.071
0.413	0.021	8.956	1.912	3.592	0.450	9.684	1.782	0.394	0.085
0.432	0.014	7.733	1.440	3.672	0.794	8.634	1.198	0.457	0.127

Table A6.5. Measured and Resolved Forces for Standard Tine

Depth [m]		FX [kN]		FY [kN]		RE [kN]		θ [Radians]	
Mean	Stdev	Mean	Stdev	Mean	Stdev	Mean	Stdev	Mean	Stdev
0.000	0.000	0.000	0.000	4.790	0.000	4.790	0.000	1.570	0.000
0.130	0.000	0.410	0.385	4.855	0.134	4.886	0.168	0.935	1.152
0.137	0.012	0.817	0.360	4.741	0.138	4.824	0.157	1.401	0.073
0.150	0.036	0.652	0.352	4.869	0.153	4.924	0.176	1.439	0.069
0.180	0.030	1.993	0.501	5.154	0.143	5.546	0.235	1.204	0.084
0.220	0.017	1.701	0.476	5.137	0.170	5.430	0.235	1.253	0.081
0.233	0.038	2.355	0.543	4.867	0.201	5.427	0.329	1.124	0.086
0.243	0.032	2.786	0.694	5.239	0.154	5.964	0.379	1.087	0.099
0.267	0.035	3.348	0.682	5.513	0.185	6.476	0.412	1.030	0.089
0.273	0.012	3.481	0.601	5.231	0.194	6.303	0.393	0.988	0.077
0.280	0.044	6.807	1.544	4.970	0.405	8.464	1.395	0.644	0.095
0.293	0.042	3.948	0.659	5.539	0.183	6.818	0.496	0.956	0.068
0.293	0.035	4.652	0.880	5.161	0.432	6.991	0.603	0.843	0.116
0.307	0.031	4.227	0.913	4.794	0.278	6.444	0.496	0.857	0.126
0.323	0.025	4.235	1.999	5.114	0.438	6.797	1.443	0.911	0.185
0.343	0.051	5.274	1.488	5.141	0.308	7.441	1.092	0.791	0.140
0.360	0.075	8.225	2.540	6.025	0.698	10.271	2.322	0.653	0.117
0.380	0.062	6.724	1.605	6.101	0.447	9.123	1.408	0.751	0.103
0.390	0.035	6.148	1.259	6.040	0.474	8.670	0.960	0.786	0.108
0.393	0.060	11.723	4.380	6.131	1.009	13.335	4.172	0.515	0.121
0.397	0.068	7.309	2.136	5.895	0.398	9.498	1.636	0.703	0.156
0.420	0.044	12.880	4.006	6.240	1.522	14.441	3.827	0.473	0.143
0.423	0.068	11.249	2.981	5.893	0.501	12.750	2.795	0.499	0.089
0.487	0.040	8.754	1.256	6.612	0.469	10.991	1.164	0.652	0.063
0.490	0.017	11.701	4.899	5.253	1.366	13.025	4.551	0.468	0.191

APPENDIX 7

Field Test Results

(Clay Soil: GAP in Türkiye-1991)

Table A7.1. Measured and Resolved Forces for Disc Plough

Depth [m]		FX [kN]		FY [kN]		RE [kN]		θ [Radians]	
Mean	Stdev	Mean	Stdev	Mean	Stdev	Mean	Stdev	Mean	Stdev
0.000	0.000	0.000	0.000	3.532	0.000	3.532	0.000	1.570	0.000
0.083	0.015	4.367	1.120	0.123	0.635	4.426	1.072	-0.004	0.194
0.084	0.015	4.298	1.185	0.241	0.717	4.382	1.114	0.027	0.228
0.088	0.016	4.343	0.882	-0.262	0.632	4.404	0.843	-0.083	0.161
0.130	0.010	6.405	1.247	0.524	0.153	6.429	1.244	0.085	0.026
0.133	0.021	6.362	1.296	0.550	0.150	6.388	1.294	0.089	0.026
0.135	0.013	6.061	0.804	0.563	0.133	6.089	0.801	0.094	0.025

Table A7.2. Measured and Resolved Forces for Mouldboard Plough

Depth [m]		FX [kN]		FY [kN]		RE [kN]		θ [Radians]	
Mean	Stdev	Mean	Stdev	Mean	Stdev	Mean	Stdev	Mean	Stdev
0.000	0.000	0.000	0.000	5.435	0.000	5.435	0.000	1.570	0.000
0.178	0.012	7.608	0.743	2.831	1.391	8.236	0.742	0.352	0.176
0.183	0.006	7.006	1.192	0.281	2.038	7.307	1.160	0.019	0.290
0.190	0.020	8.051	1.486	1.144	1.512	8.272	1.485	0.131	0.197
0.247	0.021	10.695	2.031	-1.104	1.820	10.927	1.906	-0.104	0.192
0.253	0.015	17.966	2.150	-2.102	2.131	18.223	2.067	-0.119	0.124
0.307	0.012	19.866	1.578	-6.479	0.923	20.923	1.491	-0.317	0.051

Table A7.3. Measured and Resolved Forces for Chisel

Depth [m]		FX [kN]		FY [kN]		RE [kN]		θ [Radians]	
Mean	Stdev	Mean	Stdev	Mean	Stdev	Mean	Stdev	Mean	Stdev
0.000	0.000	0.000	0.000	2.786	0.000	2.786	0.000	1.570	0.000
0.175	0.007	12.130	2.973	-2.417	1.155	12.426	2.945	0.202	0.101
0.175	0.007	10.419	2.146	-1.024	1.990	10.669	2.052	0.103	0.203
0.255	0.007	14.757	2.440	0.212	1.225	14.813	2.392	-0.017	0.095
0.275	0.043	18.743	5.379	1.443	1.538	18.844	5.431	-0.073	0.070
0.288	0.030	22.717	4.640	-1.395	2.054	22.851	4.628	0.065	0.091
0.308	0.030	25.038	5.022	1.883	2.353	25.220	4.995	-0.080	0.097

Table A7.4. Measured and Resolved Forces for Subsoiler

Depth [m]		FX [kN]		FY [kN]		RE [kN]		θ [Radians]	
Mean	Stdev	Mean	Stdev	Mean	Stdev	Mean	Stdev	Mean	Stdev
0.000	0.000	0.000	0.000	0.961	0.000	0.961	0.000	1.570	0.000
0.250	0.014	5.187	1.107	0.189	0.903	5.261	1.139	0.023	0.161
0.250	0.019	4.426	0.891	3.512	1.937	5.906	1.262	0.627	0.320
0.275	0.013	4.721	1.352	-0.429	0.277	4.756	1.328	-0.110	0.086
0.427	0.021	13.281	3.265	-0.280	0.533	13.296	3.260	-0.027	0.045
0.433	0.028	13.548	4.325	-0.318	0.633	13.567	4.320	-0.030	0.050

Table A7.5. Measured and Resolved Forces for Standard Tine

Depth [m]		FX [kN]		FY [kN]		RE [kN]		θ [Radians]	
Mean	Stdev	Mean	Stdev	Mean	Stdev	Mean	Stdev	Mean	Stdev
0.000	0.000	0.000	0.000	1.334	0.000	1.334	0.000	1.570	0.000
0.160	0.020	2.450	0.764	-1.691	0.170	3.021	0.593	-0.636	0.180
0.166	0.017	1.586	0.654	0.179	0.864	1.847	0.556	0.194	0.545
0.170	0.008	1.821	0.916	1.514	1.835	3.103	0.427	0.629	0.715
0.240	0.014	6.084	1.062	-1.891	0.390	6.378	1.090	-0.303	0.049
0.243	0.040	5.867	1.099	-1.877	0.353	6.163	1.140	-0.310	0.030
0.330	0.004	8.456	1.377	-2.594	0.522	8.852	1.433	-0.298	0.039

APPENDIX 8

Table A8.1. Geometrical Factors and Error Bands for Tools Used in Field Experiments in 1991

Depth	Disc Geometrical Factor				
[m]	Min	Max	Avg	Stdev	C.V.%
0.10	0.240001	0.273174	0.256579	0.016587	6.46
0.15	0.235630	0.291413	0.263522	0.027892	10.58
0.20	0.264790	0.331186	0.297973	0.033198	11.14
0.25	0.262488	0.547170	0.404829	0.142341	35.16
Depth	Mouldboard Geometrical Factor				
[m]	Min	Max	Avg	Stdev	C.V.%
0.10	0.384491	0.535119	0.459813	0.075314	16.38
0.15	0.448593	0.502720	0.475668	0.027064	5.69
0.20	0.445399	0.514917	0.480143	0.034759	7.24
0.25	0.499261	0.583307	0.541302	0.042023	7.76
0.30	0.504044	0.986993	0.745518	0.241475	32.39
Depth	Chisel (Curved blade) Geometrical Factor				
[m]	Min	Max	Avg	Stdev	C.V.%
0.15	0.234744	0.271637	0.253191	0.018447	7.29
0.20	0.264495	0.325474	0.294970	0.030490	10.34
0.25	0.325407	0.389286	0.357347	0.031940	8.94
0.30	0.416576	0.495998	0.456266	0.039711	8.70
0.35	0.506116	0.709280	0.607722	0.101582	16.72
Depth	Subsoiler (High lift-Without wing) Geometrical Factor				
[m]	Min	Max	Avg	Stdev	C.V.%
0.15	0.176490	0.202072	0.189269	0.012791	6.76
0.20	0.199424	0.234728	0.217091	0.017652	8.13
0.25	0.229766	0.271131	0.250431	0.020683	8.26
0.30	0.271950	0.309431	0.290670	0.018741	6.45
0.35	0.309599	0.361239	0.335419	0.025820	7.70
0.40	0.345850	0.411331	0.378591	0.032741	8.65
0.45	0.380790	0.440131	0.410460	0.029671	7.23

Source: Desbiolles (1994)

APPENDIX 9

Tine Interactions for the Chisel used in UK

Figure A9.1 shows tine arrangements on the chisel frame in field experiments in UK.

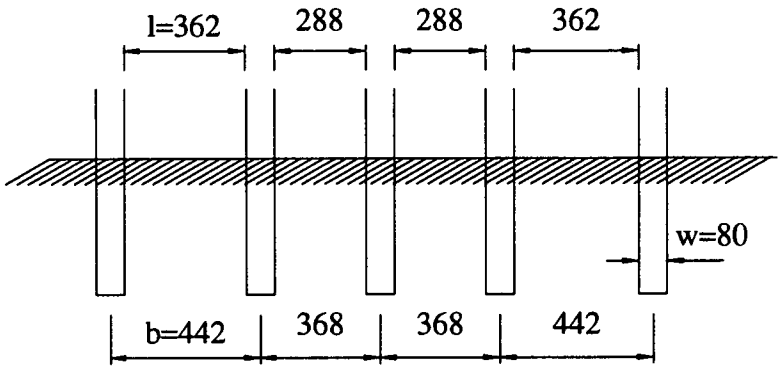

Figure A9.1. Tine arrangement of the chisel used in UK

Interaction between the tines exists only for the condition of $d \rangle l/2$ (Fig. A9.2).

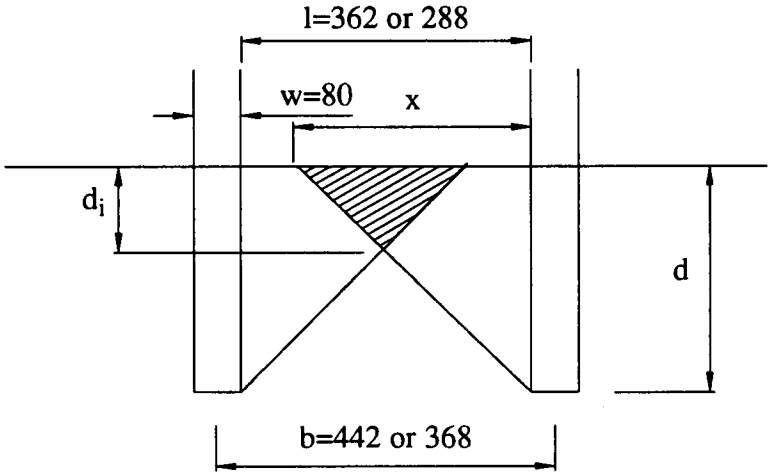

Figure A9.2. Interactions between the tines

Therefore, for the first case, i.e. $l = 362$ mm:

$d \rangle \frac{362}{2} \Rightarrow d \rangle 181$ mm and also

$d_i = (2d - l)/2$

for the second case, i.e. $l = 288$ mm:

$d \rangle \frac{288}{2} \Rightarrow d \rangle 144$ mm and also

$d_i = (2d - l)/2$

Interaction area $A_i = \frac{d_i^2}{\tan 45}$

Therefore, the interaction depth and area were calculated for the following depth range as follows:

Tine depth (d) [m]	Interaction depth1 (d_i) [m]	Interaction depth2 (d_i) [m]	Interaction area [m^2]
0.150	-	0.006	0.21×10^{-3}
0.200	0.019	0.056	11.86×10^{-3}
0.250	0.069	0.106	50.62×10^{-3}
0.300	0.119	0.156	118.64×10^{-3}
0.350	0.169	0.206	215.94×10^{-3}

Area disturbed by a single tine can be presented as $A_T = d(d \times \tan 45 + w)$

Interaction area is also stated as a percentage of total area without interaction.

Tine depth (d) [m]	Interaction area [m^2]	Total area [m^2]	% of Total area
0.150	0.21×10^{-3}	156.08×10^{-3}	0.13
0.200	11.86×10^{-3}	250.82×10^{-3}	4.73
0.250	50.62×10^{-3}	366.90×10^{-3}	13.80
0.300	118.64×10^{-3}	504.34×10^{-3}	23.52
0.350	215.94×10^{-3}	663.12×10^{-3}	32.56

The predicted draught force was corrected with the share of the interaction.

Tine depth (d) [m]	% of Total area	Predicted Draught [kN]	Corrected Draught [kN]
0.150	0.13	6.8362	6.827
0.200	4.73	11.2179	10.711
0.250	13.80	17.586	15.453
0.300	23.52	27.5674	22.318
0.350	32.56	43.5761	32.872

APPENDIX 10

Tine Interactions for the Chisel used in Türkiye

Figure A10.1 shows tine arrangements on the chisel frame used during the field experiments in Türkiye.

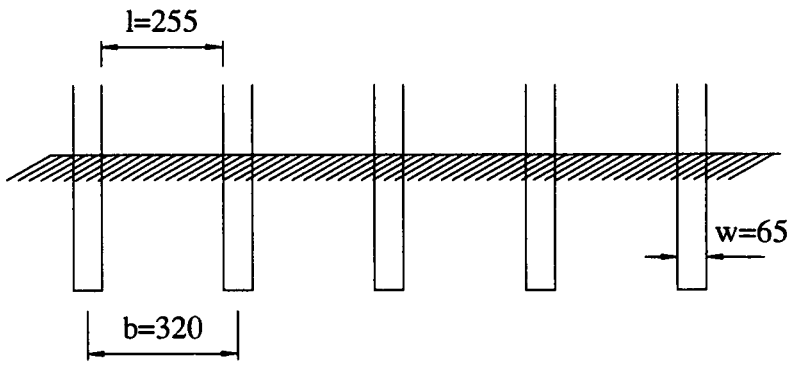

Figure A10.1. Tine arrangement of the chisel used in Türkiye

Interaction between the tines exists only for the condition of $d \rangle l/2$ (Fig. A10.2).

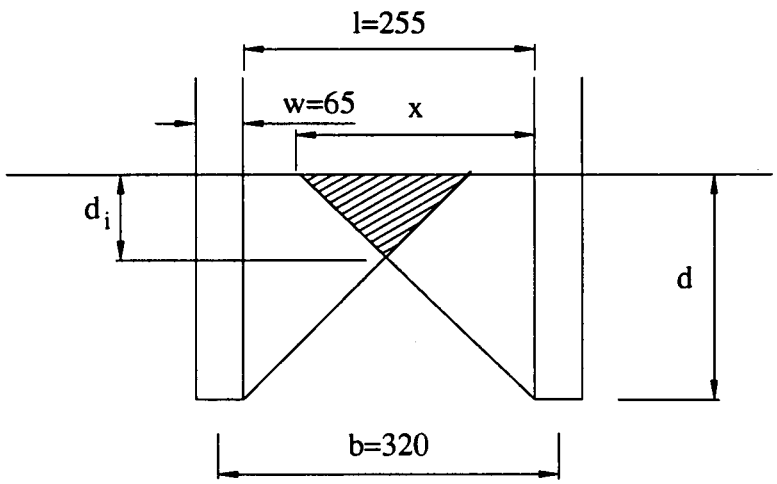

Figure A10.2. Interactions between the tines

Therefore,

$d \rangle \frac{255}{2} \Rightarrow d \rangle 127.5$ mm and also

$d_i = (2d - l)/2$

Interaction area $A_i = \frac{d_i^2}{\tan 45}$

Therefore, the interaction depth and area were calculated for the following depth range as follows:

Tine depth (d) [m]	Interaction depth (d_i) [m]	Interaction area [m^2]
0.150	0.0225	3.56×10^{-3}
0.200	0.0725	36.93×10^{-3}
0.250	0.1225	105.42×10^{-3}
0.300	0.1725	209.04×10^{-3}
0.350	0.2225	347.79×10^{-3}

Area disturbed by a single tine can be presented as $A_T = d(d \times \tan 45 + w)$

Interaction area is also stated as a percentage of total area without interaction.

Tine depth (d) [m]	Interaction area [m^2]	Total area [m^2]	% of Total area
0.150	3.56×10^{-3}	173.80×10^{-3}	2.05
0.200	36.93×10^{-3}	282.98×10^{-3}	13.05
0.250	105.42×10^{-3}	417.78×10^{-3}	25.23
0.300	209.04×10^{-3}	578.20×10^{-3}	36.15
0.350	347.79×10^{-3}	764.25×10^{-3}	45.51

The predicted draught force was corrected with the share of the interaction.

Tine depth (d) [m]	% of Total area	Predicted Draught [kN]	Corrected Draught [kN]
0.150	2.05	9.3056	9.1187
0.200	13.05	15.0290	13.2941
0.250	25.23	22.4374	17.9170
0.300	36.15	31.9779	23.4873
0.350	45.51	43.7902	30.0943

APPENDIX 11

Comparison of Measured and Predicted Draughts

Table A11.1. Prediction Errors for the Implements Used in Sandy Loam Soil: Downings Field-UK in 1991

Disc Plough							
Depth [kN]	Draught [kN]		Prediction Error [%]				D_P/D_M
	Measured	Predicted	Min	Max	Avg	C.V.	
0.10	2.313	2.506	1.35	15.36	8.35	83.89	0.923
0.15	5.204	4.269	-9.28	-26.65	-17.97	48.33	1.219
0.20	9.251	6.799	-18.31	-34.69	-26.50	30.90	1.361
0.25	14.455	11.954	11.77	-46.38	-17.30	168.03	1.209
Mouldboard Plough							
Depth [kN]	Draught [kN]		Prediction Error [%]				D_P/D_M
	Measured	Predicted	Min	Max	Avg	C.V.	
0.10	3.989	4.491	-5.85	31.03	12.59	146.48	0.888
0.15	6.315	7.706	15.08	28.96	22.02	31.52	0.820
0.20	8.863	10.956	14.67	32.57	23.62	37.89	0.809
0.25	11.631	15.983	26.75	48.08	37.42	28.51	0.728
Chisel							
Depth [kN]	Draught [kN]		Prediction Error [%]				D_P/D_M
	Measured	Predicted	Min	Max	Avg	C.V.	
0.15	5.623	6.827	12.57	30.27	21.41	41.32	0.824
0.20	8.859	10.711	8.42	33.41	20.91	59.77	0.827
0.25	12.776	15.453	10.14	31.77	20.95	51.61	0.827
0.30	17.374	22.318	17.28	39.65	28.46	39.29	0.778
0.35	22.653	32.872	20.85	69.36	45.11	53.77	0.689
Subsoiler							
Depth [kN]	Draught [kN]		Prediction Error [%]				D_P/D_M
	Measured	Predicted	Min	Max	Avg	C.V.	
0.20	2.039	1.651	-12.44	-25.61	-19.02	34.62	1.235
0.25	3.041	2.465	-12.25	-25.63	-18.95	35.33	1.234
0.30	4.241	3.512	-11.83	-22.51	-17.18	31.08	1.207
0.35	5.638	4.810	-8.12	-21.25	-14.68	44.73	1.172
0.40	7.232	6.287	-5.55	-20.59	-13.07	57.53	1.150

Table A11.2. Prediction Errors for the Implements Used in Clay Soil:

GAP-Türkiye in 1991

Disc Plough							
Depth	Draught [kN]		Prediction Error [%]				
[kN]	Measured	Predicted	Min	Max	Avg	C.V.	D_P/D_M
0.10	4.994	3.804	-18.91	-28.75	-23.83	20.66	1.313
0.15	6.861	6.478	-4.41	-15.57	-5.58	179.09	1.059
Mouldboard Plough							
Depth	Draught [kN]		Prediction Error [%]				
[kN]	Measured	Predicted	Min	Max	Avg	C.V.	D_P/D_M
0.15	5.286	7.796	39.08	55.86	47.48	17.67	0.678
0.20	9.050	11.080	13.57	31.30	22.43	39.51	0.817
0.25	13.816	16.166	7.92	26.09	17.01	53.40	0.855
Chisel							
Depth	Draught [kN]		Prediction Error [%]				
[kN]	Measured	Predicted	Min	Max	Avg	C.V.	D_P/D_M
0.15	8.328	9.119	-7.91	26.84	9.49	79.64	0.915
0.20	12.468	13.294	-11.50	23.60	6.63	134.97	1.060
0.25	17.291	17.917	-8.94	20.09	3.62	39.60	1.209
0.30	22.795	23.487	-15.39	19.43	3.04	20.06	1.321
Subsoiler							
Depth	Draught [kN]		Prediction Error [%]				
[kN]	Measured	Predicted	Min	Max	Avg	C.V.	D_P/D_M
0.20	2.845	2.505	-4.80	-19.12	-11.96	59.88	1.136
0.25	4.474	3.740	-9.51	-23.31	-16.42	42.05	1.196
0.30	6.471	5.330	-12.32	-22.94	-17.64	30.11	1.214
0.35	8.835	7.298	-11.03	-23.75	-17.39	36.56	1.211
0.40	11.566	9.539	-10.40	-24.66	-17.53	40.69	1.213
0.45	14.665	11.756	-14.04	-25.63	-19.84	29.21	1.247

APPENDIX 12

Comparison of Index Values

Table A12.1. Index Values for the Tools Used in Sandy Loam Soil: Downings Field-UK in 1991

Disc Plough						
Depth	Measured draught [kN]			Index		Error
[kN]	Implement	Tool	S.Tine	I_{GF}	I_D	[%]
0.10	2.313	0.771	0.560	1.492	1.377	7.72
0.15	5.204	1.735	1.260	1.130	1.377	-21.83
0.20	9.251	3.084	2.240	1.012	1.377	-36.03
0.25	14.455	4.818	3.500	1.138	1.377	-20.97
Mouldboard Plough						
Depth	Measured draught [kN]			Index		Error
[kN]	Implement	Tool	S.Tine	I_{GF}	I_D	[%]
0.10	3.989	1.330	0.560	2.674	2.374	11.20
0.15	6.315	2.105	1.260	2.040	1.671	18.11
0.20	8.863	2.954	2.240	1.631	1.319	19.14
0.25	11.631	3.877	3.500	1.522	1.108	27.22
Chisel						
Depth	Measured draught [kN]			Index		Error
[kN]	Implement	Tool	S.Tine	I_{GF}	I_D	[%]
0.20	8.859	1.856	2.240	1.002	0.828	17.33
0.25	12.776	2.908	3.500	1.005	0.831	17.33
0.30	17.374	4.292	5.039	1.094	0.852	22.14
0.35	22.653	6.006	6.859	1.271	0.876	31.11
Subsoiler						
Depth	Measured draught [kN]			Index		Error
[kN]	Implement	Tool	S.Tine	I_{GF}	I_D	[%]
0.25	3.041	3.041	3.500	0.704	0.869	-23.42
0.30	4.241	4.241	5.039	0.697	0.842	-20.75
0.35	5.638	5.638	6.859	0.702	0.822	-17.09
0.40	7.232	7.232	8.959	0.702	0.807	-14.99

Table A12.2. Index Values for the Tools Used in Clay Soil: GAP-Türkiye in 1991

Disc Plough						
Depth	Measured draught [kN]			Index		Error
[kN]	Implement	Tool	S.Tine	I_{GF}	I_D	[%]
0.10	4.994	1.665	0.850	1.492	1.959	-31.27
0.15	6.861	2.287	1.912	1.130	1.196	-5.85
Mouldboard Plough						
Depth	Measured draught [kN]			Index		Error
[kN]	Implement	Tool	S.Tine	I_{GF}	I_D	[%]
0.10	2.523	0.841	0.850	2.674	0.989	63.00
0.15	5.286	1.762	1.912	2.040	0.922	54.83
0.20	9.050	3.017	3.398	1.631	0.888	45.57
0.25	13.816	4.605	5.310	1.522	0.867	43.02
Chisel						
Depth	Measured draught [kN]			Index		Error
[kN]	Implement	Tool	S.Tine	I_{GF}	I_D	[%]
0.15	8.328	1.391	1.912	0.812	0.728	11.33
0.20	12.468	2.349	3.398	0.737	0.691	6.24
0.25	17.291	3.609	5.310	0.704	0.680	3.41
0.30	22.795	5.173	7.646	0.697	0.677	2.87
Subsoiler						
Depth	Measured draught [kN]			Index		Error
[kN]	Implement	Tool	S.Tine	I_{GF}	I_D	[%]
0.20	2.845	2.845	3.398	0.737	0.837	-13.60
0.25	4.474	4.474	5.310	0.704	0.843	-19.68
0.30	6.471	6.471	7.646	0.697	0.846	-21.42
0.35	8.835	8.835	10.407	0.702	0.849	-20.93
0.40	11.566	11.566	13.593	0.702	0.851	-21.21

APPENDIX 13

Soil Strength Factors for the Fields in 1993

Table A13.1. Fitted Draught Requirement of the Standard Tine: Showground Field in UK in 1993

Depth	Sandy Loam Soil (Showground Field)			
[m]	Min	Max	Avg	C.V.%
0.00	0.000	0.000	0.000	0.00
0.05	0.497	0.831	0.664	25.16
0.10	1.179	1.733	1.456	19.04
0.15	2.043	2.706	2.375	13.96
0.20	3.089	3.754	3.422	9.72
0.25	4.307	4.885	4.596	6.29
0.30	5.667	6.128	5.898	3.91
0.35	7.072	7.582	7.327	3.48
0.40	8.453	9.314	8.884	4.85
0.45	9.861	11.276	10.568	6.69
0.50	11.323	13.437	12.380	8.54

Table A13.2. Fitted Draught Requirement of the Standard Tine: Millbrook Field in UK in 1993

Depth	Sandy Loam Soil (Millbrook Field)			
[m]	Min	Max	Avg	C.V.%
0.00	0.000	0.000	0.000	0.00
0.05	-0.122	0.376	0.127	196.06
0.10	0.153	0.999	0.576	73.44
0.15	0.823	1.821	1.347	37.06
0.20	1.884	2.995	2.440	22.77
0.25	3.328	4.381	3.855	13.66
0.30	5.129	6.055	5.592	8.28
0.35	7.217	8.085	7.651	5.67
0.40	9.479	10.585	10.032	5.51
0.45	11.894	13.577	12.735	6.61
0.50	14.505	17.015	15.760	7.96

Table A13.3. Fitted Draught Requirement of the Standard Tine: Copse Field in UK in 1993

Depth	Clay Soil (Copse Field)			
[m]	Min	Max	Avg	C.V.%
0.00	0.000	0.000	0.000	0.00
0.05	0.982	1.384	1.183	16.99
0.10	2.336	2.997	2.666	12.40
0.15	4.059	4.842	4.451	8.80
0.20	6.144	6.928	6.536	6.00
0.25	8.569	9.277	8.923	3.97
0.30	11.268	11.952	11.610	2.95
0.35	14.137	15.058	14.598	3.15
0.40	17.161	18.613	17.887	4.06
0.45	20.375	22.579	21.477	5.13
0.50	23.800	26.935	25.368	6.18

APPENDIX 14

Geometrical and Soil Strength Factors for the Validation Tests in 1993

Table A14.1. Geometrical Factors (GF) for Winged Subsoiler Used in UK in 1993

Subsoiler (High lift-With wing)						
Depth [m]	Geometrical Factor					Index $GF_{Tool}/GF_{S.Tine}$
	Min	Max	Avg	Stdev	C.V.%	
0.10	0.292865	0.328463	0.310664	0.017799	5.73	1.807
0.15	0.383086	0.422637	0.402862	0.019776	4.91	1.728
0.20	0.465274	0.505495	0.485384	0.020111	4.14	1.648
0.25	0.538350	0.578114	0.558232	0.019882	3.56	1.570
0.30	0.600267	0.642583	0.621404	0.021158	3.40	1.490
0.35	0.648651	0.701200	0.674902	0.026275	3.89	1.412
0.40	0.682693	0.754808	0.718778	0.036058	5.02	1.333
0.45	0.703020	0.802782	0.752931	0.049881	6.62	1.254

Table A14.2. Soil Strength Factors (SSF) for the Fields in UK in 1993

Depth [m]	Showground Field (Sandy Loam Soil)	Millbrook Field (Sandy Loam Soil)	Copse Field (Clay Soil)
0.00	0.0000	0.0000	0.0000
0.05	5.9972	1.1469	10.6832
0.10	8.4648	3.3494	15.5027
0.15	10.1837	5.7760	19.0862
0.20	11.6207	8.2869	22.1981
0.25	12.9213	10.8385	25.0875
0.30	14.1460	13.4130	27.8477
0.35	15.3238	16.0014	30.5305
0.40	16.4704	18.5991	33.1621
0.45	17.5958	21.2033	35.7583
0.50	18.7054	23.8120	38.3289

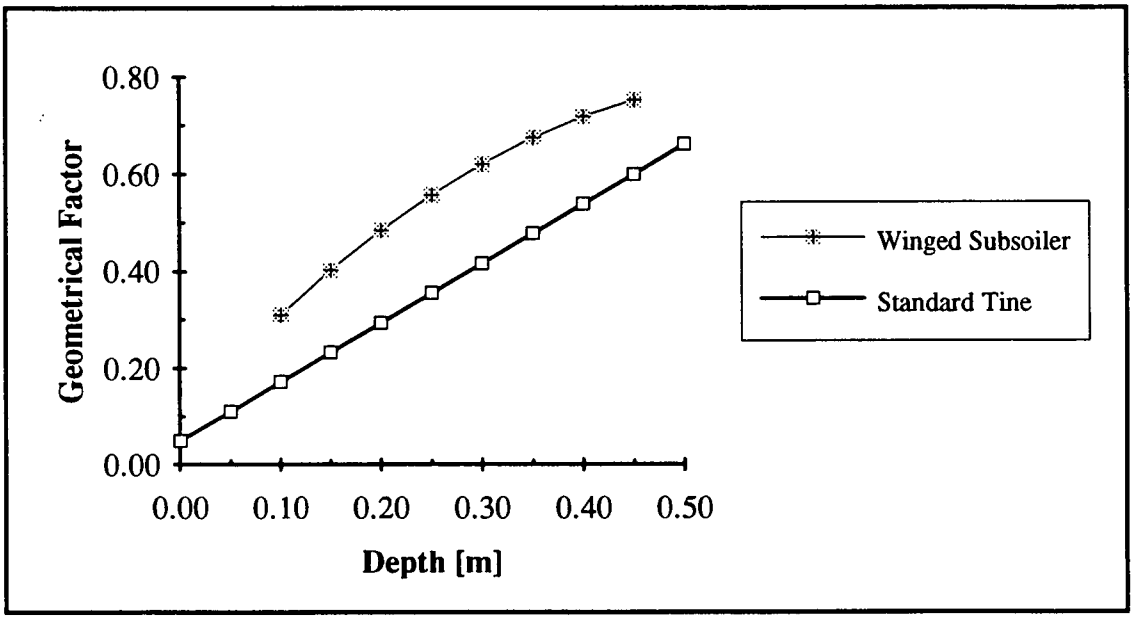

Figure A14.1. Geometrical factors for winged subsoiler and standard tine used in 1993

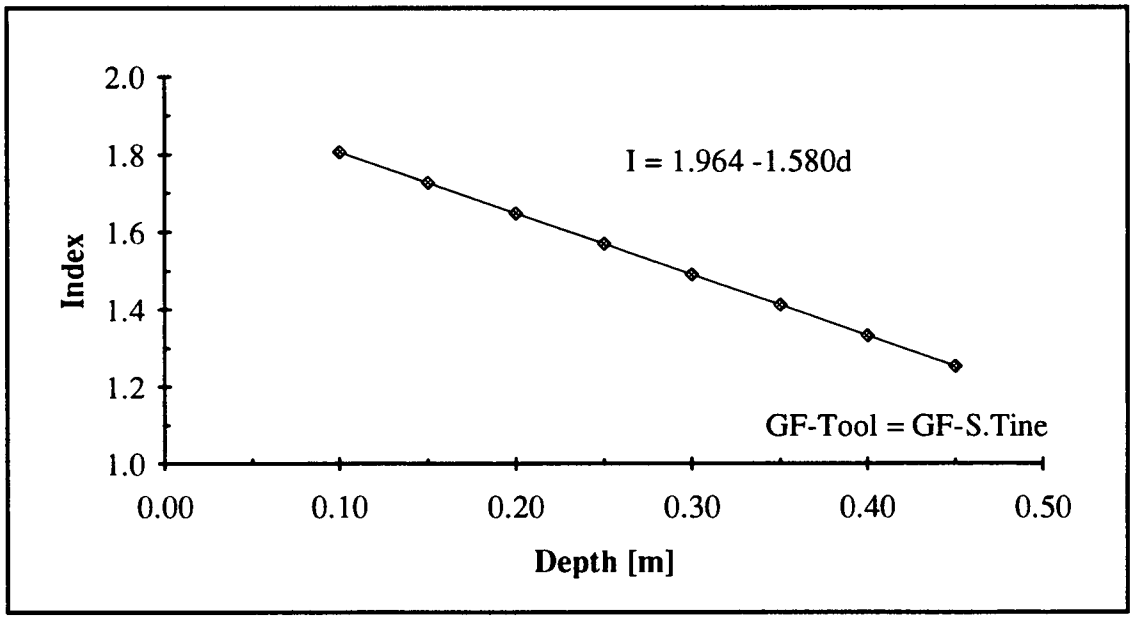

Figure A14.2. Index curve based on geometrical factors for winged subsoiler used in 1993

APPENDIX 15

Predicting the Draught Forces

Table A15.1. Working Depths Accepted for Draught Predictions

Implement	Working depth [m]		
	d_1	d_2	d_3
Disc plough	0.10	0.15	0.20
Mouldboard plough	0.15	0.20	0.25
Chisel	0.25	0.30	0.35
Subsoiler	0.30	0.35	0.40

It is assumed that the speed for both sandy loam and clay soil conditions is 3.6 and 6.6 km/h for all implements, respectively.

During the predictions, in addition to the implements and soil characteristics, the following parameters are also considered:

for ASAE:

Soil type

clay soil : Decatur clay loam for disc plough

: silty clay (South Texas) for mouldboard plough

: medium or clay loam for subsoiler

sandy loam soil : Davidson loam for disc plough

: Loam (Saskatchewan) for chisel

*These are the closest soil descriptions.

for Witney (1988)

Plough type : semi-digger

Compaction level : stubble

Soil type : sandy loam & silty clay

Table A15.2. Draught Forces Predicted by Different Methods for the Implements Under Sandy loam and Clay Soil Conditions

Disc Plough						
Depth [m]	Draught force [kN]					
	ASAE		Witney		Kirişci	
	Sandy	Clay	Sandy	Clay	Sandy	Clay
0.10	8.502	13.142	-	-	2.506	3.804
0.15	12.754	19.713	-	-	4.269	6.478
0.20	17.005	26.285	-	-	6.799	10.314
Mouldboard Plough						
Depth [m]	Draught force [kN]					
	ASAE		Witney		Kirişci	
	Sandy	Clay	Sandy	Clay	Sandy	Clay
0.15	5.387	8.145	11.327	2.517	7.706	7.796
0.20	7.182	10.860	15.102	3.356	10.956	11.080
0.25	8.978	13.573	18.878	4.195	15.893	16.166
Chisel						
Depth [m]	Draught force [kN]					
	ASAE		Witney		Kirişci	
	Sandy	Clay	Sandy	Clay	Sandy	Clay
0.25	38.690	42.000	-	-	15.453	17.917
0.30	55.714	50.400	-	-	22.318	23.487
0.35	75.833	58.800	-	-	32.872	30.094
Subsoiler						
Depth [m]	Draught force [kN]					
	ASAE		Witney		Kirişci	
	Sandy	Clay	Sandy	Clay	Sandy	Clay
0.30	3.600	8.400	-	-	3.512	5.330
0.35	4.200	9.800	-	-	4.810	7.298
0.40	4.800	11.200	-	-	6.287	9.539